Romain Maurand
CEA Grenoble, France

Hole spin qubits in silicon : Coherence “sweetspots” and coupling to MW cavity

Swiss National Science Foundation

Outline

- Spin Qubits quick recap
- Holes / Spin-Orbit Interaction
- Silicon-on- insulator nanowire devices
- Coherence “sweetspots”
- Spin-photon coupling

Spins in semiconductor Quantum dot

PHYSICAL REVIEW A VOLUME 57, NUMBER 1 JANUARY 1998

Quantum computation with quantum dots

Daniel Loss[1,2,*] and David P. DiVincenzo[1,3,†]
[1]*Institute for Theoretical Physics, University of California, Santa Barbara, Santa Barbara, California 93106-4030*
[2]*Department of Physics and Astronomy, University of Basel, Klingelbergstrasse 82, 4056 Basel, Switzerland*
[3]*IBM Research Division, T.J. Watson Research Center, P.O. Box 218, Yorktown Heights, New York 10598*
(Received 9 January 1997; revised manuscript received 22 July 1997)

We propose an implementation of a universal set of one- and two-quantum-bit gates for quantum computation using the spin states of coupled single-electron quantum dots. Desired operations are effected by the gating of the tunneling barrier between neighboring dots. Several measures of the gate quality are computed within a recently derived spin master equation incorporating decoherence caused by a prototypical magnetic environment. Dot-array experiments that would provide an initial demonstration of the desired nonequilibrium spin dynamics are proposed. [S1050-2947(98)04501-6]

Spins in semiconductor Quantum dot

PHYSICAL REVIEW A VOLUME 57, NUMBER 1 JANUARY 1998

Quantum computation with quantum dots

Daniel Loss[1,2,*] and David P. DiVincenzo[1,3,†]
[1]*Institute for Theoretical Physics, University of California, Santa Barbara, Santa Barbara, California 93106-4030*
[2]*Department of Physics and Astronomy, University of Basel, Klingelbergstrasse 82, 4056 Basel, Switzerland*
[3]*IBM Research Division, T.J. Watson Research Center, P.O. Box 218, Yorktown Heights, New York 10598*
(Received 9 January 1997; revised manuscript received 22 July 1997)

We propose an implementation of a universal set of one- and two-quantum-bit gates for quantum computation using the spin states of coupled single-electron quantum dots. Desired operations are effected by the gating of the tunneling barrier between neighboring dots. Several measures of the gate quality are computed within a recently derived spin master equation incorporating decoherence caused by a prototypical magnetic environment. Dot-array experiments that would provide an initial demonstration of the desired nonequilibrium spin dynamics are proposed. [S1050-2947(98)04501-6]

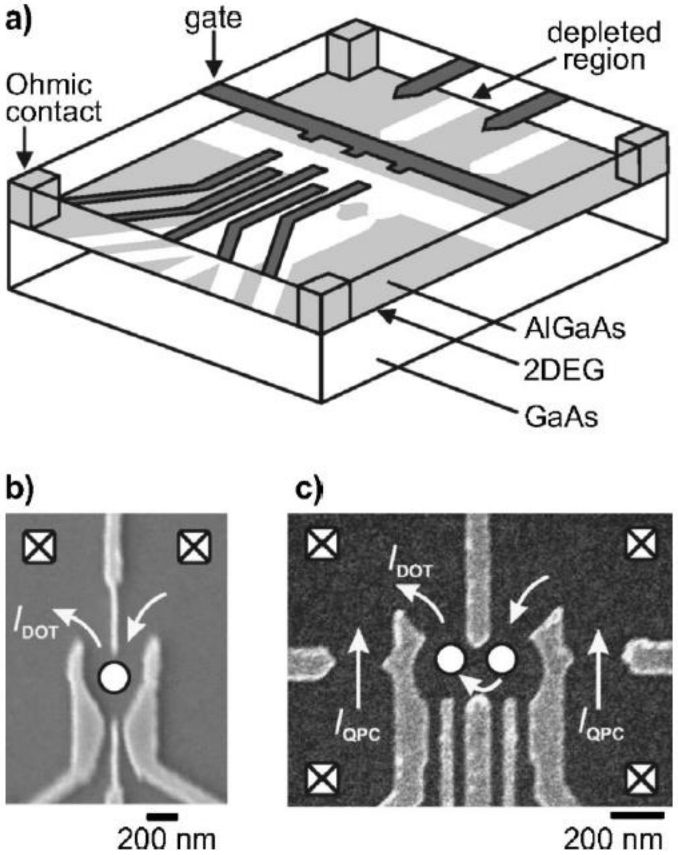

First realizations in GaAs/AlGaAs heterostructures

R. Hanson, L. Kouwenhoven, and J. Petta, Rev. Mod. ***79****, (2007).*

Singlet/Triplet qubit 2005

J. R. Petta, Science ***309****, 2180 (2005).*

Coherence : few tens of ns

Single spin Qubit 2006

F. H. L. Koppens, Nature ***442****, 766 (2006).*

Spins in semiconductor Quantum dot

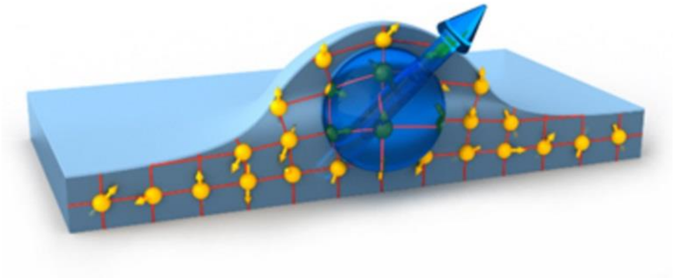

Hyperfine interaction limits coherence times in GaAs/AlGaAs

Decoupling sequences: Echo → T_2=1μs
CPMG→T_2=200 μs

III-V
No stable spin-free isotope

Si
^{28}Si (92.2%) S=0
^{29}Si (4.7%) S=1/2
^{30}Si (3.1%) S=0

Ge
^{70}Ge (20.4%) S=0
^{72}Ge (27.3%) S=0
^{73}Ge (7.8%) S=9/2
^{74}Ge (36.7%) S=0
^{76}Ge (7.8%) S=0

host	$\mathcal{N}_T$	$\mathcal{N}_S$	$\mathcal{A}$	$\delta\mathcal{A}$	T_2^*
GaAs	10^6	10^6	92 μeV (3.6 T)	92 neV	7.2 ns
Natural Si	10^5	5000	210 neV (1.85 mT)	3.0 neV	0.22 μs
100% ^{29}Si	10^5	10^5	4.3 μeV (37 mT)	13.6 neV	49 ns
0.01% ^{29}Si	10^5	10	0.43 neV (3.7 μT)	0.136 neV	4.9 μs

L. V. C. Assali,Phys. Rev. B ***83****, 165301 (2011).*

Spin qubit in purified silicon

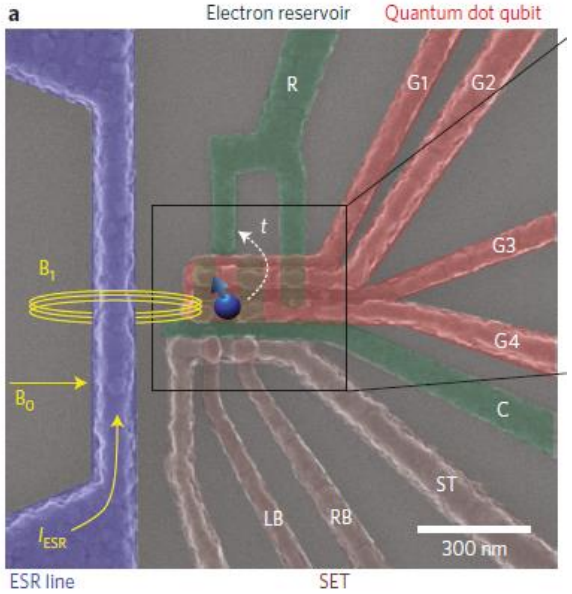

Si quantum dot in ^{28}Si (800ppm ^{29}Si

*M. Veldhorst, Nat. Nanotechnol. **9**, 981 (2014).*

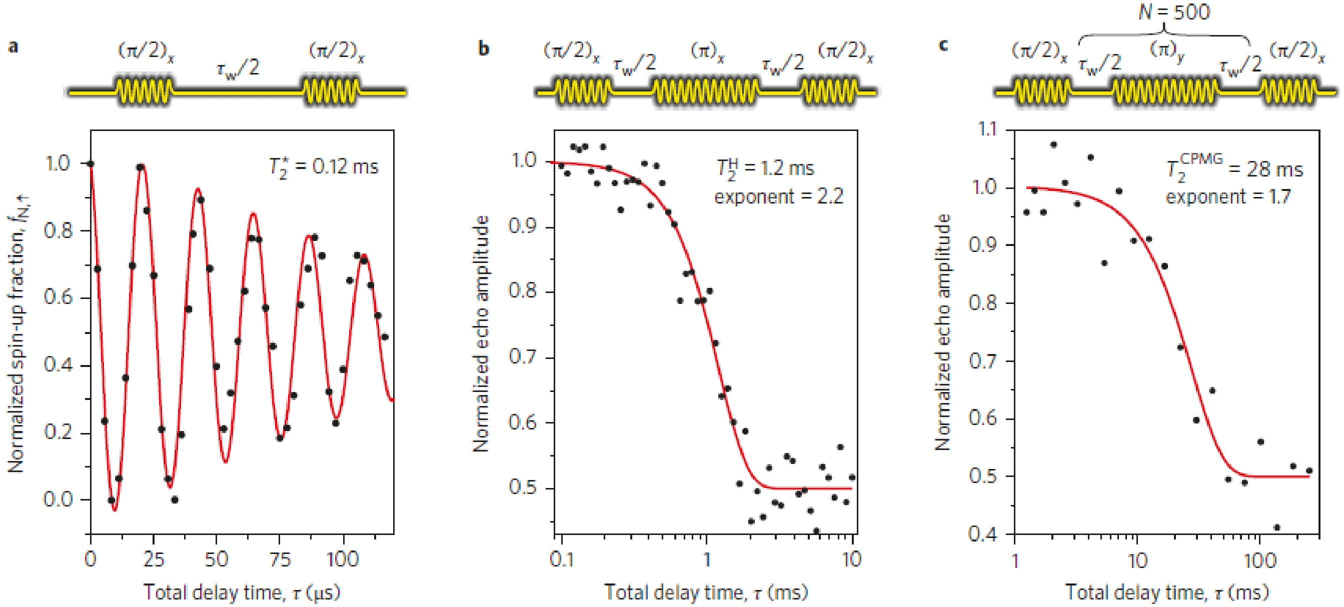

Spin qubit in purified silicon

Si quantum dot in ^{28}Si (800ppm ^{29}Si

M. Veldhorst, Nat. Nanotechnol. ***9****, 981 (2014).*

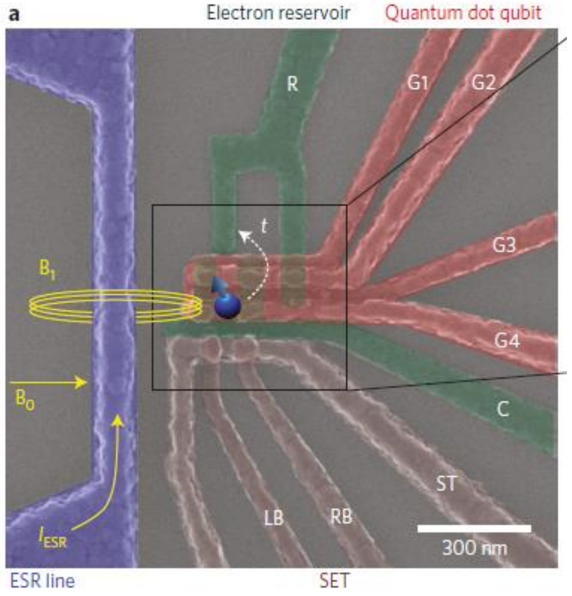

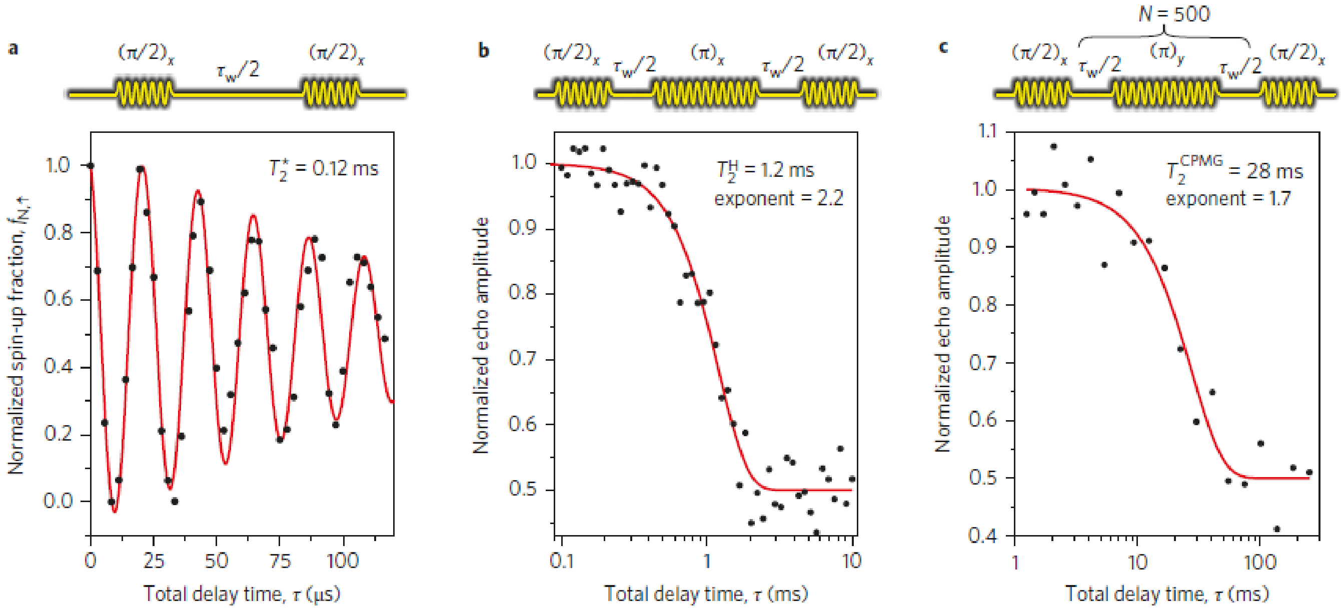

ESR line : bulky, addressability difficult, slow Rabi frequencies

Other means for spin resonance?

Magnetic field gradient

Electrically driven single-electron spin resonance in a slanting Zeeman field

Pioro-Ladriere, et al. Nature Phys. 4, 776 (2008)

Artificial Spin-Orbit Interaction

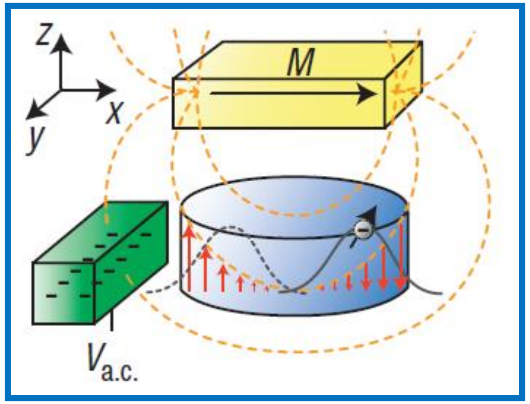

Magnetic field gradient

Electrically driven single-electron spin resonance in a slanting Zeeman field

Pioro-Ladriere, et al. Nature Phys. 4, 776 (2008)

Artificial Spin-Orbit Interaction

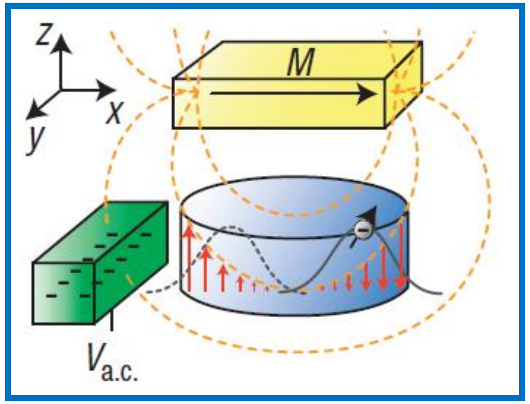

First demonstration in Silicon

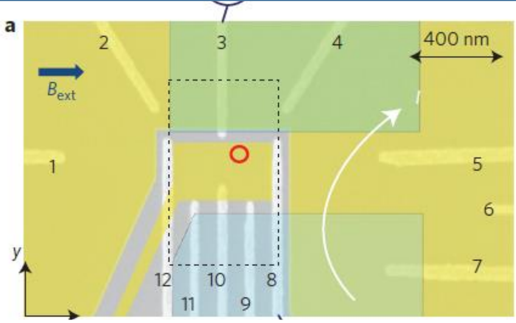

Kawakami, et al. Nature Nano. 9, 666 (2014)

99.9% Single Qubit Fidelity

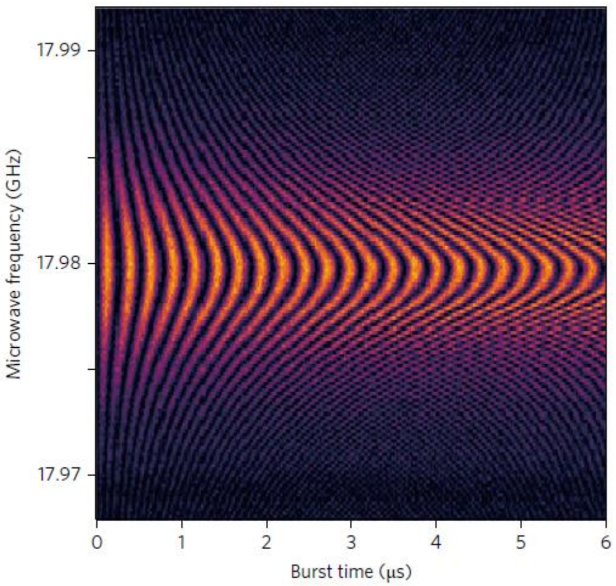

Yoneda et al. Nature Nano 13, 102 (2018)

6 Qubit Universal Control

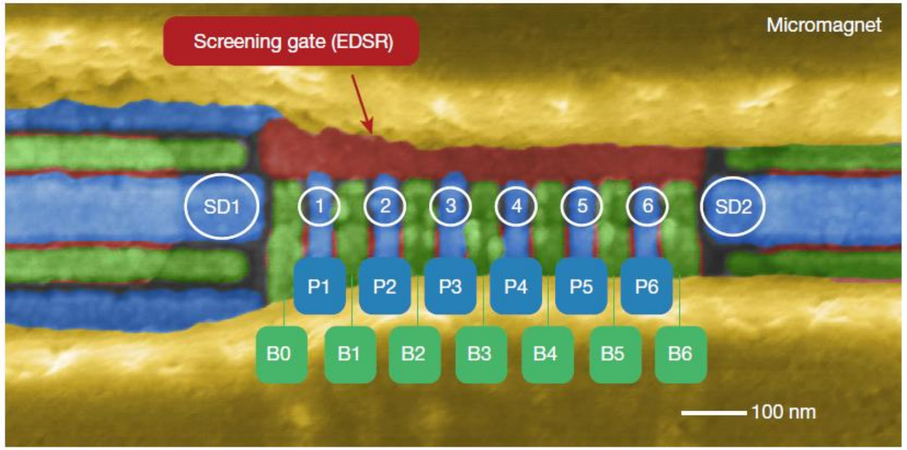

Philips et al. Nature 609, 919 (2022)

Intrinsic spin-orbit interaction

Intrinsic 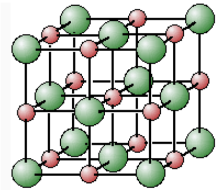

Band structure entangles $\vec{S}$ and $\vec{L}$ by spin-orbit interaction

Effective spin Hamiltonian : $H \ = \frac{1}{2}\mu_B{}^t\boldsymbol{\sigma} \cdot \hat{g} \cdot \boldsymbol{B}$

$$\hat{g} = \begin{bmatrix} g_{xx} & g_{yx} & g_{zx} \\ g_{xy} & g_{yy} & g_{zy} \\ g_{xz} & g_{yz} & g_{zz} \end{bmatrix}$$

Intrinsic spin-orbit interaction

Intrinsic

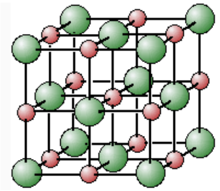

Band structure entangles $\vec{S}$ and $\vec{L}$ by spin-orbit interaction

Effective spin Hamiltonian : $H = \frac{1}{2}\mu_B {}^t\boldsymbol{\sigma} \cdot \hat{g} \cdot \boldsymbol{B}$

$$\hat{g} = \begin{bmatrix} g_{xx} & g_{yx} & g_{zx} \\ g_{xy} & g_{yy} & g_{zy} \\ g_{xz} & g_{yz} & g_{zz} \end{bmatrix}$$

Modulation of the spin precession vector

↓

Spin Resonance

Intrinsic spin-orbit interaction

Intrinsic

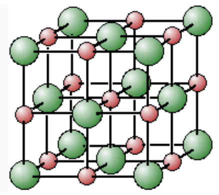

Band structure entangles $\vec{S}$ and $\vec{L}$ by spin-orbit interaction

Effective spin Hamiltonian : $H = \frac{1}{2}\mu_B {}^t\boldsymbol{\sigma} \cdot \hat{g} \cdot \boldsymbol{B}$

$$\hat{g} = \begin{bmatrix} g_{xx} & g_{yx} & g_{zx} \\ g_{xy} & g_{yy} & g_{zy} \\ g_{xz} & g_{yz} & g_{zz} \end{bmatrix}$$

Modulation of g-matrix

↓

Spin Resonance

Gigahertz Electron Spin Manipulation Using Voltage-Controlled g-Tensor Modulation

Y. Kato,[1,2] R. C. Myers,[1] D. C. Driscoll,[1] A. C. Gossard,[1] J. Levy,[1,2] D. D. Awschalom[1,2*]

Science 2003

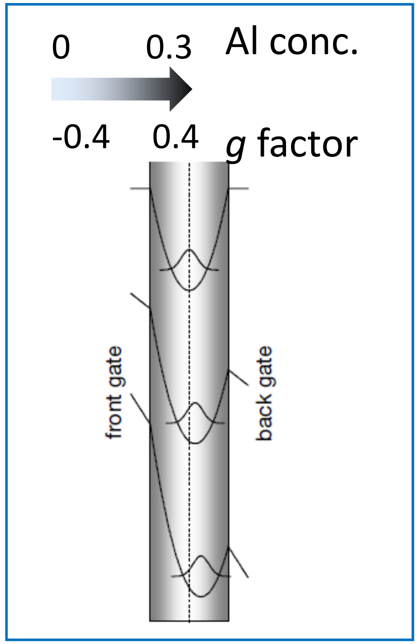

or

Gate voltage dependent confinement

Intrinsic spin-orbit interaction

Intrinsic

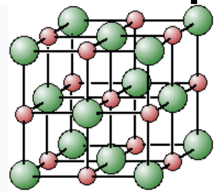

Band structure entangles $\vec{S}$ and $\vec{L}$ by spin-orbit interaction

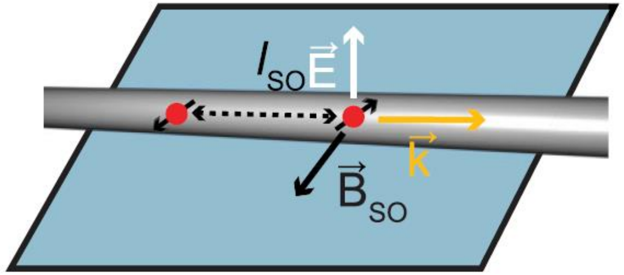

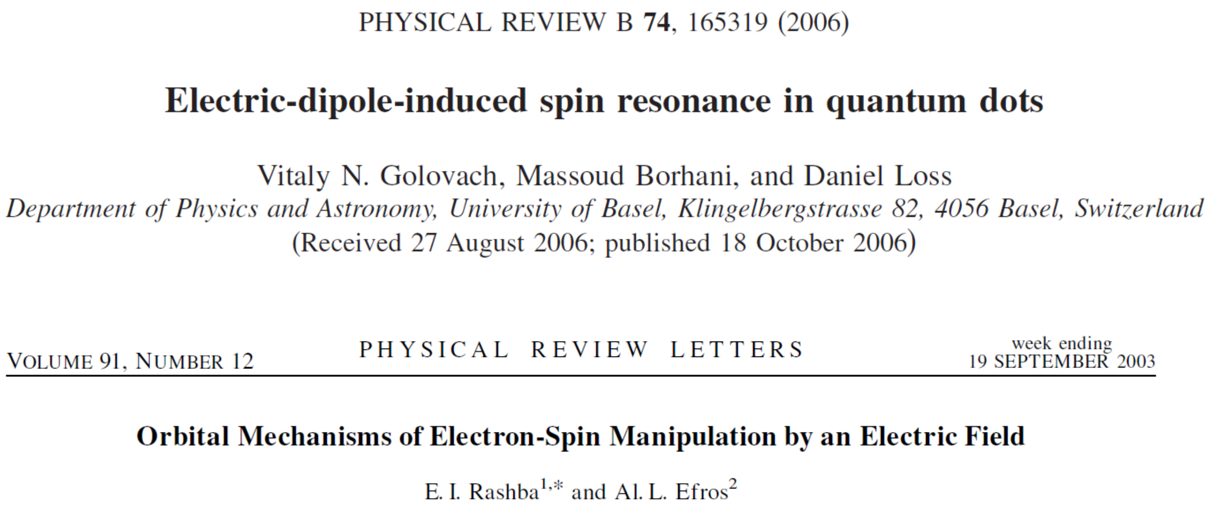

PHYSICAL REVIEW B **74**, 165319 (2006)

Electric-dipole-induced spin resonance in quantum dots

Vitaly N. Golovach, Massoud Borhani, and Daniel Loss
Department of Physics and Astronomy, University of Basel, Klingelbergstrasse 82, 4056 Basel, Switzerland
(Received 27 August 2006; published 18 October 2006)

VOLUME 91, NUMBER 12 PHYSICAL REVIEW LETTERS week ending 19 SEPTEMBER 2003

Orbital Mechanisms of Electron-Spin Manipulation by an Electric Field

E. I. Rashba[1,*] and Al. L. Efros[2]

Intrinsic spin-orbit interaction

Intrinsic

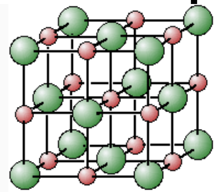

Band structure entangles $\vec{S}$ and $\vec{L}$ by spin-orbit interaction

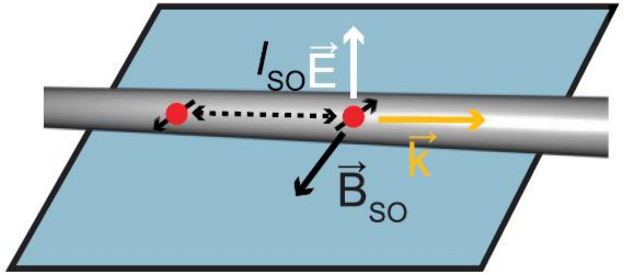

PHYSICAL REVIEW B **74**, 165319 (2006)

Electric-dipole-induced spin resonance in quantum dots

Vitaly N. Golovach, Massoud Borhani, and Daniel Loss
Department of Physics and Astronomy, University of Basel, Klingelbergstrasse 82, 4056 Basel, Switzerland
(Received 27 August 2006; published 18 October 2006)

VOLUME 91, NUMBER 12 PHYSICAL REVIEW LETTERS week ending 19 SEPTEMBER 2003

Orbital Mechanisms of Electron-Spin Manipulation by an Electric Field

E. I. Rashba[1,*] and Al. L. Efros[2]

Moving the dot as a whole in a Spin-Orbit Field

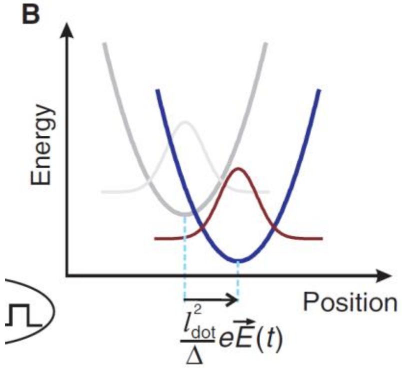

$$|\mathbf{B}_{\text{eff}}(t)| = 2\,|\mathbf{B}_{\text{ext}}|\,\frac{l_{\text{dot}}}{l_{\text{SO}}}\,\frac{e|\mathbf{E}(t)|l_{\text{dot}}}{\Delta}$$

GaAs

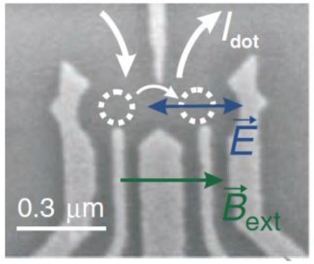

InAs

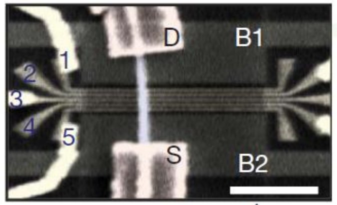

Nadj-Perge et al. Nature ***468****, 1084–1087 (2010)*

InSb with electron and hole

van den Berg, J. W. G. et al. Phys. Rev. Lett. ***110****, 66806 (2013)*

Pribiag, V. S. et al. Nat. Nanotechnol. ***8****, 170–174 (2013)*

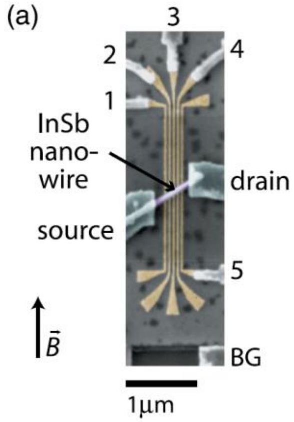

Outline

- Spin Qubits quick recap
- Hole spin in semiconductor
- Silicon-on- insulator nanowire devices
- Coherence “sweetspots”
- Spin-photon coupling

Holes

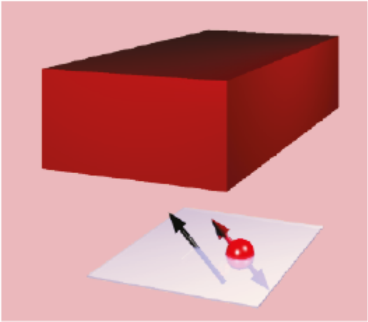

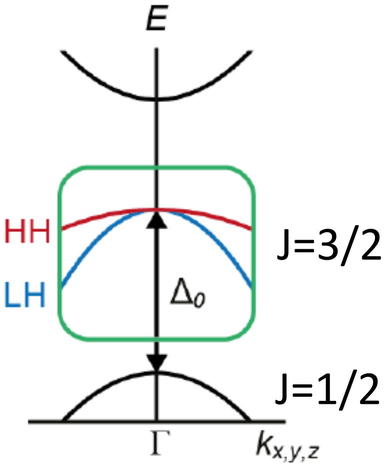

Bulk

Fang, Y., *et al.* Recent advances in hole-spin qubits. *Mater. Quantum Technol.* **3**, (2023).
Scappucci, G. *et al.* The germanium quantum information route. *Nat. Rev. Mater.* **6**, 926–943 (2021).

Holes

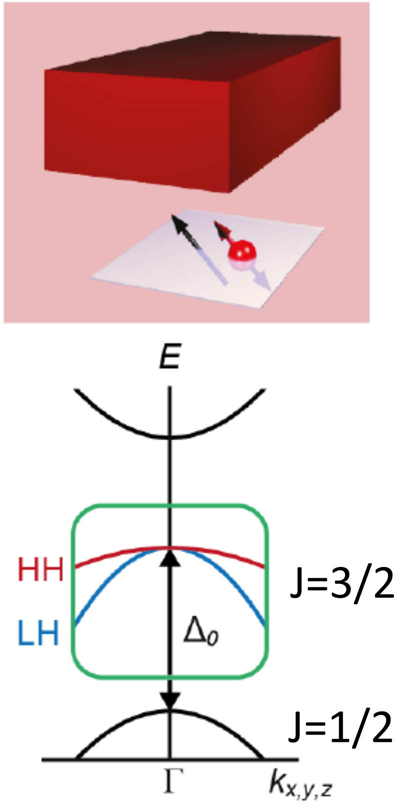

Bulk

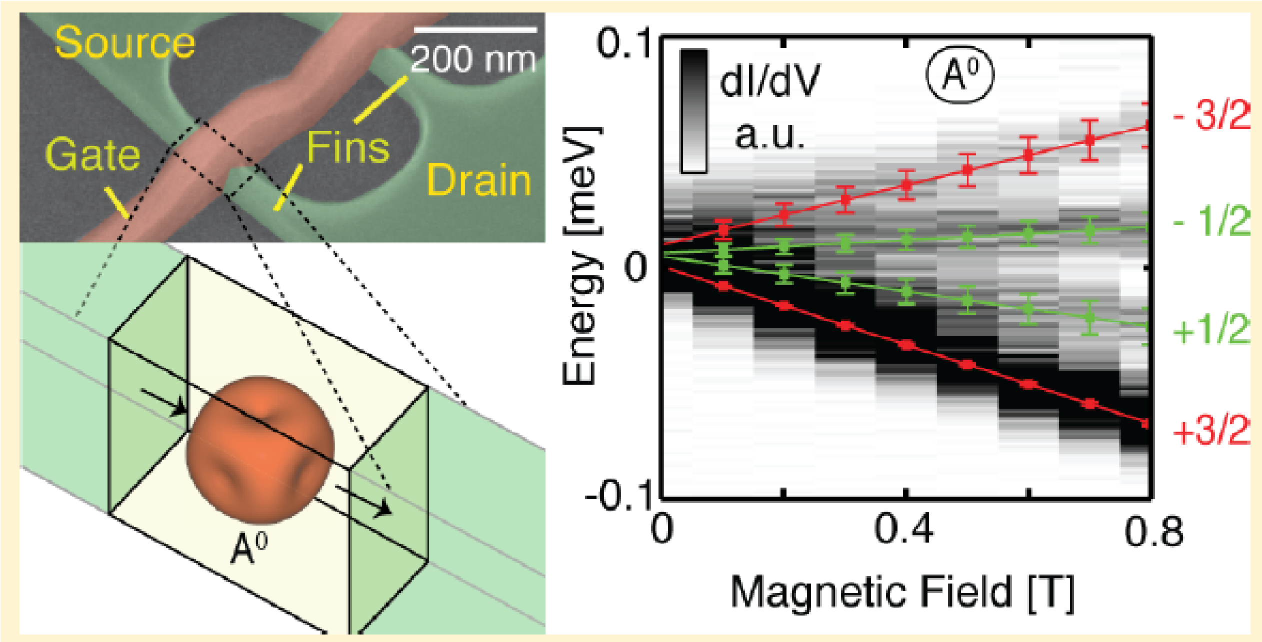

Single hole on a Boron Acceptor

Van Der Heijden, J. et al. Nano Lett. **14**, 1492–1496 (2014).

Fang, Y., *et al.* Recent advances in hole-spin qubits. *Mater. Quantum Technol.* **3**, (2023).
Scappucci, G. *et al.* The germanium quantum information route. *Nat. Rev. Mater.* **6**, 926–943 (2021).

Holes

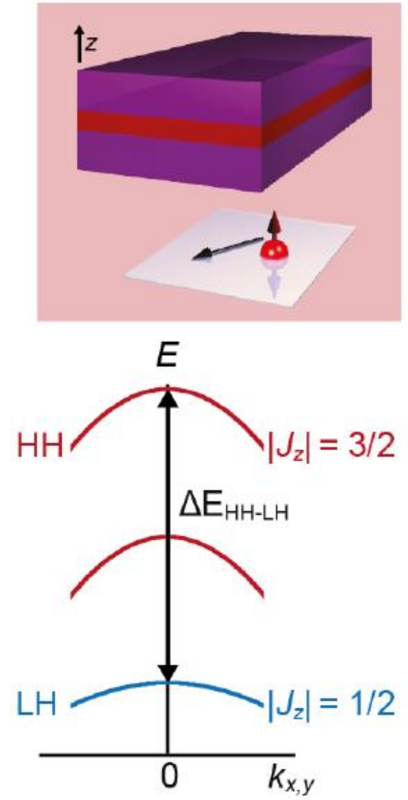

2D

Fang, Y., *et al.* Recent advances in hole-spin qubits. *Mater. Quantum Technol.* **3**, (2023).
Scappucci, G. *et al.* The germanium quantum information route. *Nat. Rev. Mater.* **6**, 926–943 (2021).

Holes

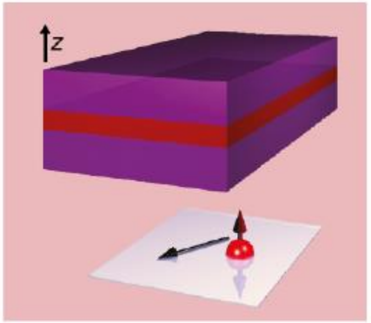

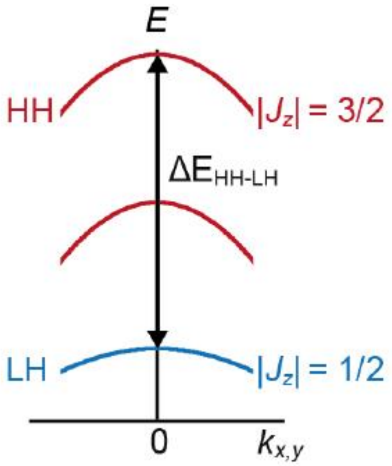

2D

Heavy Hole ground state

$$H = \frac{1}{2}\mu_B {}^t\boldsymbol{\sigma} \cdot \hat{g} \cdot \boldsymbol{B}$$

$$\mathbf{G} = \begin{bmatrix} \mathbf{0} & & \\ & \mathbf{0} & \\ & & \boldsymbol{6K} \end{bmatrix}$$

Spin is locked out-of-plane

Hendrickx et al. TU Delft

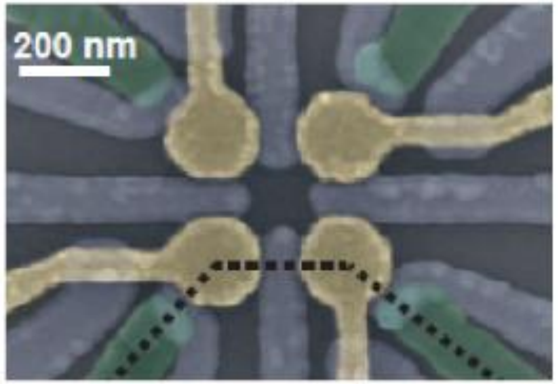

In-plane g-factor ~0.05-0.3
Out-of-plane g-factor ~ 7 - 15

Fang, Y., *et al.* Recent advances in hole-spin qubits. *Mater. Quantum Technol.* **3**, (2023).
Scappucci, G. *et al.* The germanium quantum information route. *Nat. Rev. Mater.* **6**, 926–943 (2021).

Holes

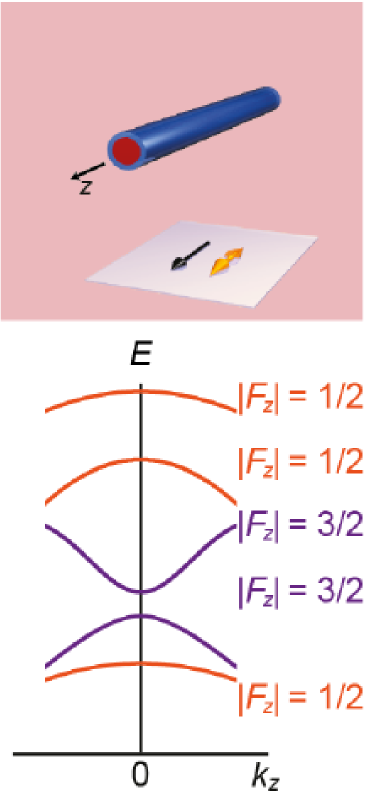

1D

Fang, Y., *et al.* Recent advances in hole-spin qubits. *Mater. Quantum Technol.* **3**, (2023).
Scappucci, G. *et al.* The germanium quantum information route. *Nat. Rev. Mater.* **6**, 926–943 (2021).

Holes

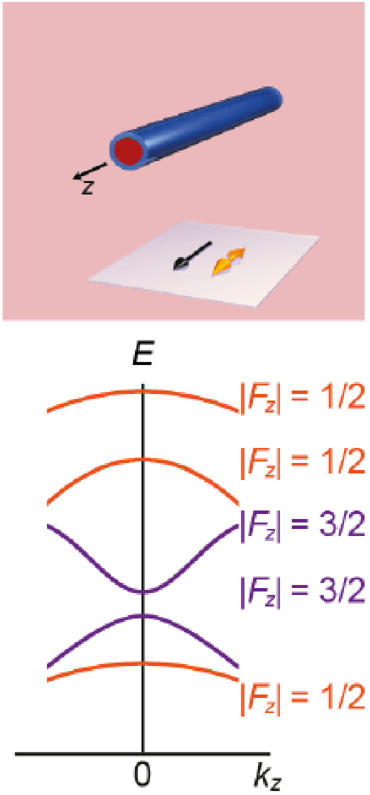

1D

Strong HH-LH mixing

$$H = \frac{1}{2}\mu_B {}^t\boldsymbol{\sigma} \cdot \hat{g} \cdot \boldsymbol{B}$$

$$\mathbf{G} = \begin{bmatrix} \boldsymbol{4K} & & \\ & \boldsymbol{4K} & \\ & & \boldsymbol{2K} \end{bmatrix}$$

Enhanced Rashba linear-in k Spin-Orbit Interaction

Spin-Orbit Length ~ 10-100nm

Kloeffel, C. et. al. Direct Rashba spin-orbit interaction in Si and Ge nanowires with different growth directions. *Phys. Rev. B* **97**, 235422 (2018).

Fang, Y., *et al.* Recent advances in hole-spin qubits. *Mater. Quantum Technol.* **3**, (2023).
Scappucci, G. *et al.* The germanium quantum information route. *Nat. Rev. Mater.* **6**, 926–943 (2021).

Hole spin qubits

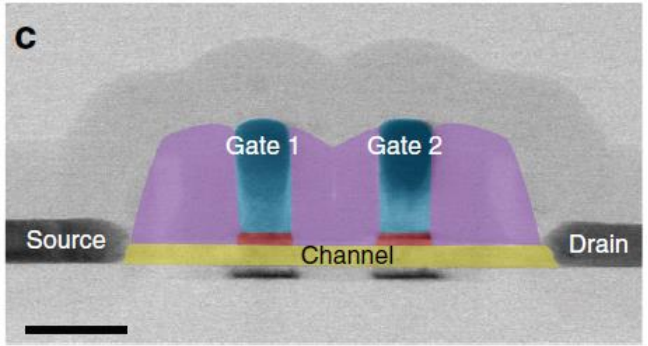

RM *et al. Nat. Commun.* **7**, 3–8 (2016)

Ge Hut Nanowire

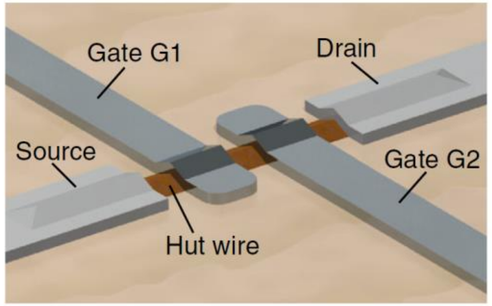

Watzinger, H. *et al. Nat. Commun.* **9**, 3902 (2018).

FinFET

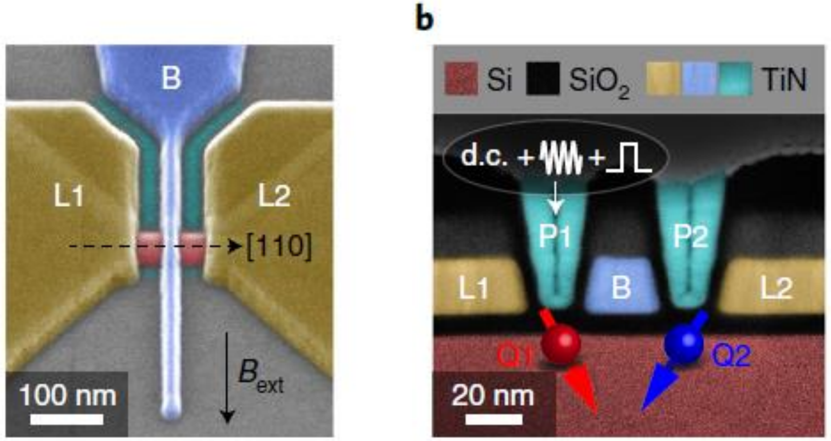

Camenzind, L. C. *et al. Nat. Electron.* (2022)

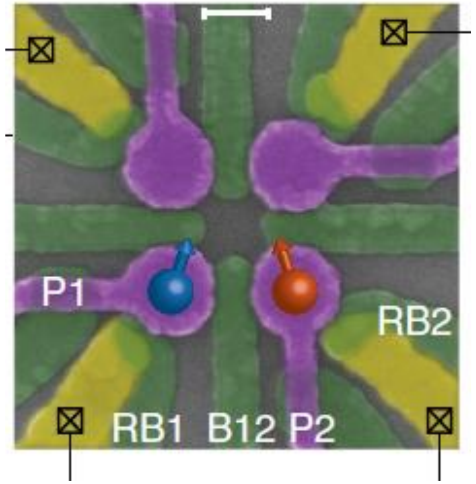

Hendrickx, N. W. *et al. Nat. Commun.* **11**, (2020).

- f_{Rabi} ~ 10 – 200 MHz
- T_2 ~ 10 ns – 5 µs

Ge/Si Nanowire

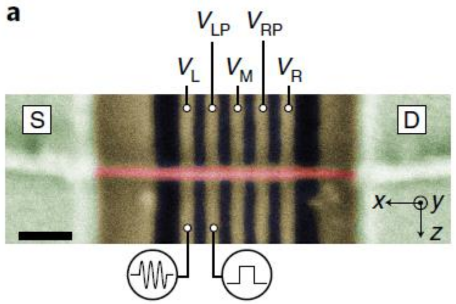

Froning, F. N. M. *Nat. Nanotechnol.* **16**, 308–312 (2021).

Outline

- Spin Qubits quick recap
- Hole spin in semiconductor
- Silicon-on- insulator nanowire devices
- Coherence “sweetspots”
- Spin-photon coupling

MOS technology for spin qubit

- 300mm SOI wafers
  T_{Si}/T_{BOx} = 10nm to 20nm/145nm
- Active mesa patterning
- Thermal oxidation
- Oxide/MG stack dep. & patterning
  5nm SiO_2/5nm TiN/50nm Poly Si
- Channel protection Spacers
  32nm SiN
- Raised S/D epi in-situ Boron doped
  18nm Si
- Salicide and back-end-of-line

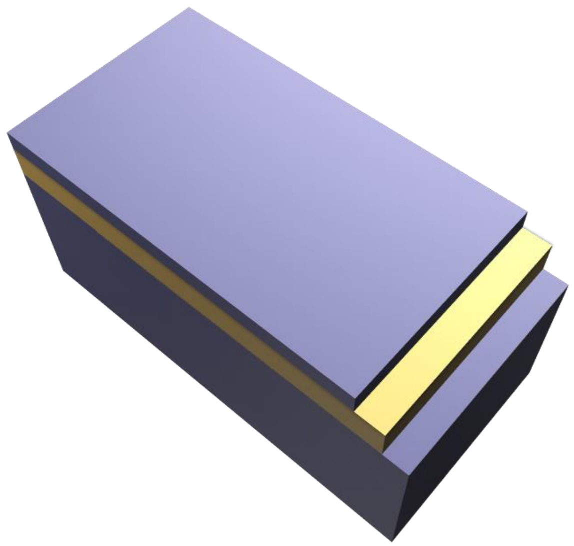

MOS technology for spin qubit

- 300mm SOI wafers
  T_{Si}/T_{BOx} = 12nm/145nm
- Active mesa patterning
- Thermal oxidation
- Oxide/MG stack dep. & patterning
  5nm SiO_2/5nm TiN/50nm Poly Si
- Channel protection Spacers
  32nm SiN
- Raised S/D epi in-situ Boron doped
  18nm Si
- Salicide and back-end-of-line

MOS technology for spin qubit

- 300mm SOI wafers
  T_{Si}/T_{BOx} = 12nm/145nm
- Active mesa patterning
- Thermal oxidation
- Oxide/MG stack dep. & patterning
  5nm SiO_2/5nm TiN/50nm Poly Si
- Channel protection Spacers
  32nm SiN
- Raised S/D epi in-situ Boron doped
  18nm Si
- Salicide and back-end-of-line

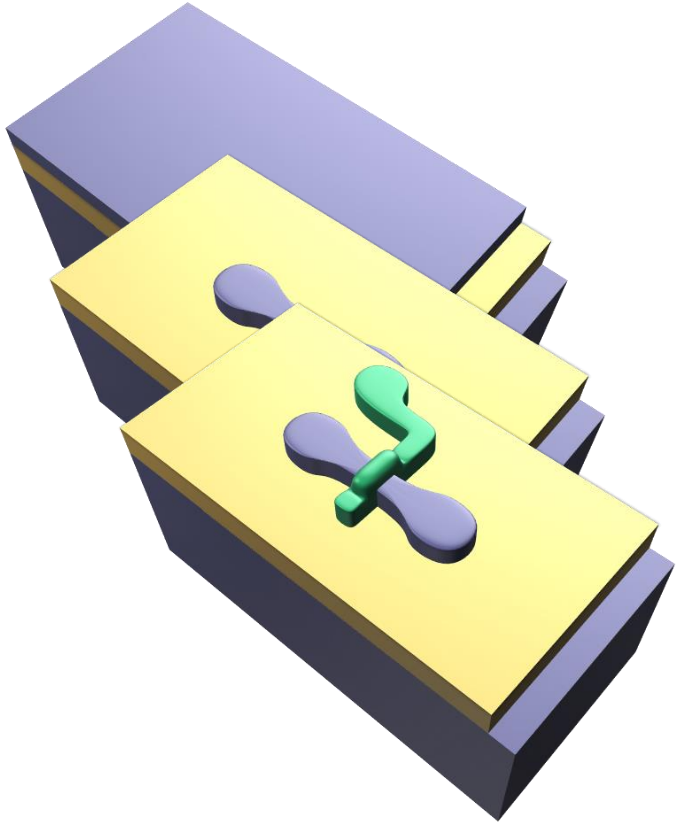

MOS technology for spin qubit

- 300mm SOI wafers
  T_{Si}/T_{BOx} = 12nm/145nm
- Active mesa patterning
- Thermal oxidation
- Oxide/MG stack dep. & patterning
  5nm SiO_2/5nm TiN/50nm Poly Si
- Channel protection Spacers
  32nm SiN
- Raised S/D epi in-situ Boron doped
  18nm Si
- Salicide and back-end-of-line

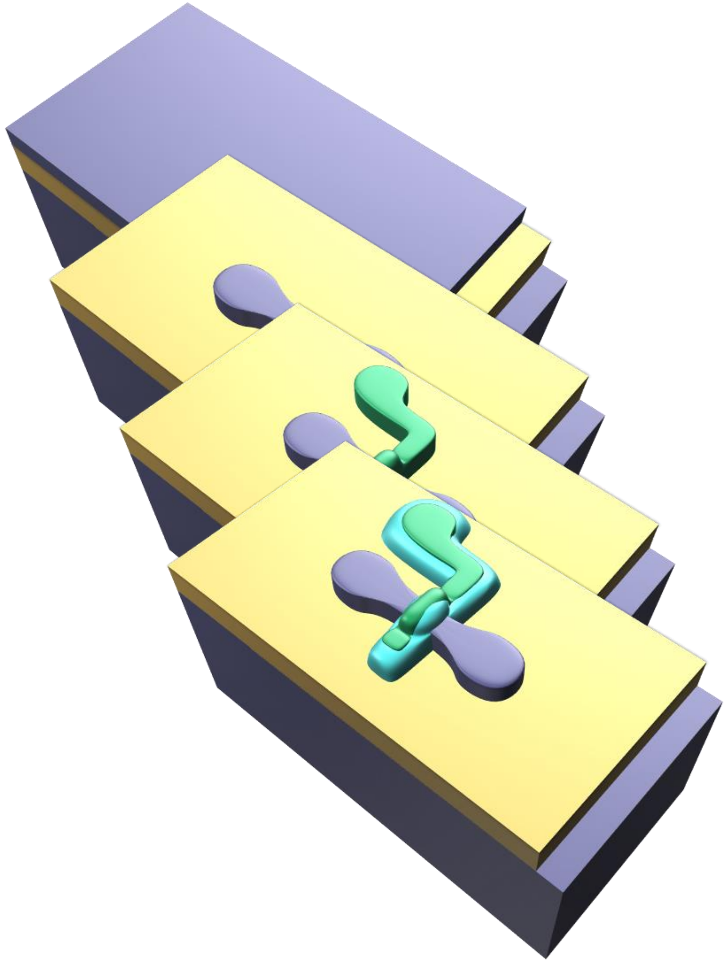

MOS technology for spin qubit

- 300mm SOI wafers
  T_{Si}/T_{BOx} = 12nm/145nm
- Active mesa patterning
- Thermal oxidation
- Oxide/MG stack dep. & patterning
  5nm SiO_2/5nm TiN/50nm Poly Si
- Channel protection Spacers
  32nm SiN
- Raised S/D epi in-situ Boron doped
  18nm Si
- Salicide and back-end-of-line

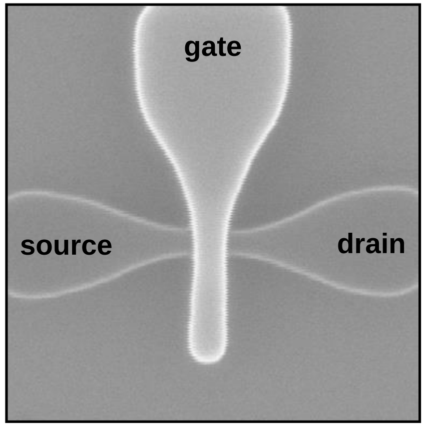

Silicon-on-Insulator trigate nanowire transistor

S. Barraud IEEE 33, 1526 (2012)

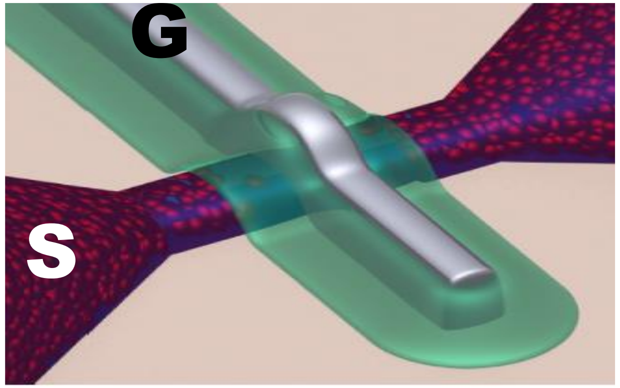

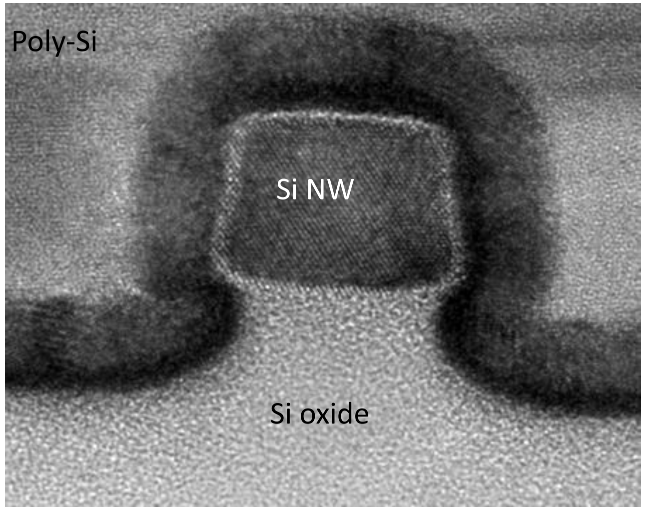

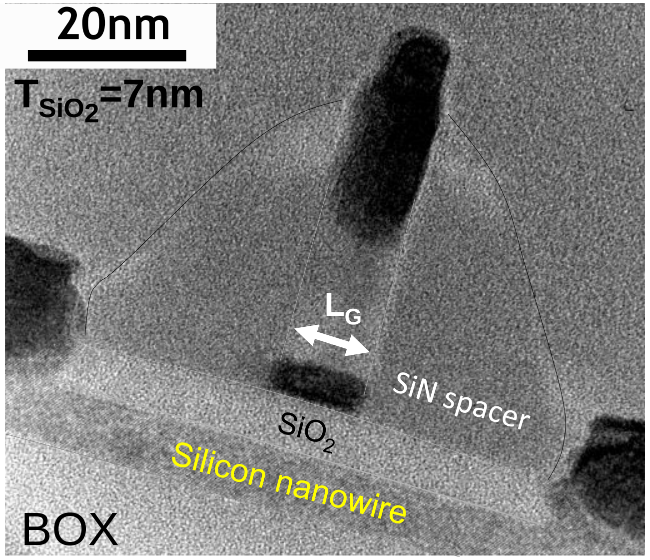

Outline

- Spin Qubits manipulation quick recap
- Holes / Spin-Orbit Interaction
- Silicon-on- insulator nanowire devices
- Coherence “sweetspots”
- Spin-photon coupling

N. Piot[1,5], B. Brun[1,5]✉, V. Schmitt[1], S. Zihlmann[1], V. P. Michal[2], A. Apra[1], J. C. Abadillo-Uriel[2], X. Jehl[1], B. Bertrand[3], H. Niebojewski[3], L. Hutin[3], M. Vinet[3], M. Urdampilleta[4], T. Meunier[4], Y.-M. Niquet[2], R. Maurand[1]✉ and S. De Franceschi[1]✉

A single hole spin with enhanced coherence in natural silicon

Nat. Nanotechnol. 17, 1072–1077 (2022)

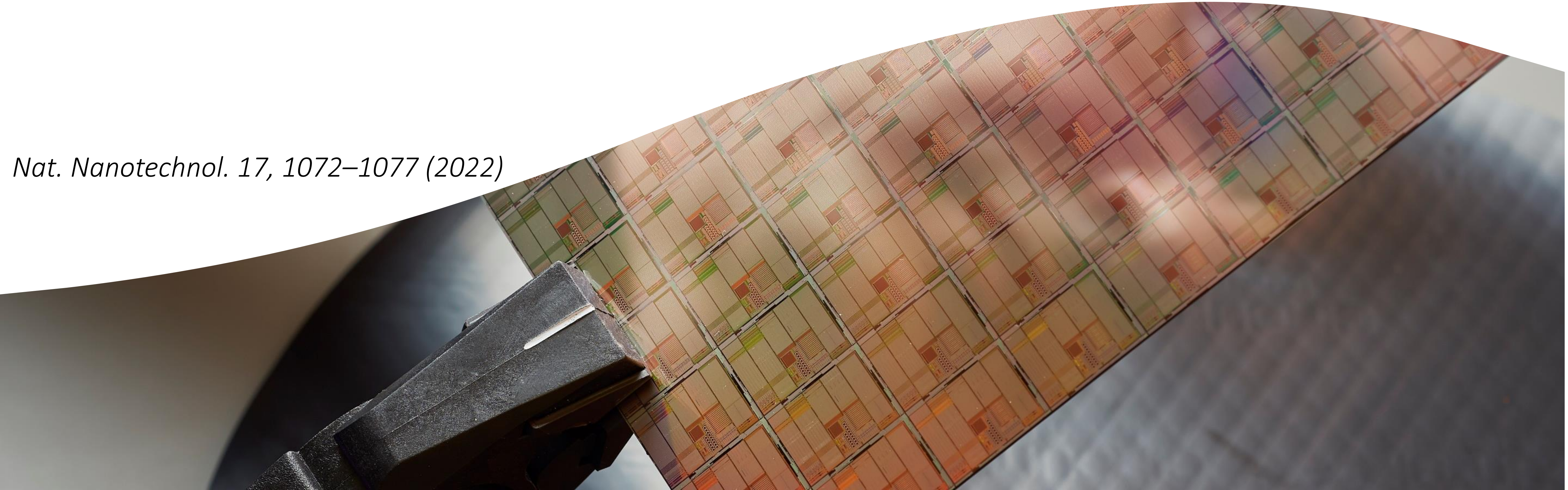

Fast single shot of the first hole in CMOS device

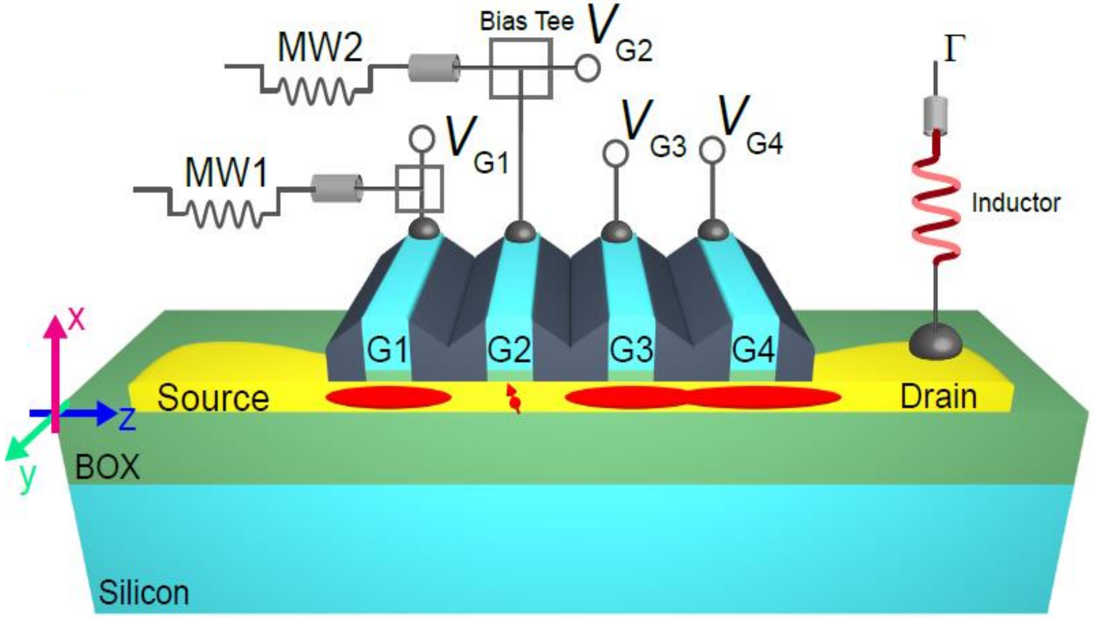

$W = 100\ nm$ $L_g = 40\ nm$ $S_h = 40\ nm$

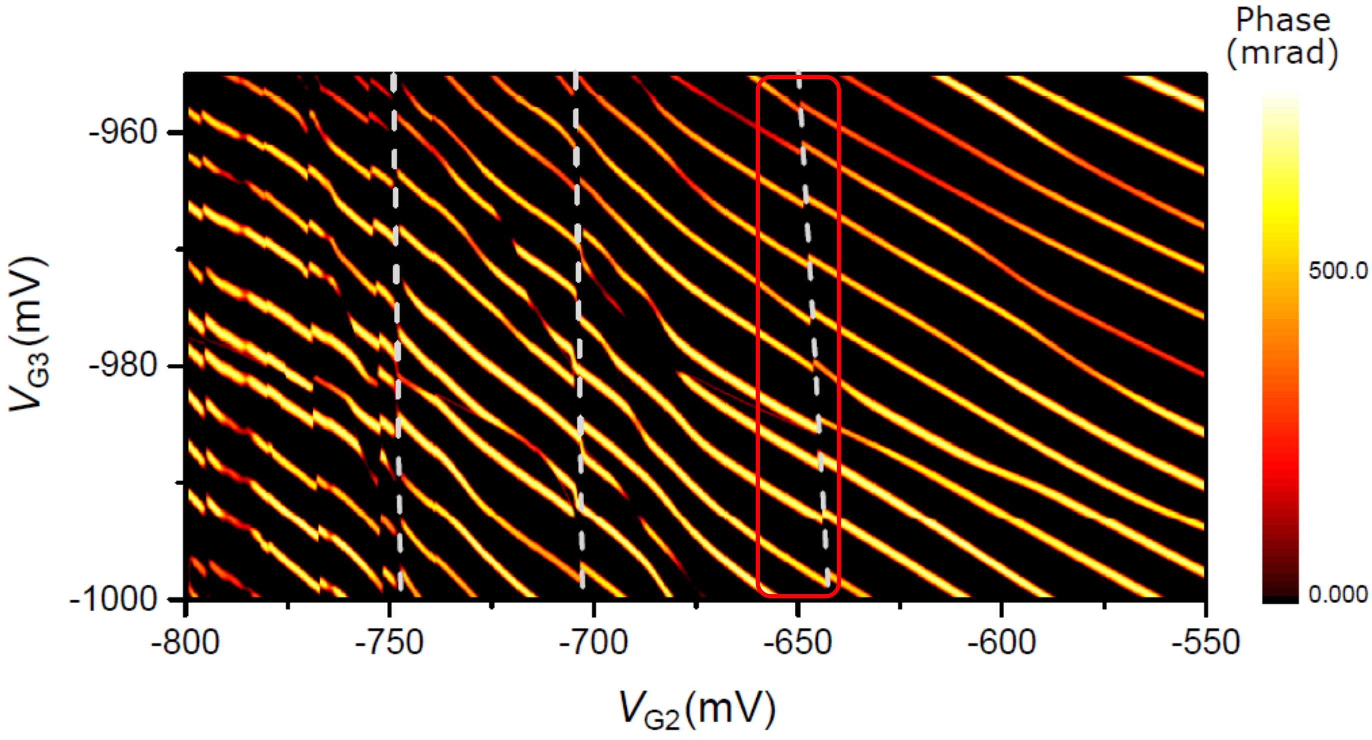

Gyromagnetic factor characterization

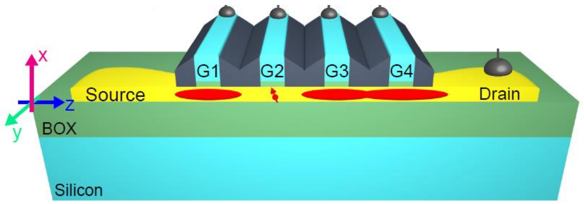

Effective spin Hamiltonian : $H = \frac{1}{2}\mu_B{}^t\boldsymbol{\sigma} \cdot \hat{g} \cdot \boldsymbol{B}$

$$\hat{g} = \begin{bmatrix} g_{\boldsymbol{xx}} & g_{\boldsymbol{yx}} & g_{\boldsymbol{zx}} \\ g_{\boldsymbol{xy}} & g_{\boldsymbol{yy}} & g_{\boldsymbol{zy}} \\ g_{\boldsymbol{xz}} & g_{\boldsymbol{yz}} & g_{\boldsymbol{zz}} \end{bmatrix}$$

Zwanenburg, F. A Nano Lett. ***9****, 1071–1079 (2009).*
Ares, N. Phys. Rev. Lett. ***110****, 46602 (2013).*
Bogan, A. et al. Phys. Rev. Lett. ***118****, 1–5 (2017).*
Liles, S. D. et al. Phys. Rev. B ***104****, 235303 (2021).*
Tanttu, T. et al. Phys. Rev. X ***9****, 21028 (2019).*

Gyromagnetic factor characterization

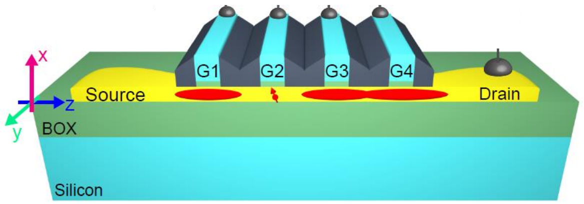

Effective spin Hamiltonian : $H = \frac{1}{2}\mu_B {}^t\boldsymbol{\sigma} \cdot \hat{g} \cdot \boldsymbol{B}$

$$\hat{g} = \begin{bmatrix} g_{xx} & g_{yx} & g_{zx} \\ g_{xy} & g_{yy} & g_{zy} \\ g_{xz} & g_{yz} & g_{zz} \end{bmatrix}$$

Zwanenburg, F. A Nano Lett. ***9****, 1071–1079 (2009).*
Ares, N. Phys. Rev. Lett. ***110****, 46602 (2013).*
Bogan, A. et al. Phys. Rev. Lett. ***118****, 1–5 (2017).*
Liles, S. D. et al. Phys. Rev. B ***104****, 235303 (2021).*
Tanttu, T. et al. Phys. Rev. X ***9****, 21028 (2019).*

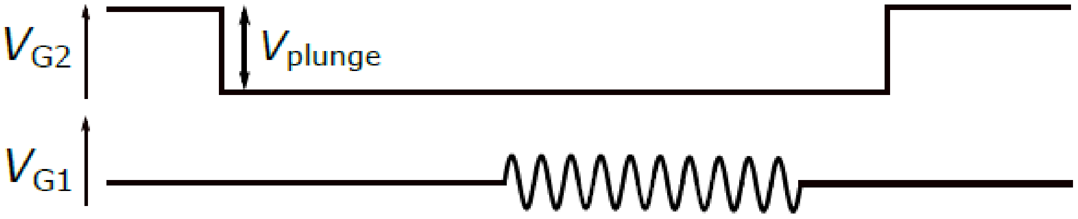

$$f_{larmor} = \frac{g^* \mu_B B}{h} = F_{MW1}$$

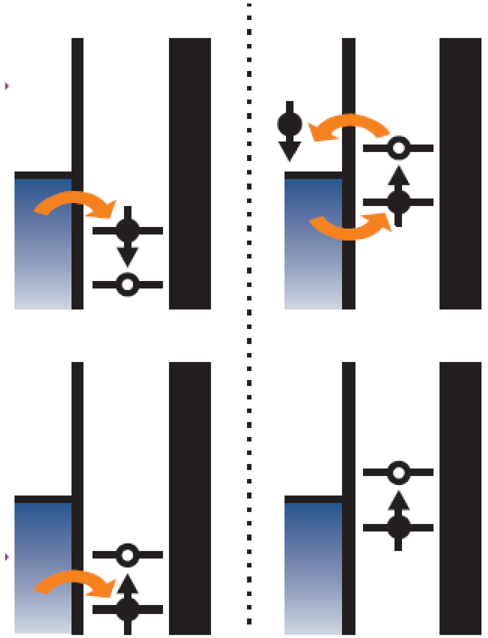

Elzermann Nature 2003

Gyromagnetic factor characterization

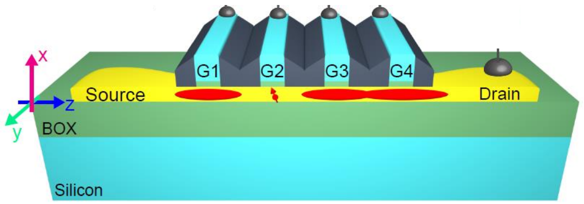

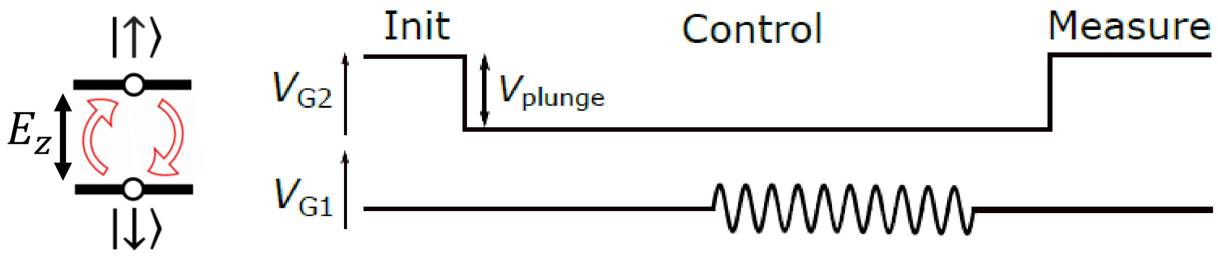

$g^* (\boldsymbol{B})$

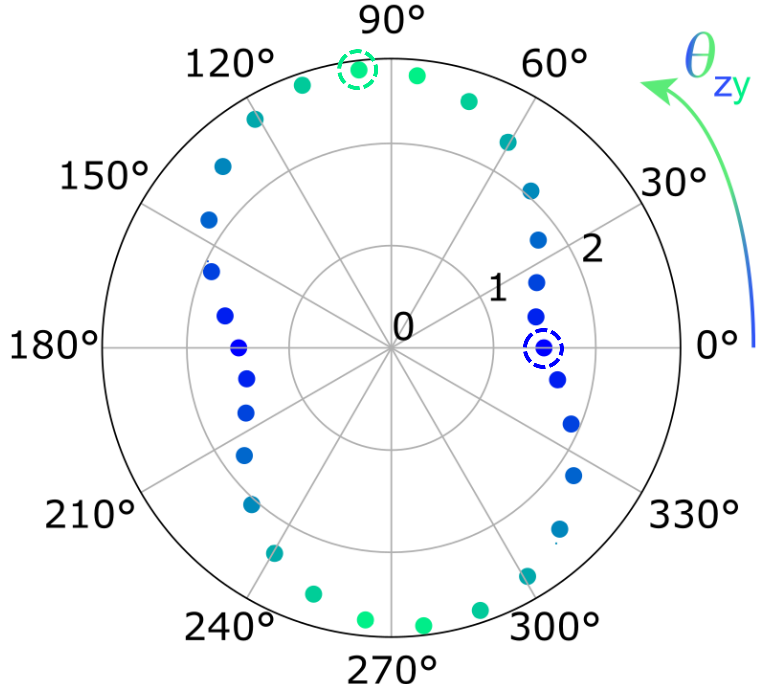

In plane : ⊥ the wire

$g_y^*(\theta_{zy} = 99°) \approx 2.7$

In plane : Along the wire

$g_z^*(\theta_{zy} = 0°) \approx 1.5$

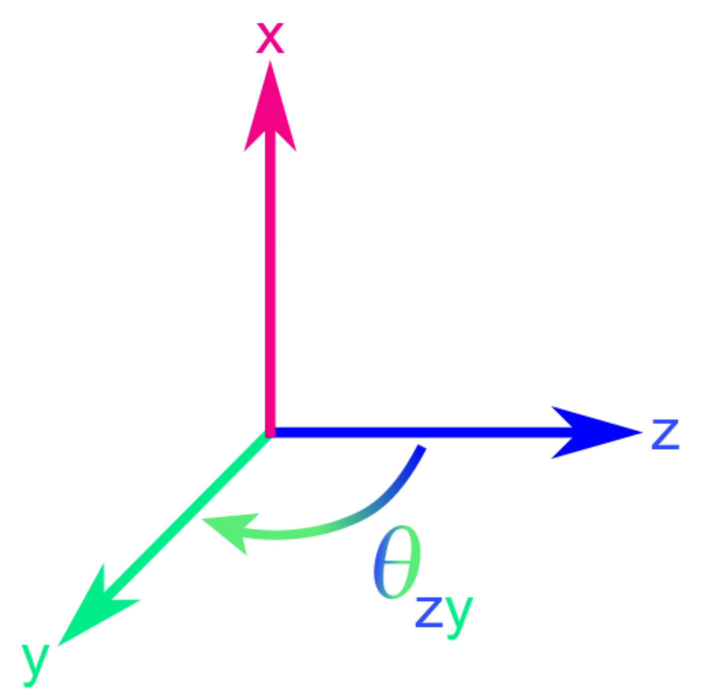

Gyromagnetic factor characterization

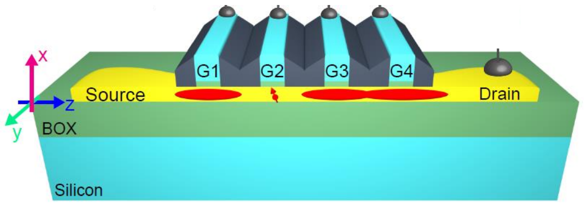

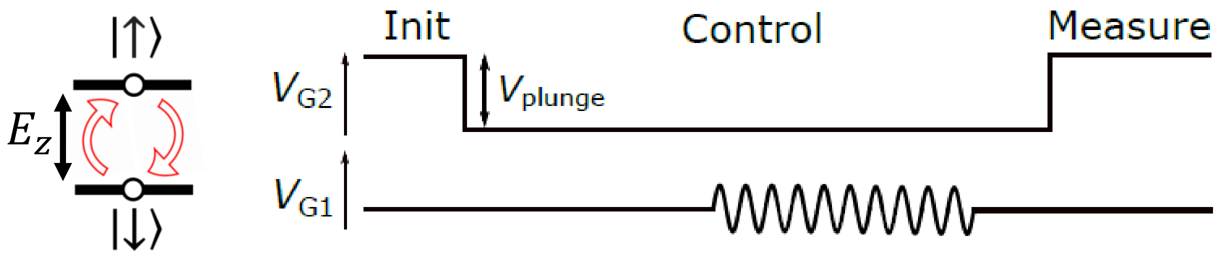

$g^*(\boldsymbol{B})$

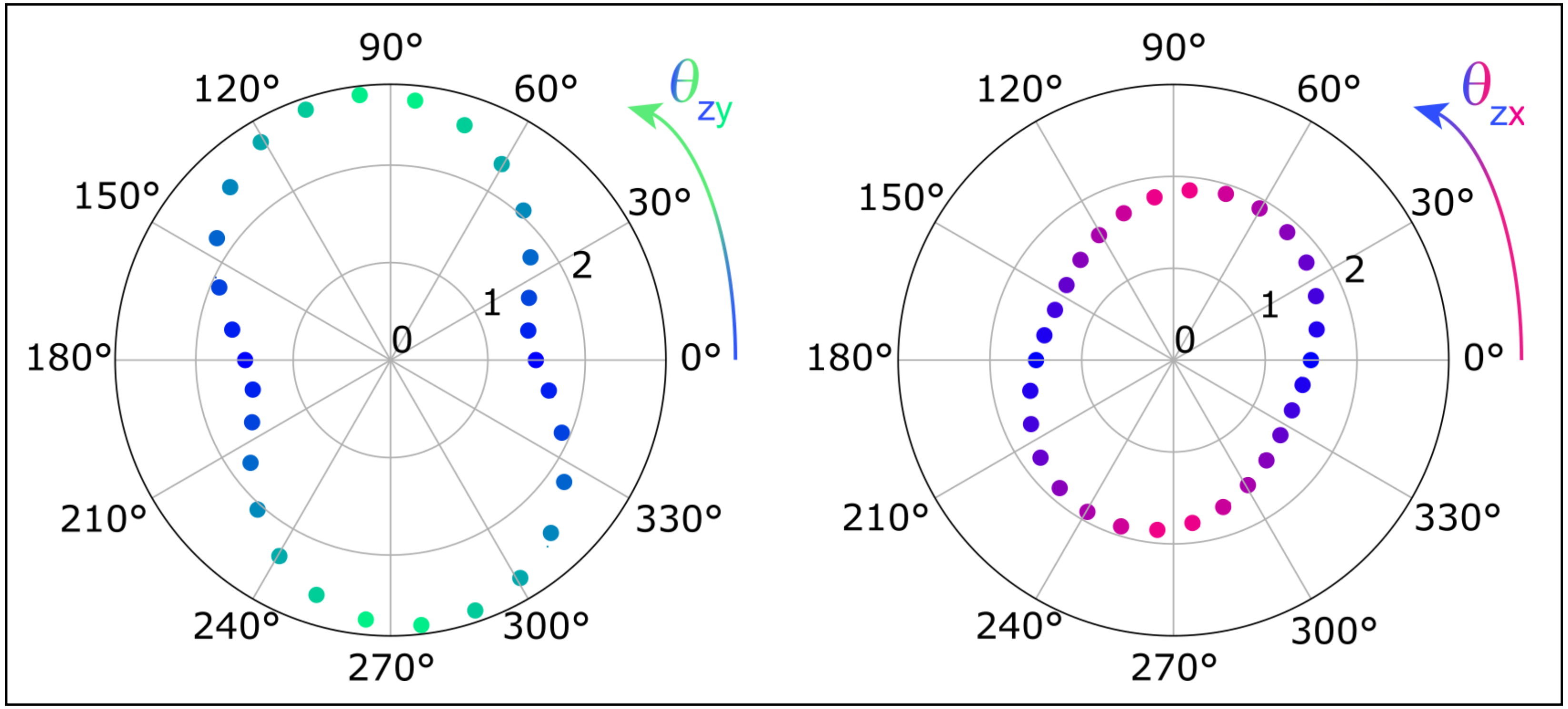

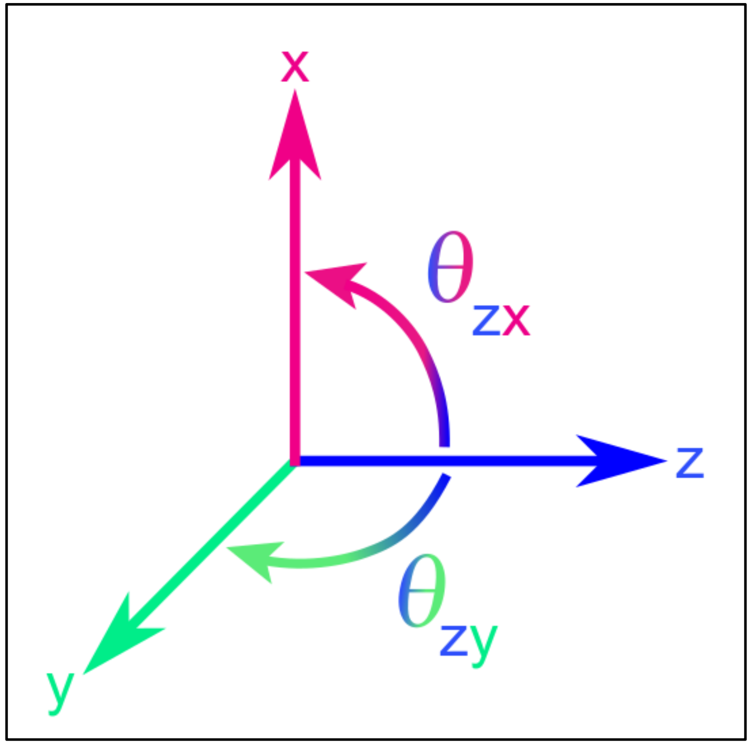

Gyromagnetic factor characterization

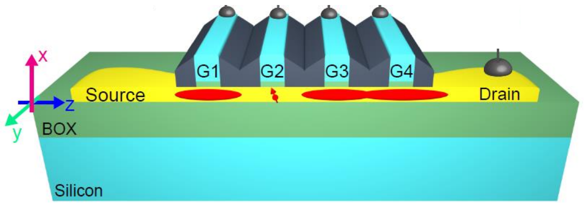

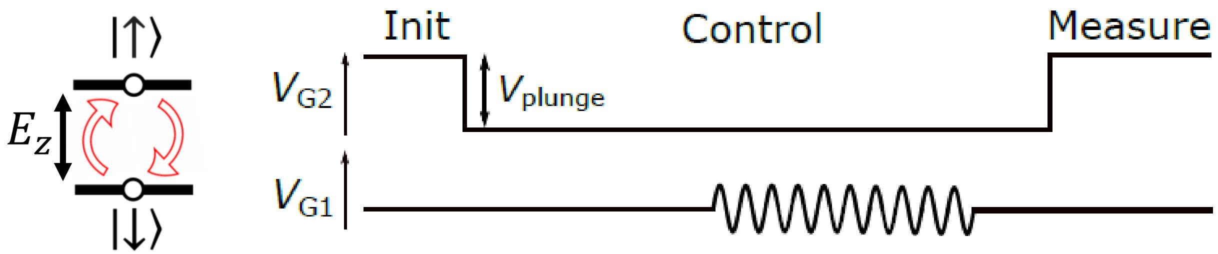

$g^* (\boldsymbol{B})$

Y.M. Niquet's group, CEA-Grenoble

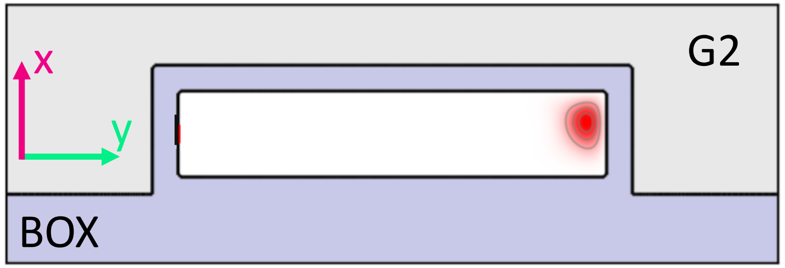

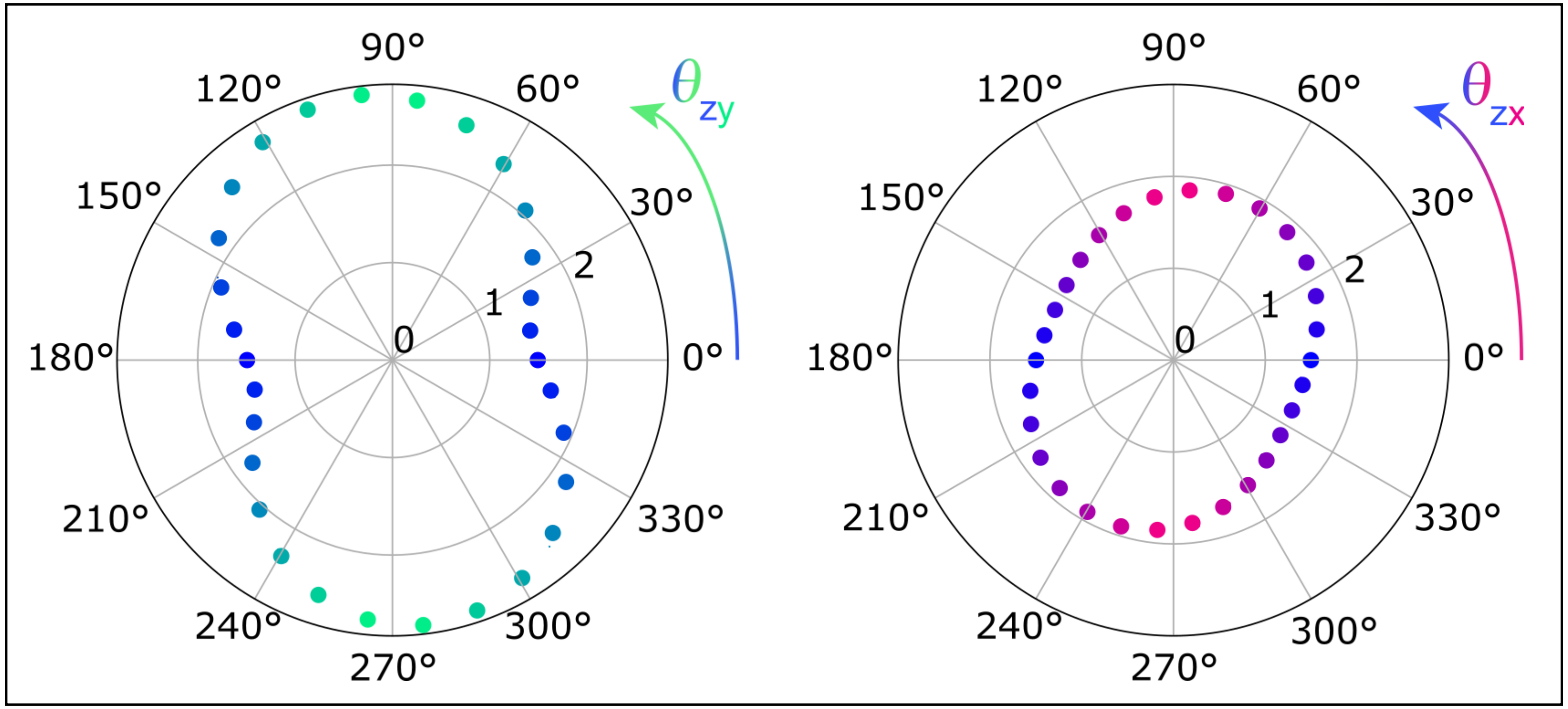

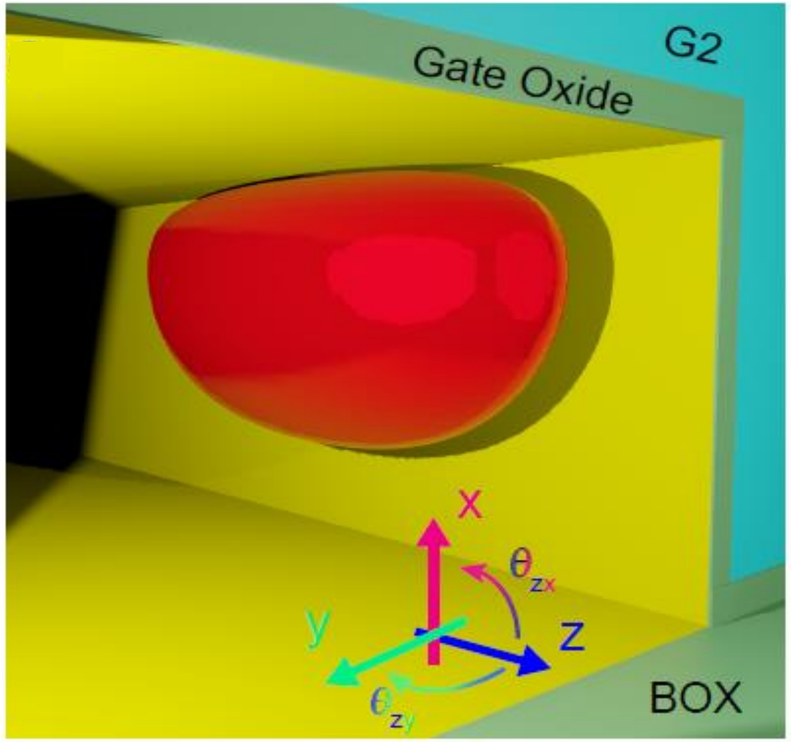

Gyromagnetic factor characterization

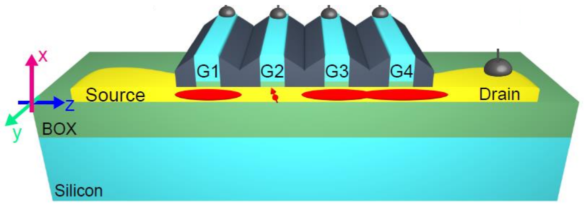

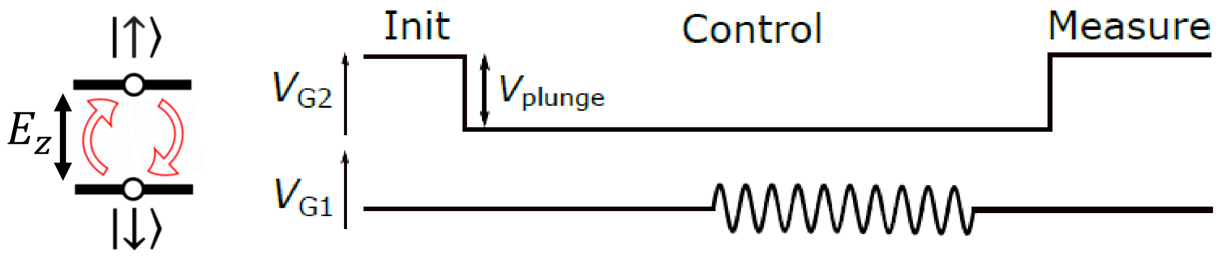

$g^* (\boldsymbol{B})$

Y.M. Niquet's group, CEA-Grenoble

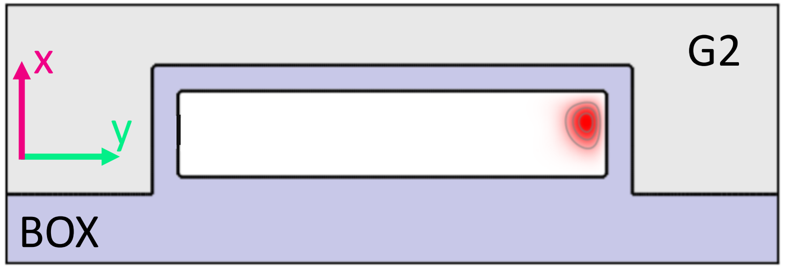

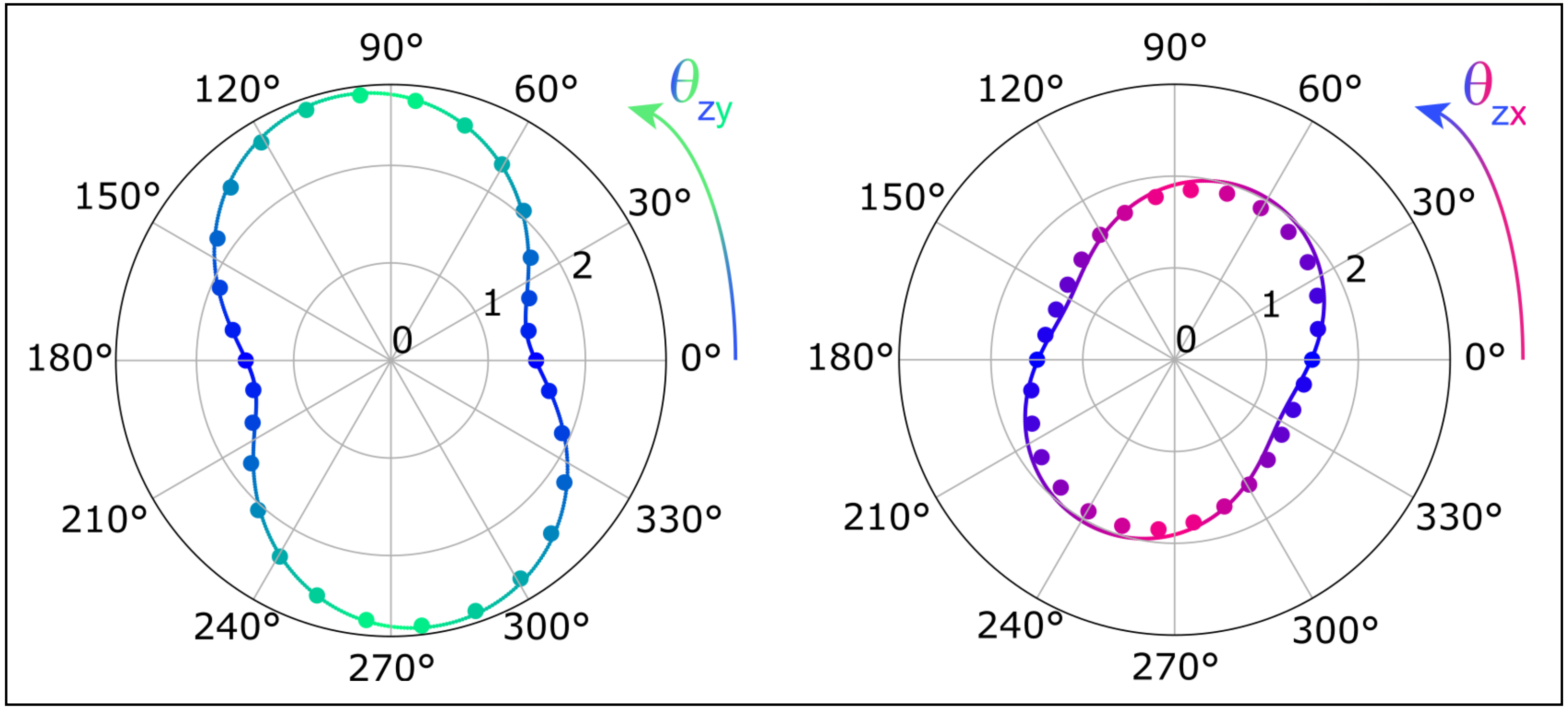

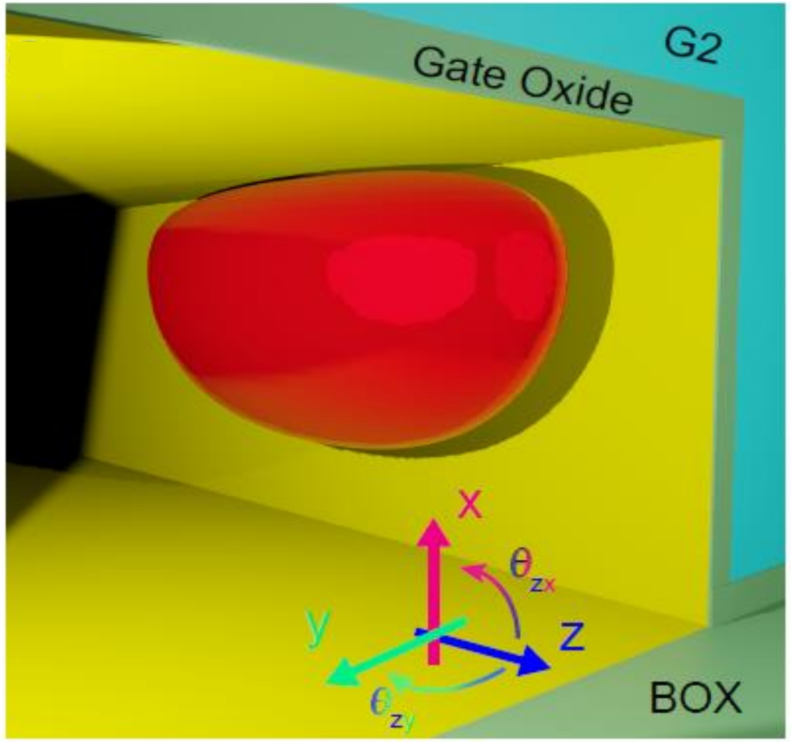

Complex response to electric driving field

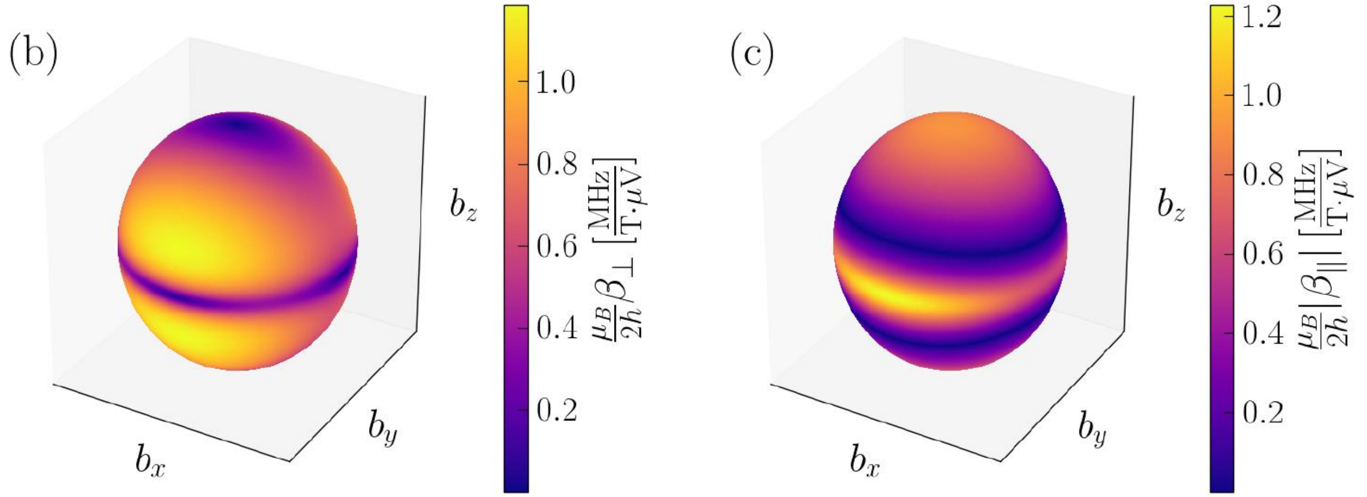

Michal, V *et al. Phys.Rev. B* 107, L041303 (2023)

Transverse and Longitudinal coupling strength depends on the B-field orientation

Complex response to EDSR driving field

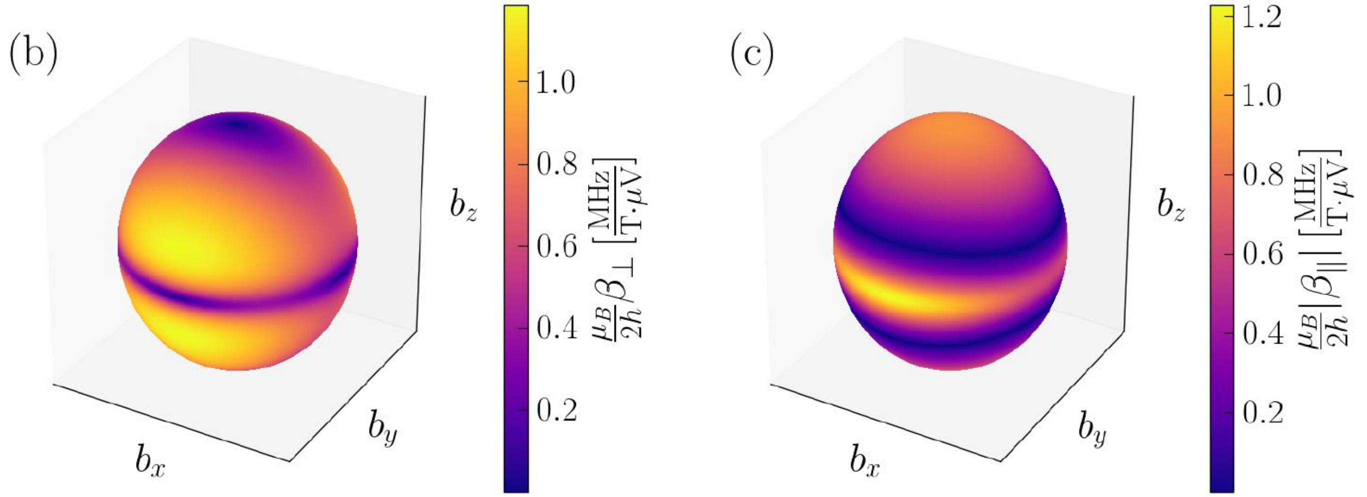

Michal, V *et al. Phys.Rev. B* 107, L041303 (2023)

Transverse and Longitudinal coupling strength depends on the B-field orientation

Can we find operation sweet spots?
i.e. Zero Longitudinal Coupling

Longitudinal spin electric susceptibility (LSES)

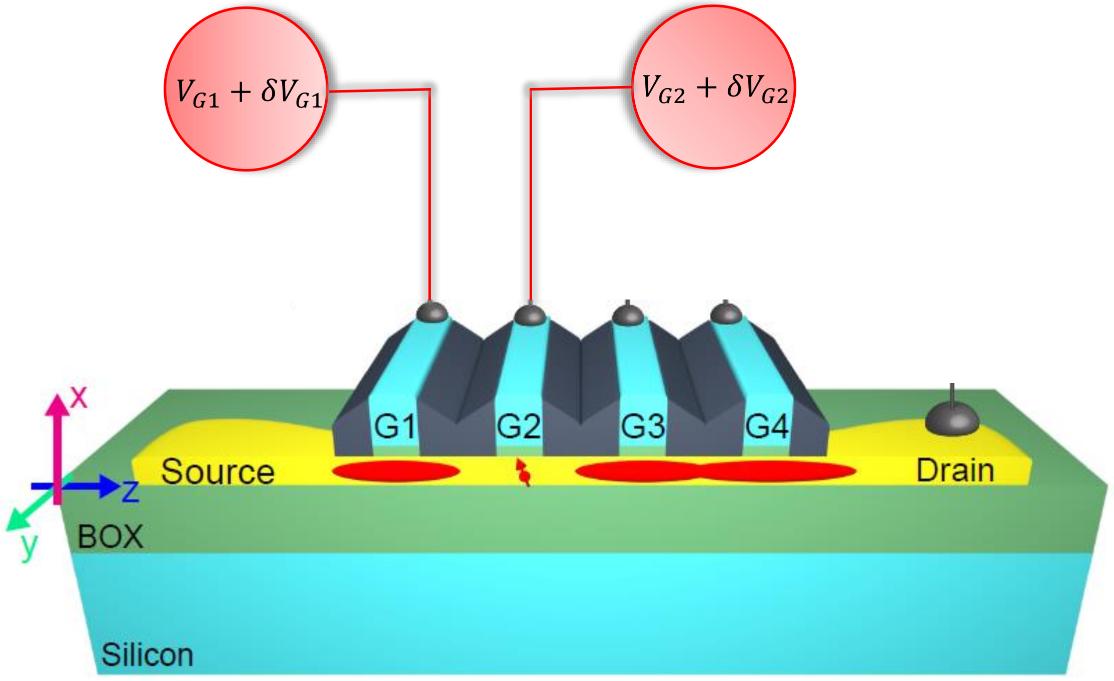

Longitudinal Larmor sensitivity

$$\frac{\delta f_L}{\delta V_{G2}} = LSESG_2$$

$$\frac{\delta f_L}{\delta V_{G1}} = LSESG_1$$

Longitudinal spin electric susceptibility (LSESG2)

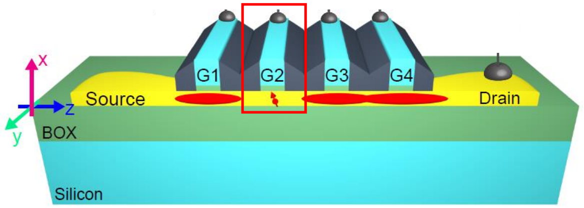

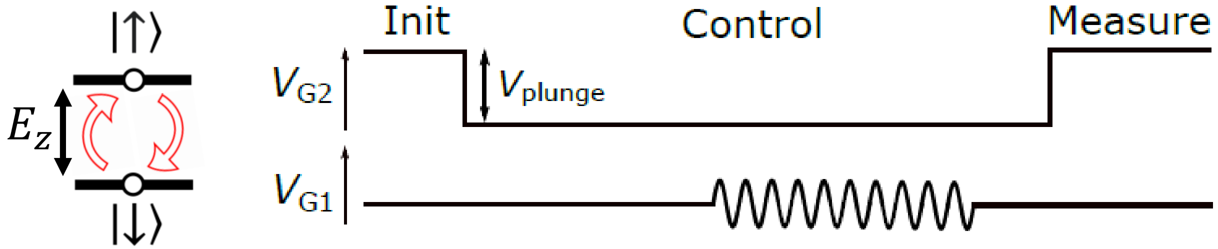

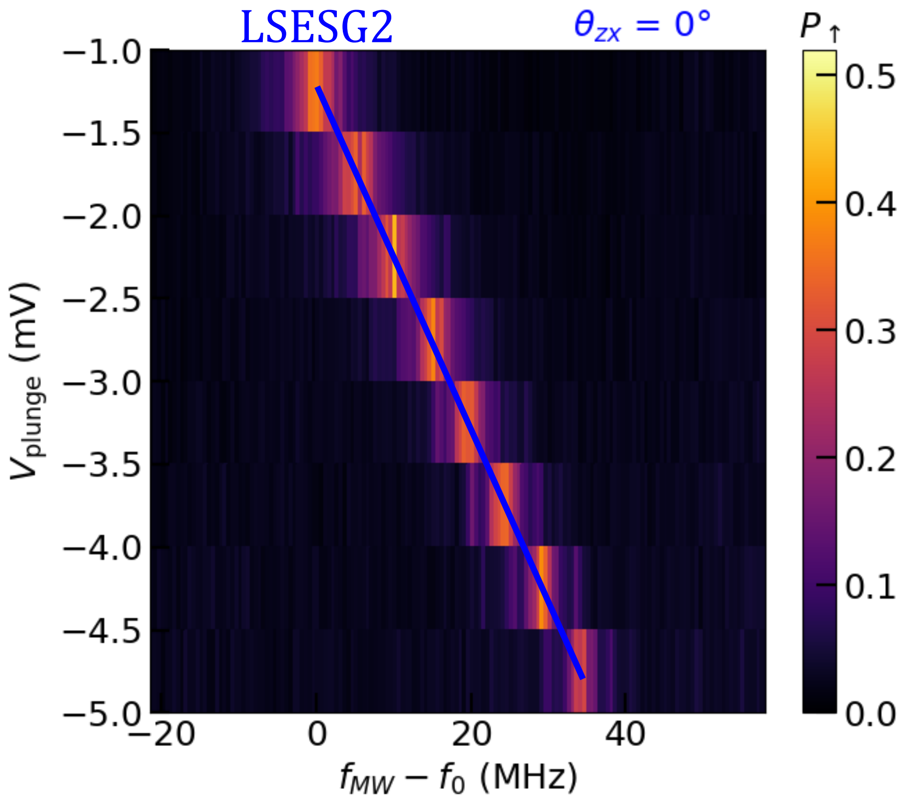

$\mathrm{LSESG2}(\theta)$

Longitudinal spin electric susceptibility (LSESG2)

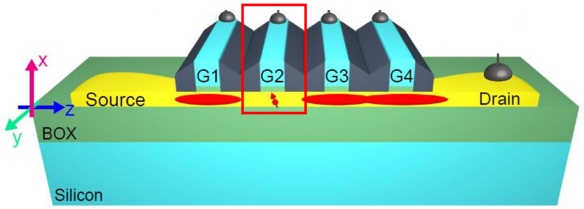

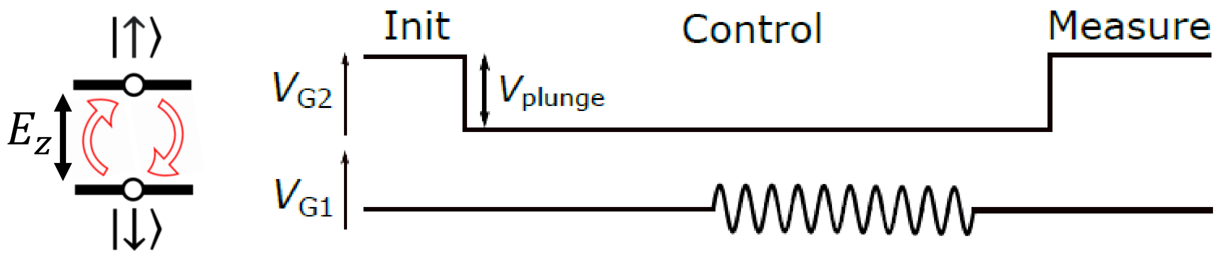

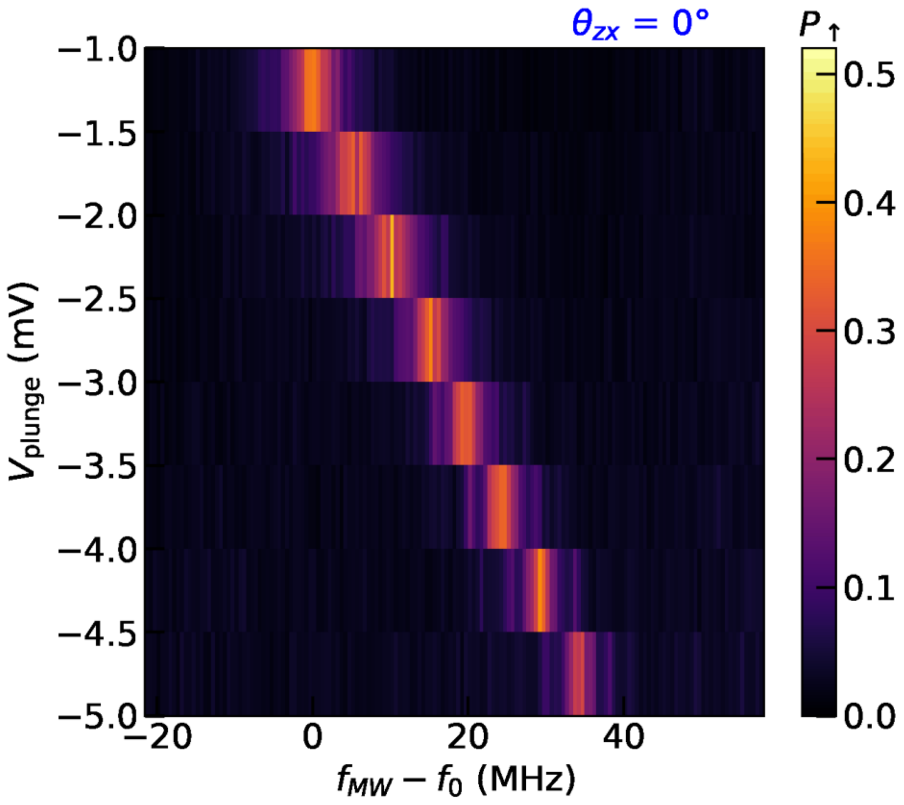

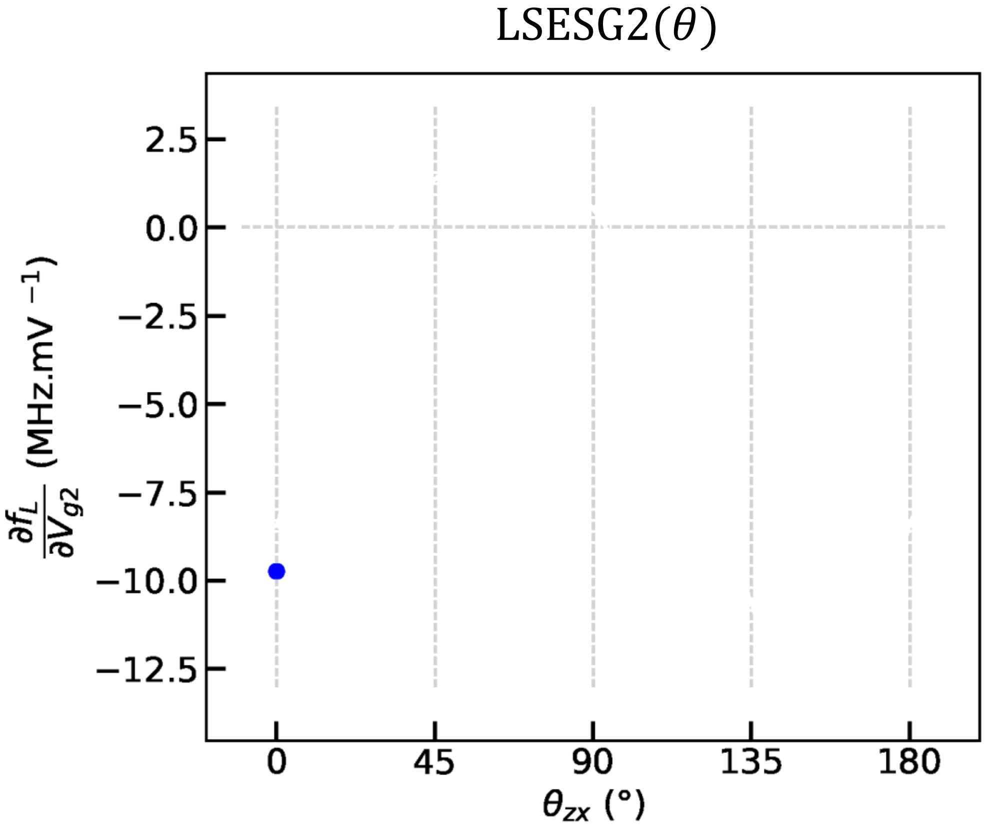

Longitudinal spin electric susceptibility (LSESG2)

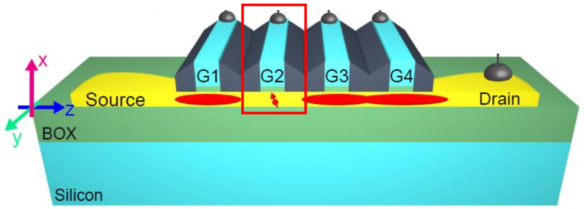

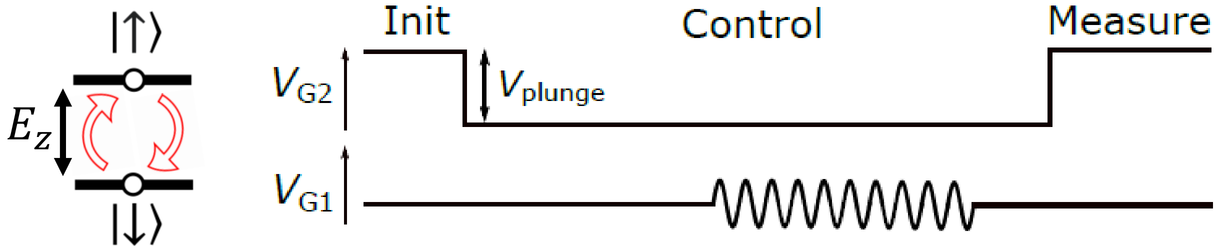

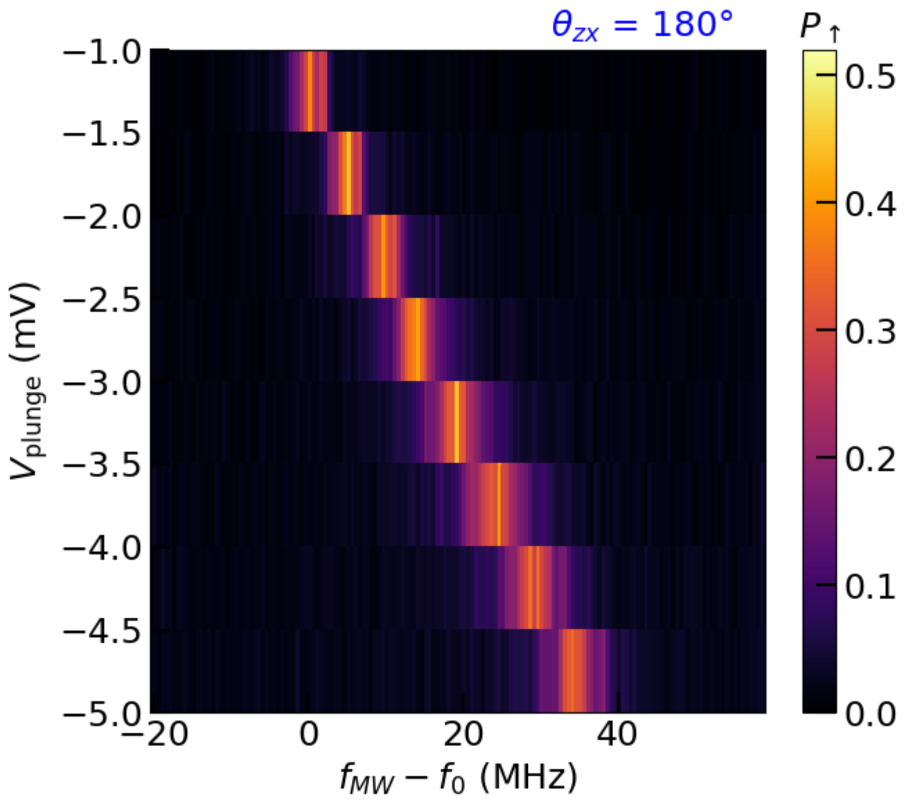

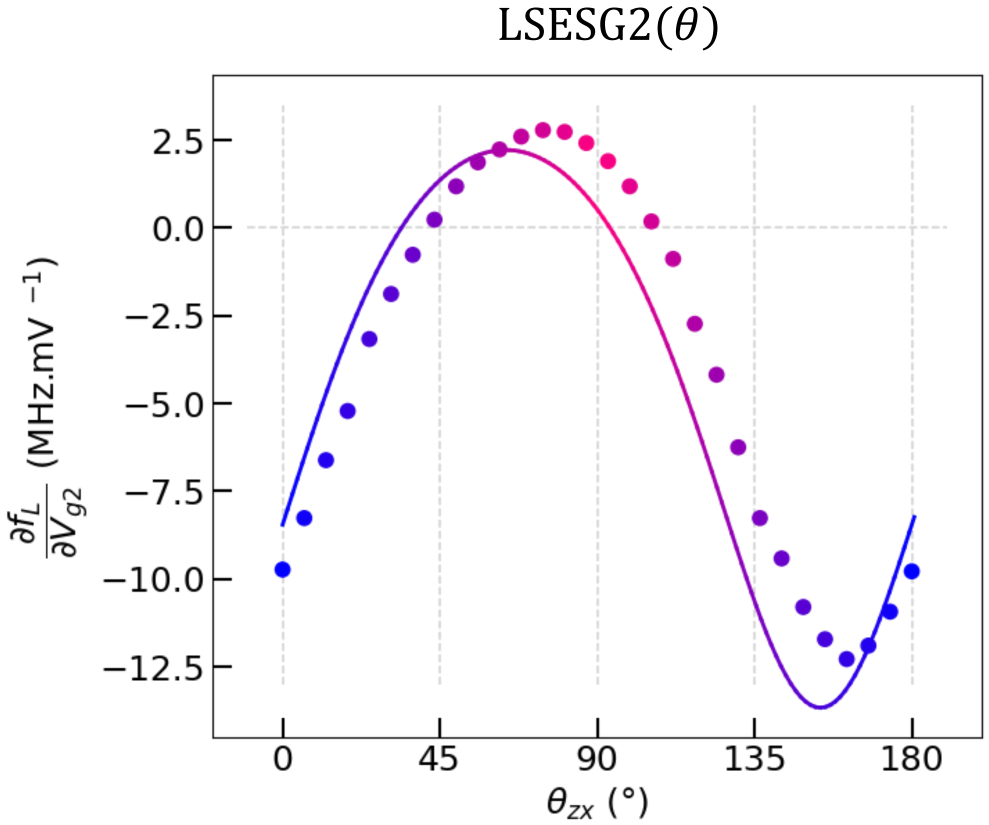

Longitudinal spin electric susceptibility (LSESG2)

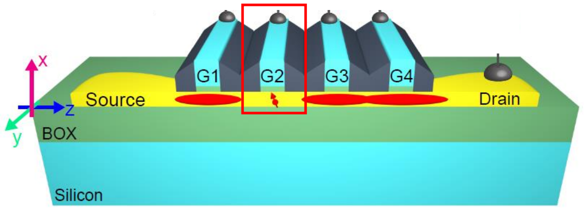

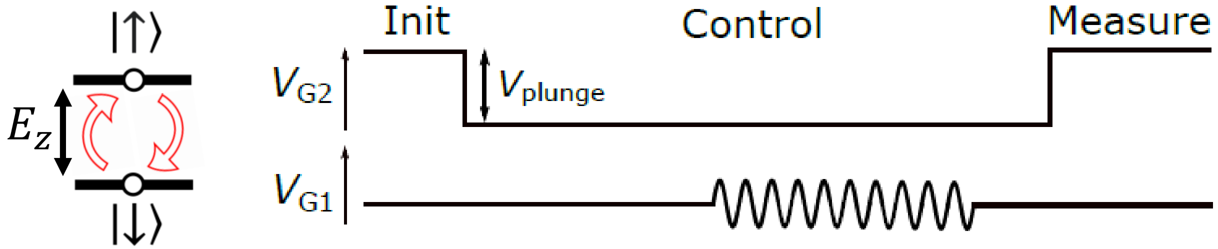

2 sweet spots for noise ⊥ to the wire

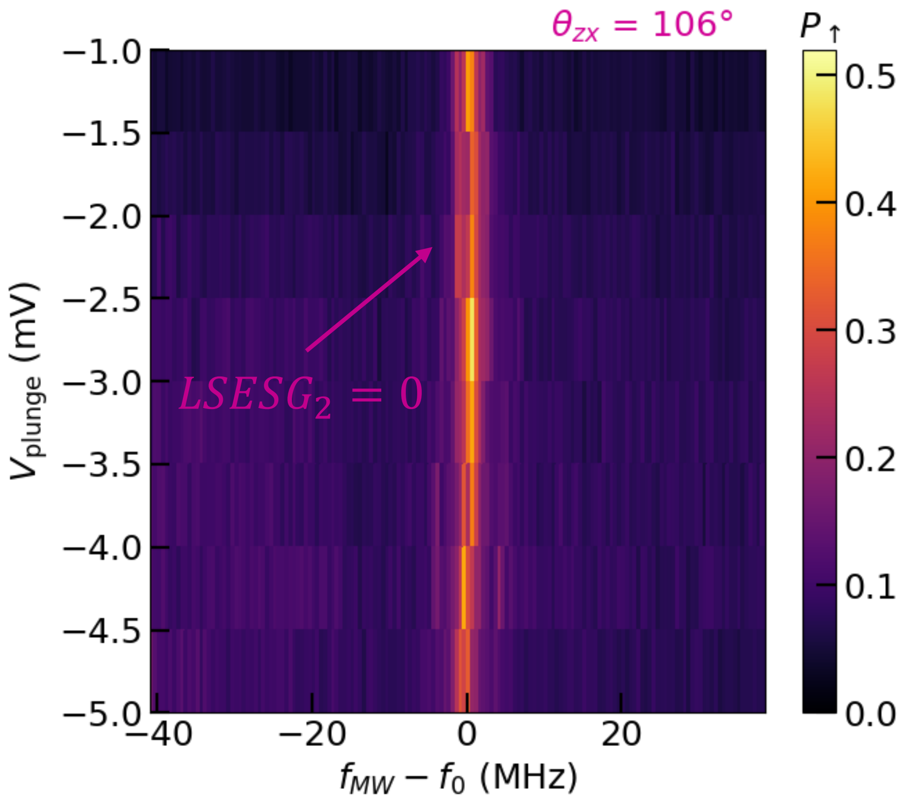

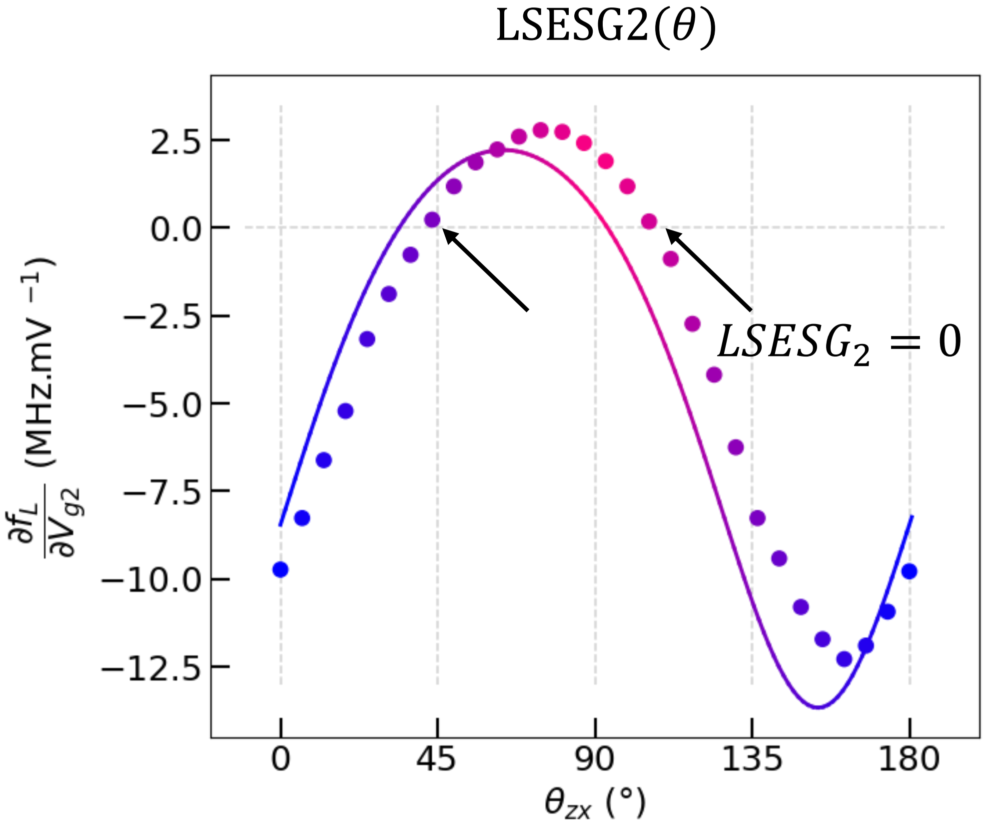

Longitudinal spin electric susceptibility (LSESG1)

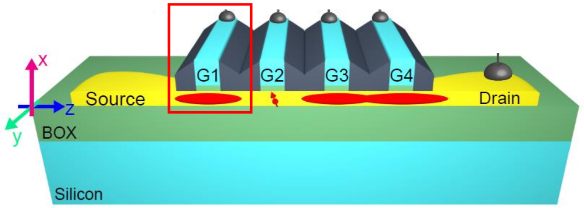

Phase Gate

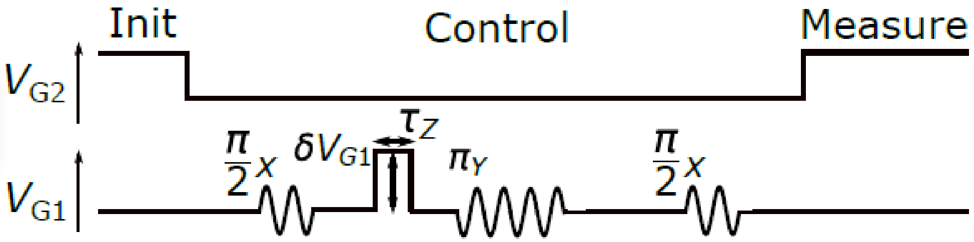

$\Leftrightarrow$ — R_ϕ — $\begin{bmatrix} 1 & 0 \\ 0 & e^{i\phi} \end{bmatrix}$ $\phi \propto |f_L(\delta V_{G1}) - F_L^0|$

Longitudinal spin electric susceptibility (LSESG1)

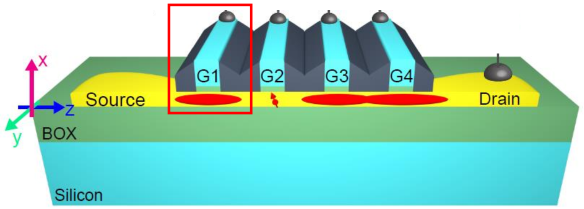

Phase Gate

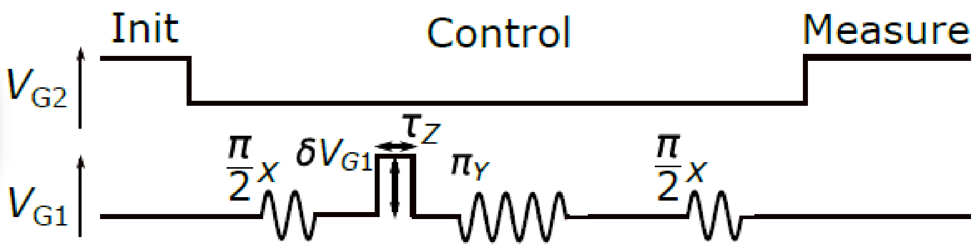

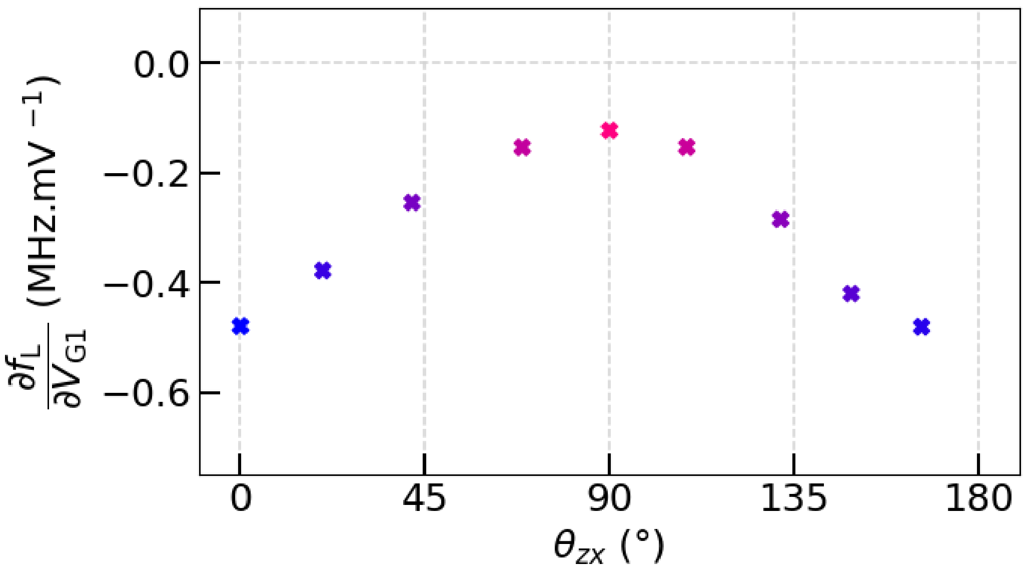

Longitudinal spin electric susceptibility (LSESG1)

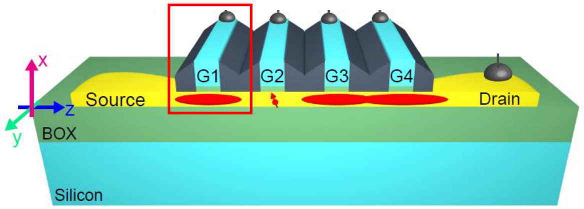

Phase Gate

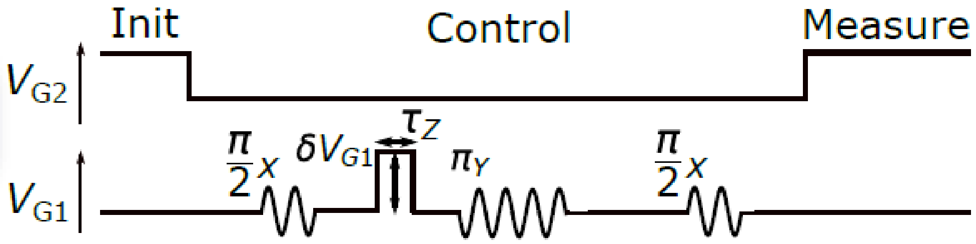

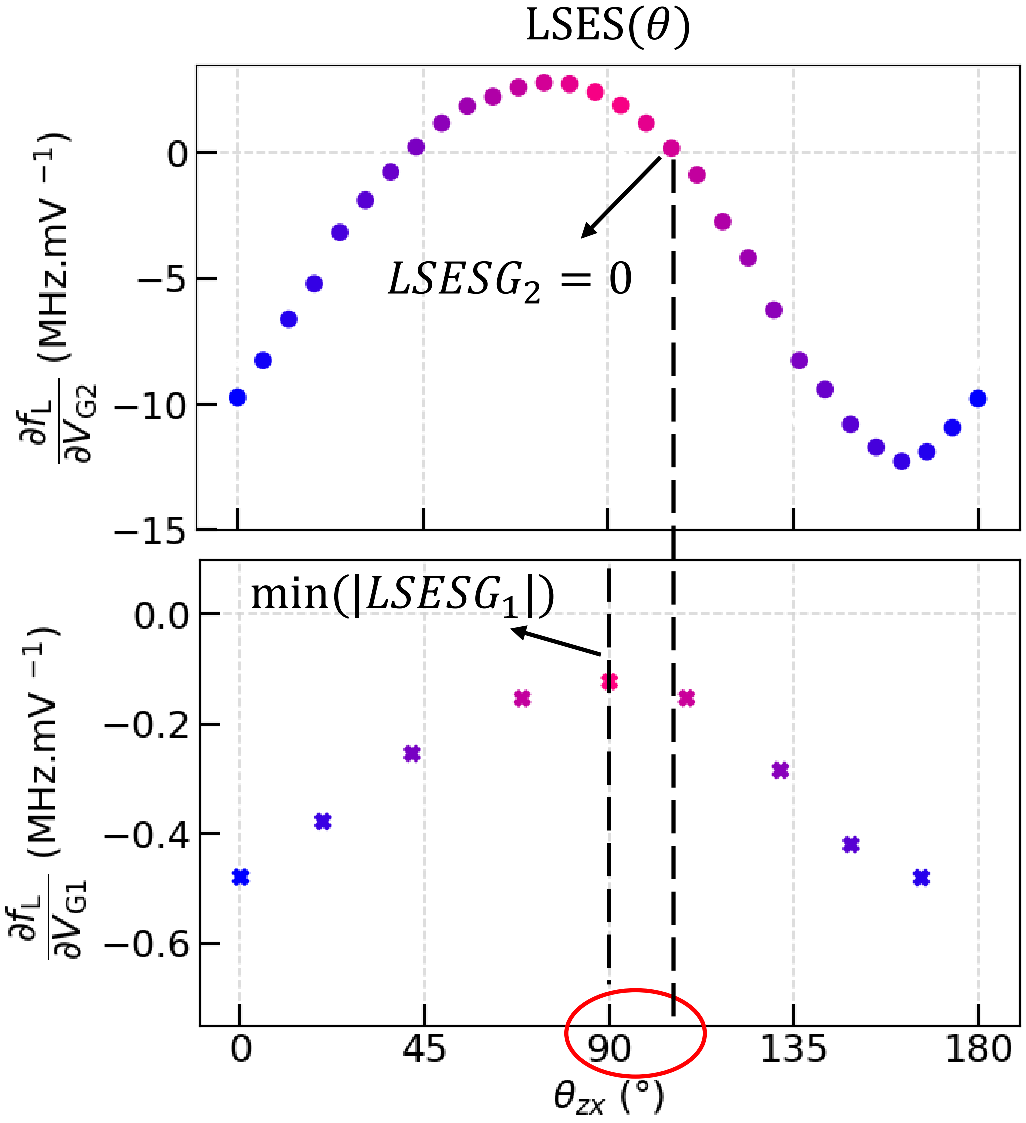

Hahn echo coherence time

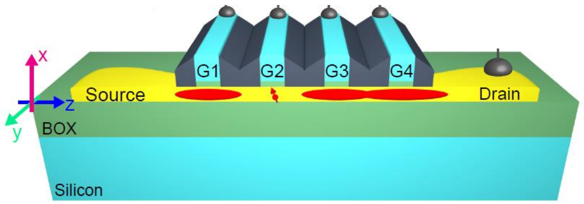

$$- - - \quad fit: \exp(-(\tau_{wait}/T_2^E)^\beta \quad \beta \approx 1.5$$

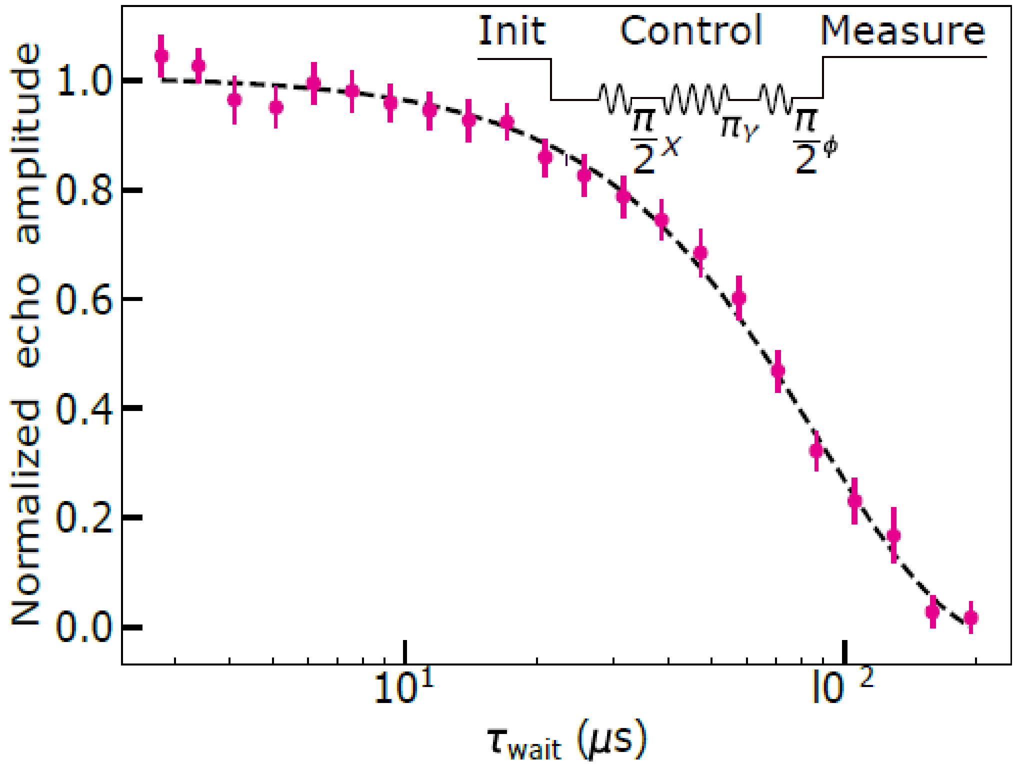

Hahn echo coherence time

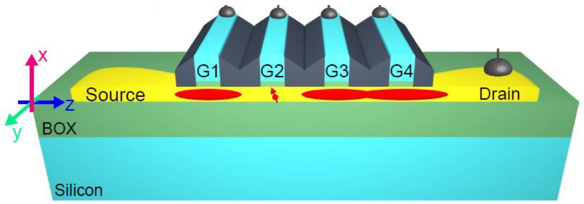

- - - $fit: \exp(-(\tau_{wait}/T_2^E)^\beta \;\; \beta \approx 1.5$

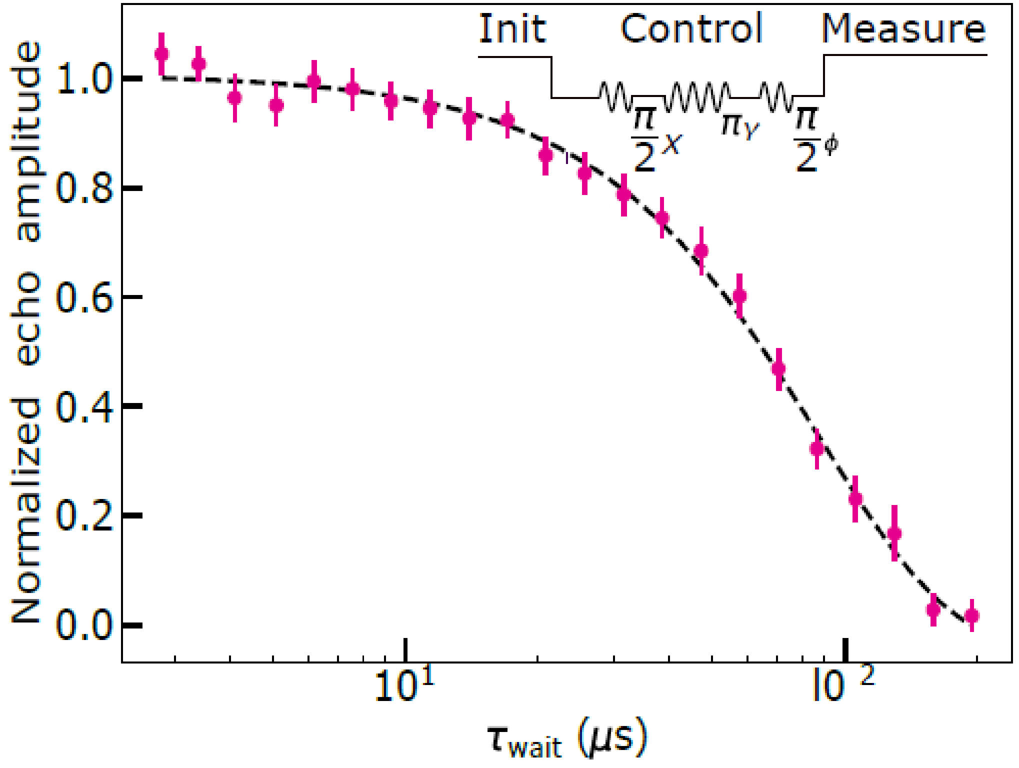

$T_2^E(\theta)$

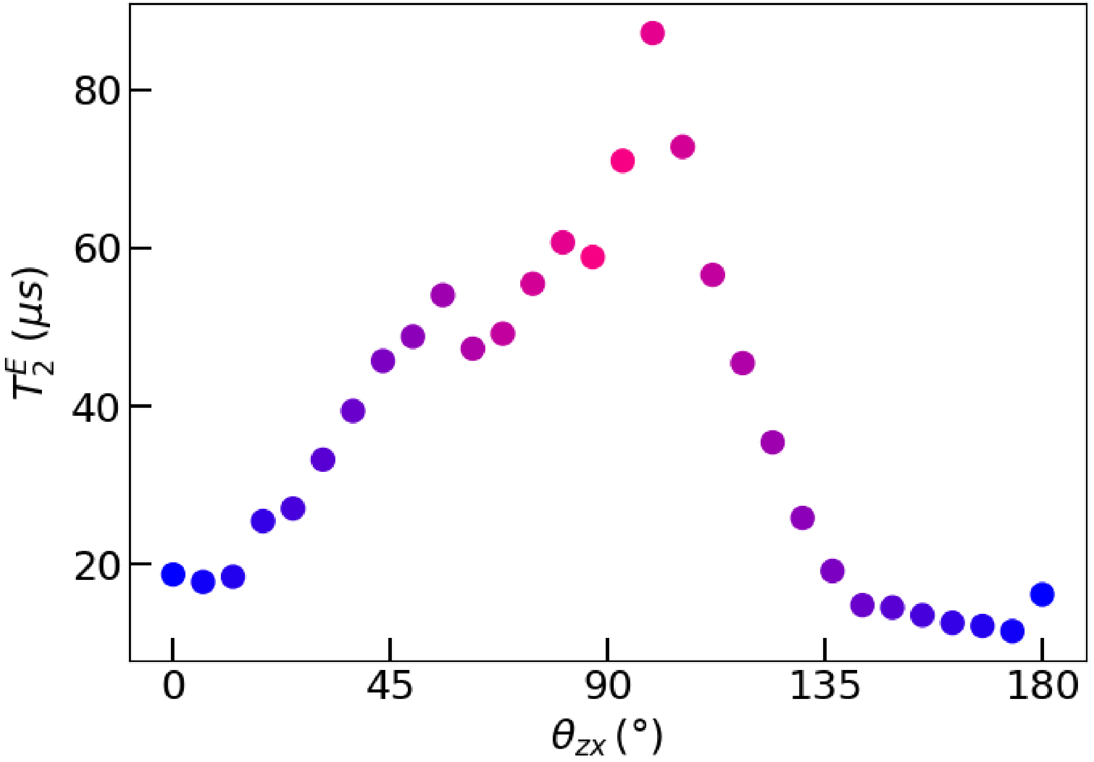

Hahn echo coherence time

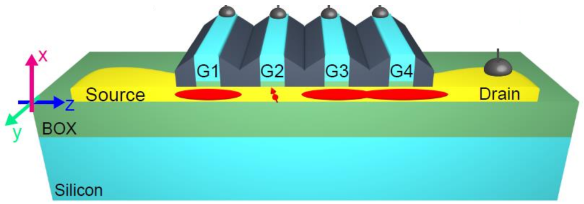

$$S_{Gi}(f) = S^{\mathrm{hf}}_{Gi}(f_0/f)^{0.5}$$

$$\frac{1}{T_2^{\mathrm{E}}} \approx 7.8 f_0^{1/3}\left(\sum_i \left(\frac{\partial f_L}{\partial V_{Gi}}\right)^2 S^{\mathrm{hf}}_{Gi}\right)^{2/3}$$

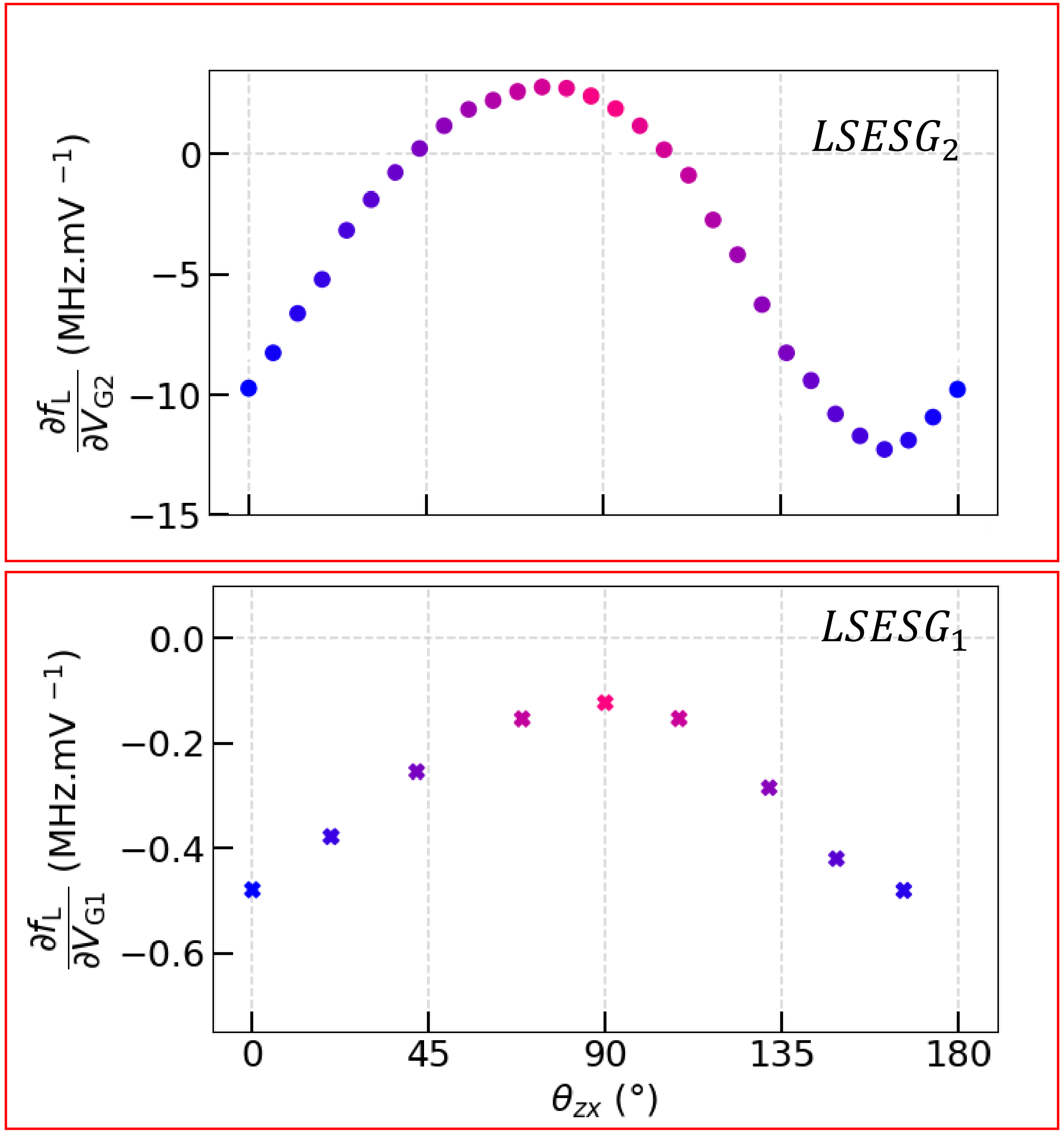

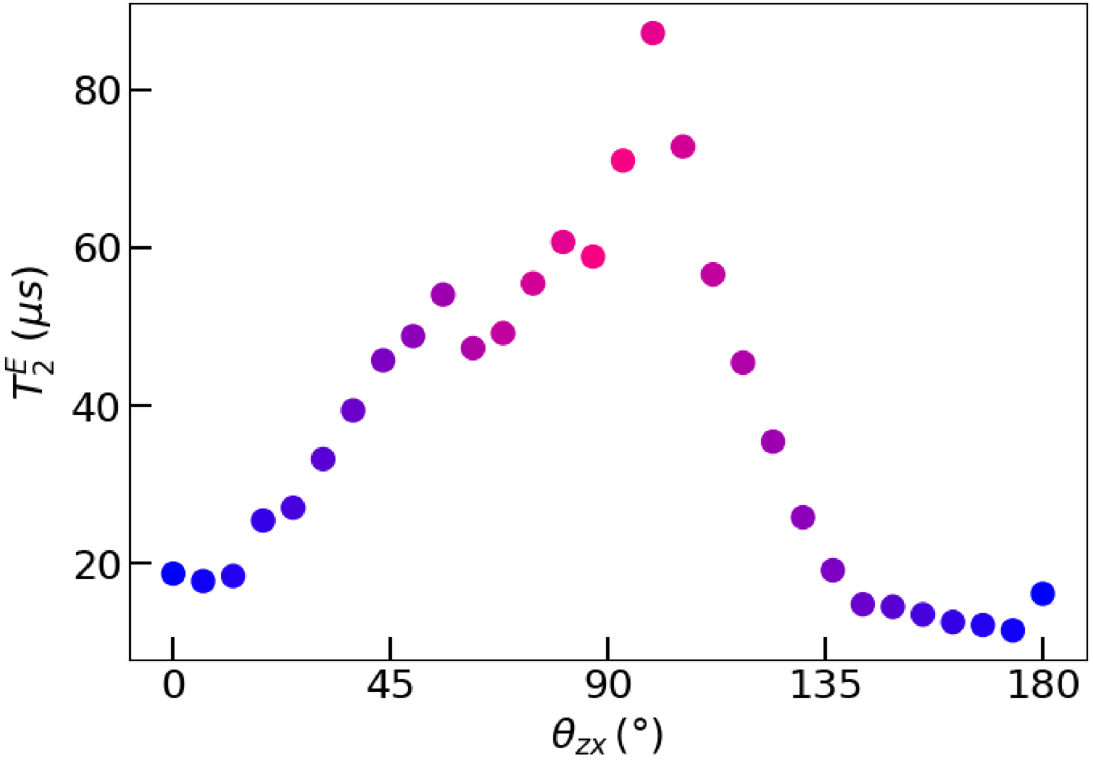

Hahn echo coherence time

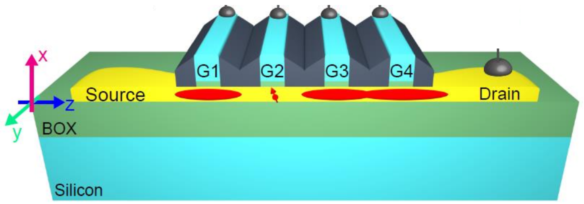

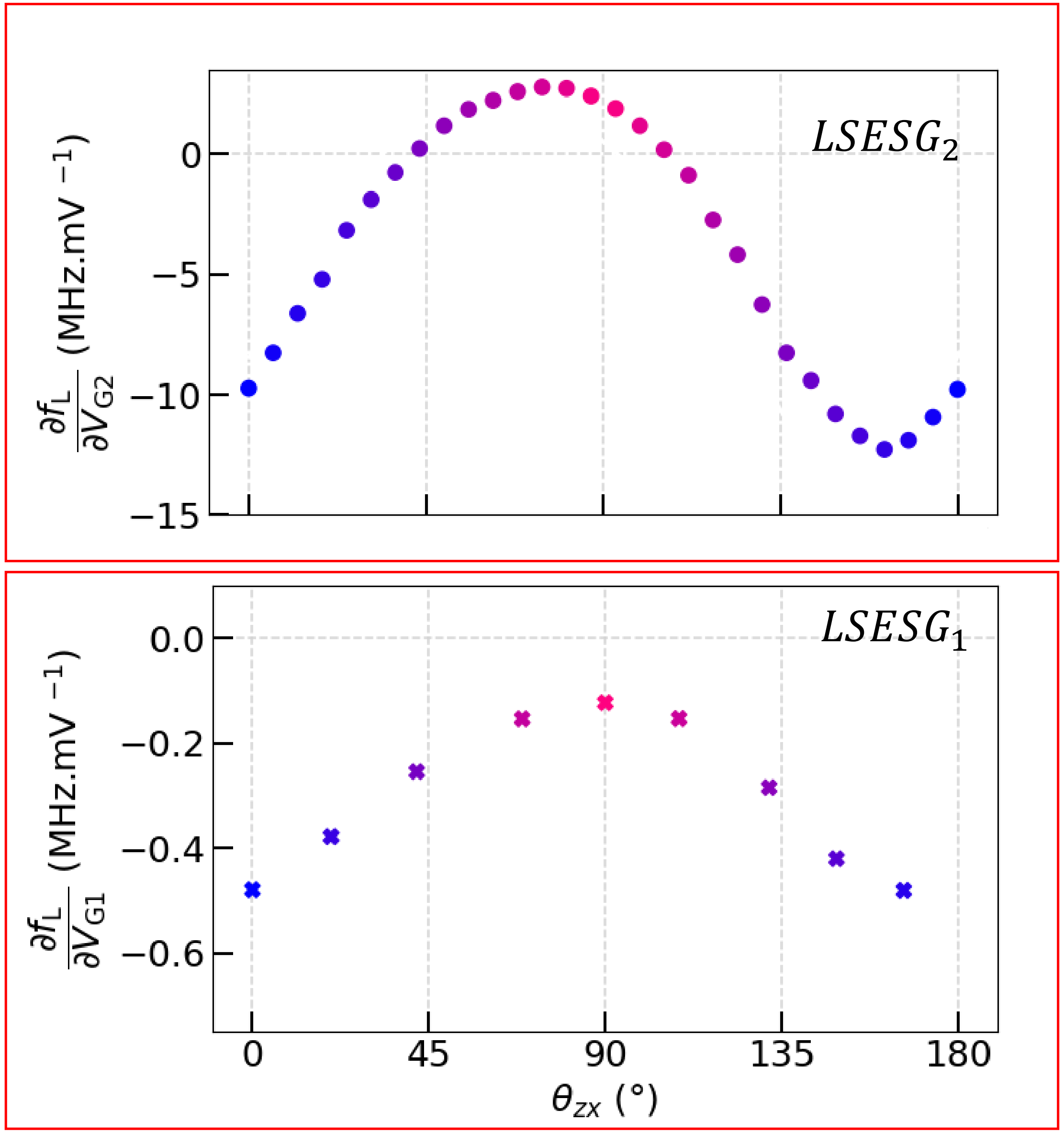

$$S_{Gi}(f) = S^{\mathrm{hf}}_{Gi}(f_0/f)^{0.5}$$

$$\frac{1}{T_2^{\mathrm{E}}} \approx 7.8 f_0^{1/3}\left(\sum_i \left(\frac{\partial f_L}{\partial V_{Gi}}\right)^2 S^{\mathrm{hf}}_{Gi}\right)^{2/3}$$

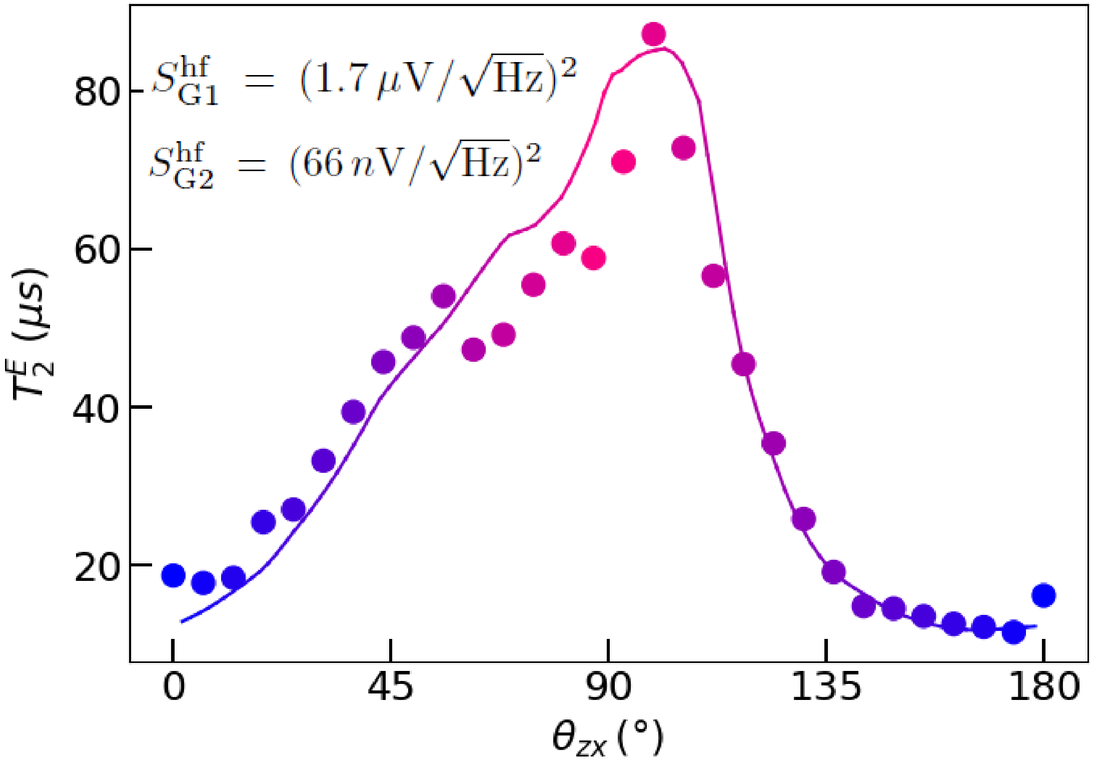

Take home message

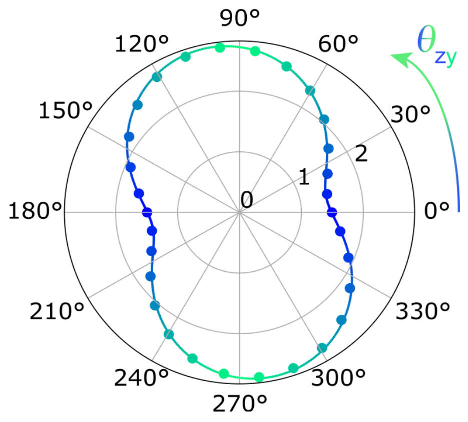

❑ G-tensor → DNA of the hole

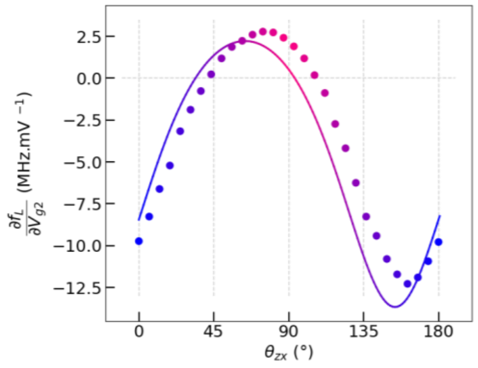

❑ BField direction minimize Longitudinal coupling

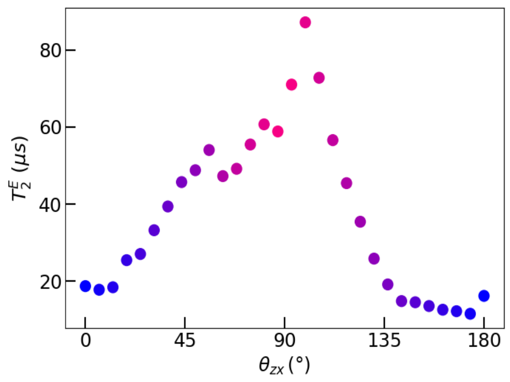

❑ T2Echo enhanced to 100µs

Outline

- Spin Qubits manipulation quick recap
- Holes / Spin-Orbit Interaction
- Silicon-on- insulator nanowire devices
- Coherence “sweetspots”
- Spin-photon coupling


Cécile X. Yu[1,4], Simon Zihlmann[1,4]✉, José C. Abadillo-Uriel[2], Vincent P. Michal[2], Nils Rambal[3], Heimanu Niebojewski[3], Thomas Bedecarrats[3], Maud Vinet[3], Étienne Dumur[1], Michele Filippone[2], Benoit Bertrand[3], Silvano De Franceschi[1], Yann-Michel Niquet[2] & Romain Maurand[1]✉

Strong photon coupling to a hole spin in silicon

Nat. Nanotechnol. (2023).
https://doi.org/10.1038/s41565-023-01332-3

Léo Noirot

Spin-photon interaction

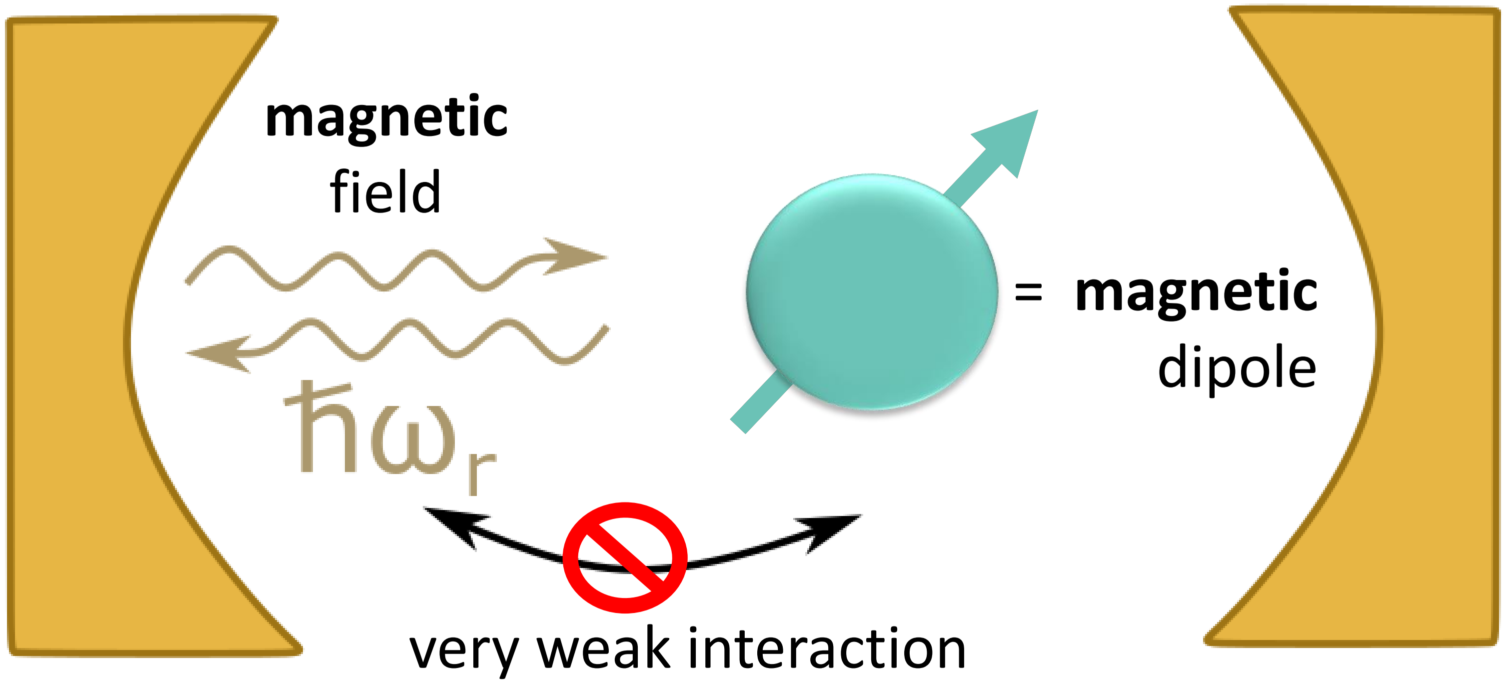

Charge-Photon Interaction g_c

$\vec{B} = 0\ T$

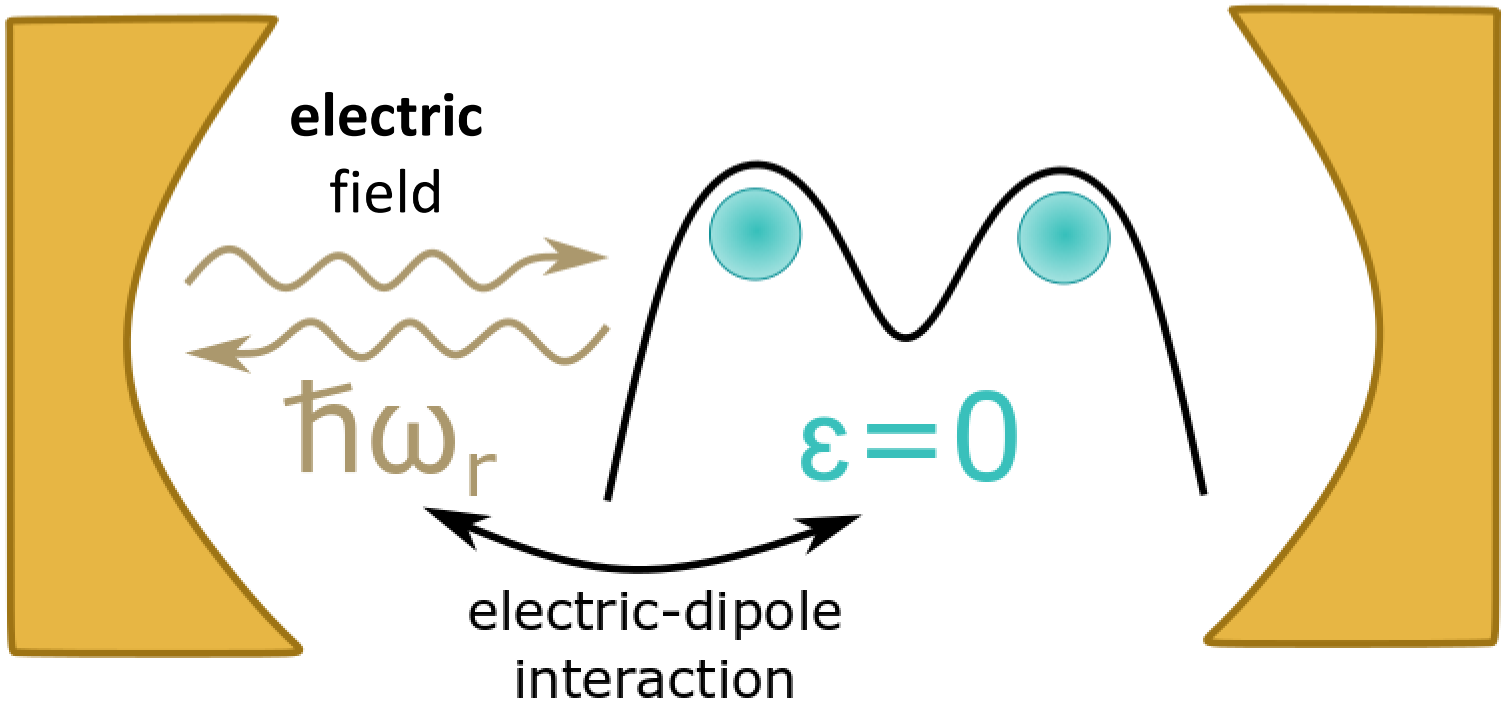

Frey et al. Phys. Rev. Lett. 108, 046807 (2012)
Mi et al. Science 355 156 (2016)
Stockklauser, Scarlino et al., PRX 7 011030 (2017)

Spin-photon interaction g_s with SOI

$\vec{B} \neq 0\ T$

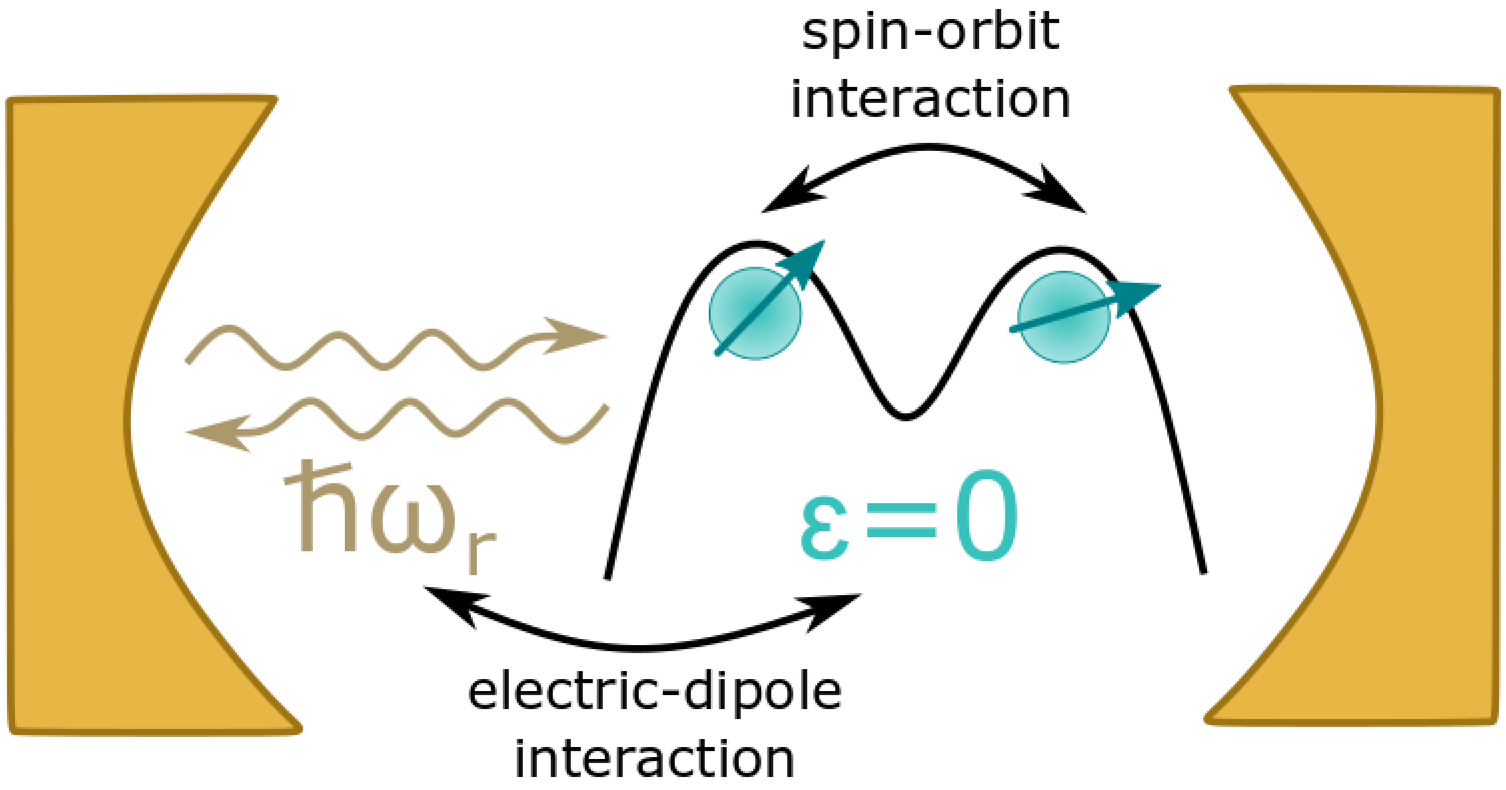

Spin-photon coupling = electric-dipole interaction + spin-orbit interaction

Si **electron** spin – photon interface

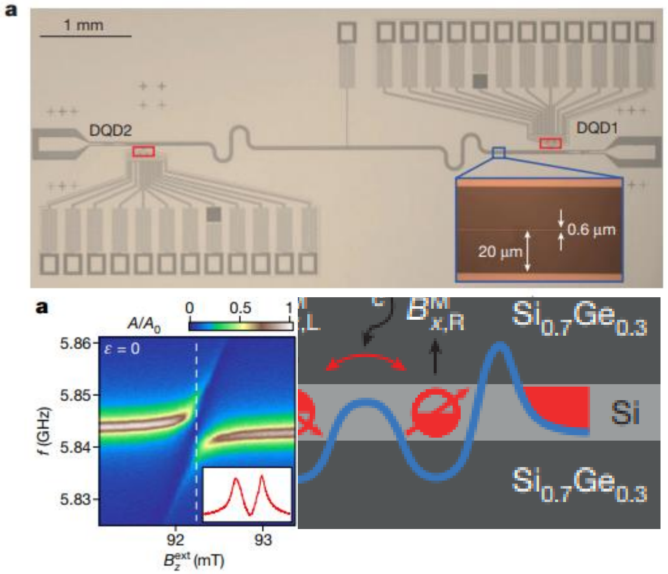

- $g_c/(2\pi) = 40\ MHz$
- $g_s/(2\pi) = 5.5\ MHz$
- $\mathrm{C} = \frac{4g_s^2}{\gamma\kappa} \sim 40$

Mi et al. Nature 555, 590 (2018)

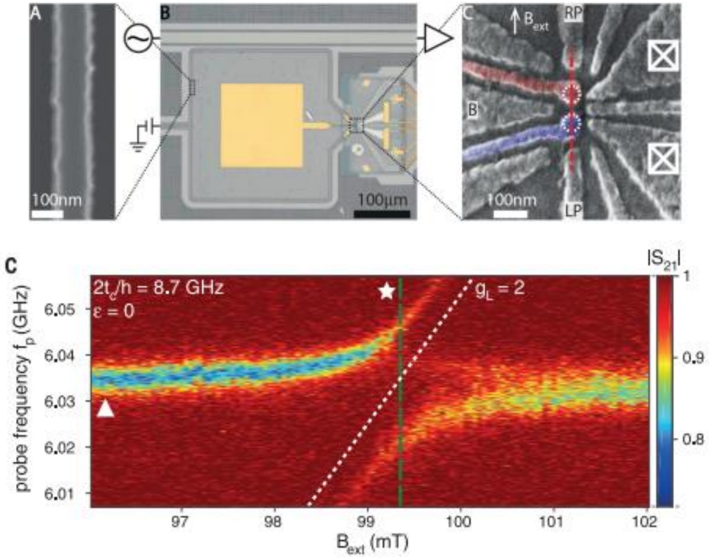

- $g_c/(2\pi) = 200\ MHz$
- $g_s/(2\pi) = 13\ MHz$
- $\mathrm{C} = \frac{4g_s^2}{\gamma\kappa} \sim 180$

Samkharadze et al. Science 359, 1123 (2018)

Si **electron** spin – photon interface

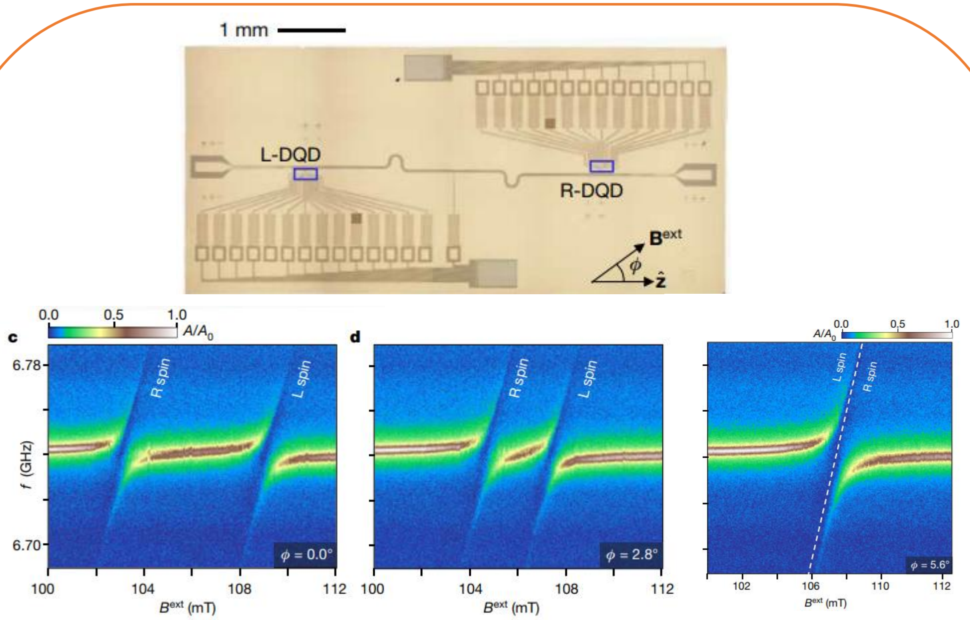

- $g_c/(2\pi) = 40\ MHz$
- $g_s/(2\pi) = 9.4\ MHz$
- $C = \frac{4g_s^2}{\gamma\kappa} \sim 40$

Borjans et al., Nature **577** (2020)

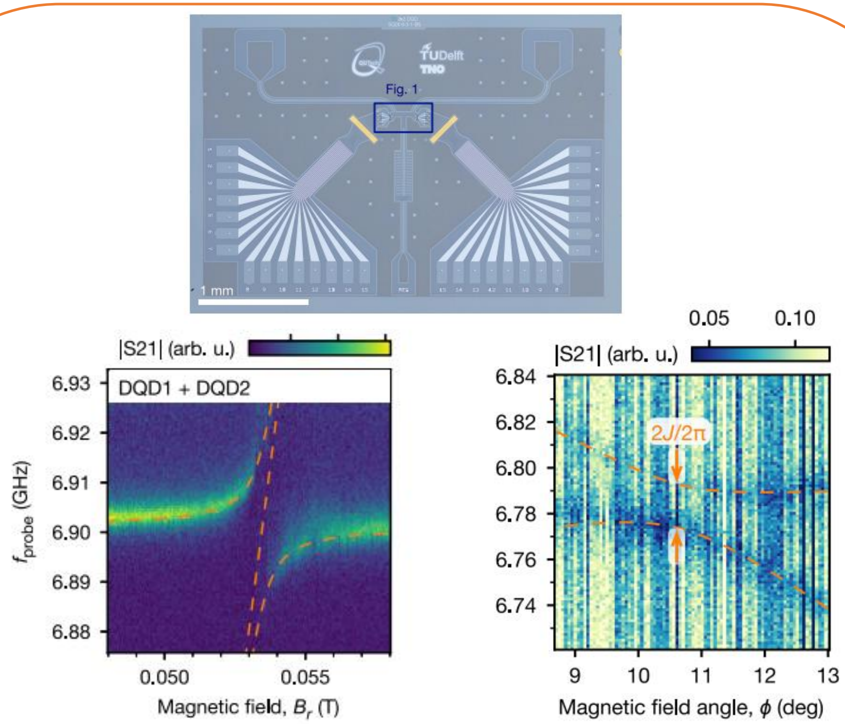

- $g_c/(2\pi) = 192\ MHz$
- $g_s/(2\pi) = 33\ MHz$
- $C = \frac{4g_s^2}{\gamma\kappa} \sim 400$

Harvey-Collard et al., PRX **12** (2022)

NbN resonators

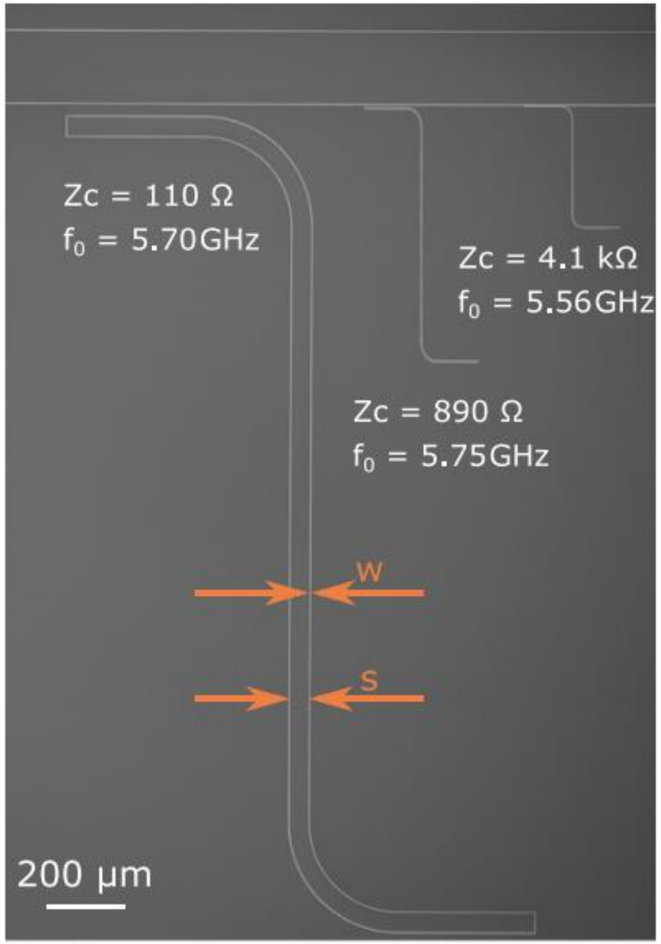

- 10 nm NbN
- Disordered superconductor
- CPW - resonators
- Large kinetic inductance 190 pH/sq

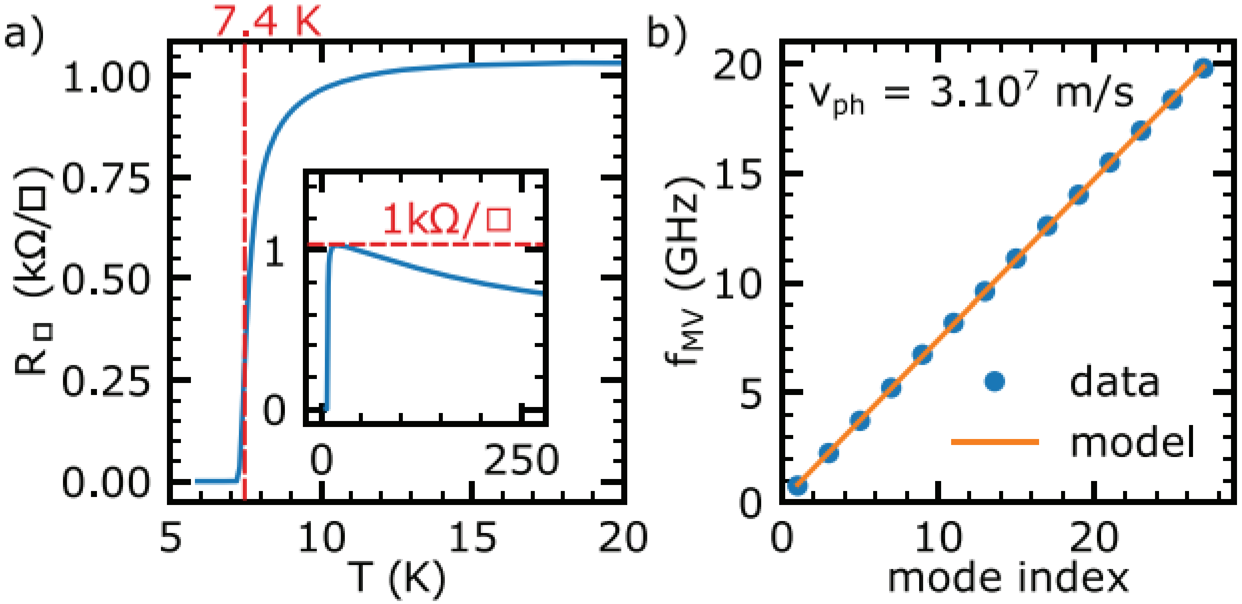

Yu et al. Appl. Phys. Lett. 118, 054001 (2021)

NbN resonators

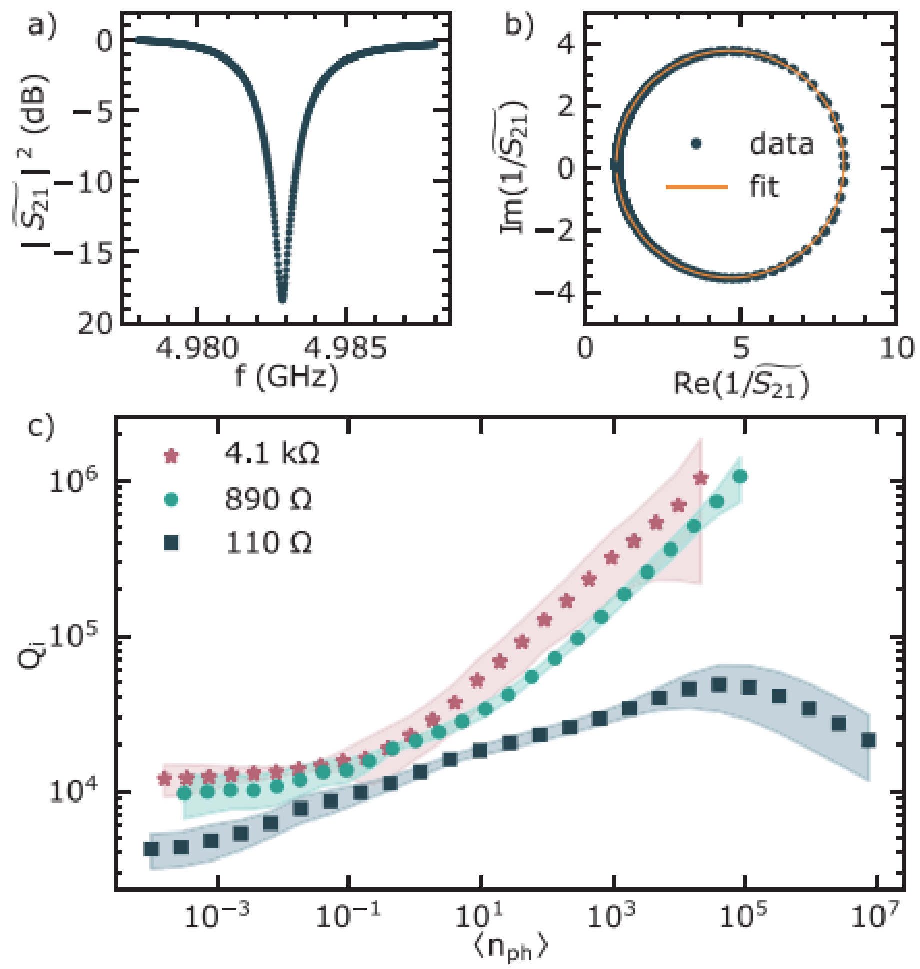

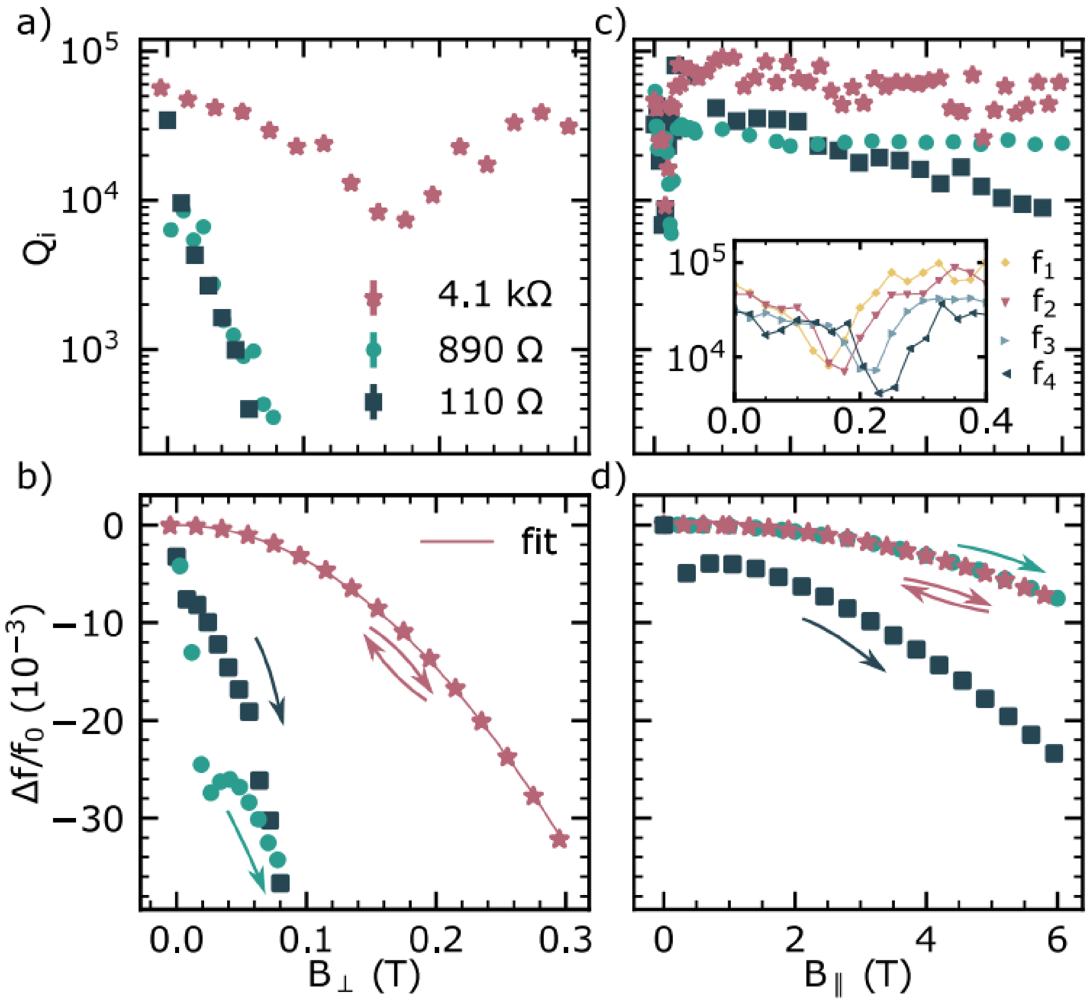

Yu et al. Appl. Phys. Lett. 118, 054001 (2021)

Hybrid circuit QED architecture with hole spins

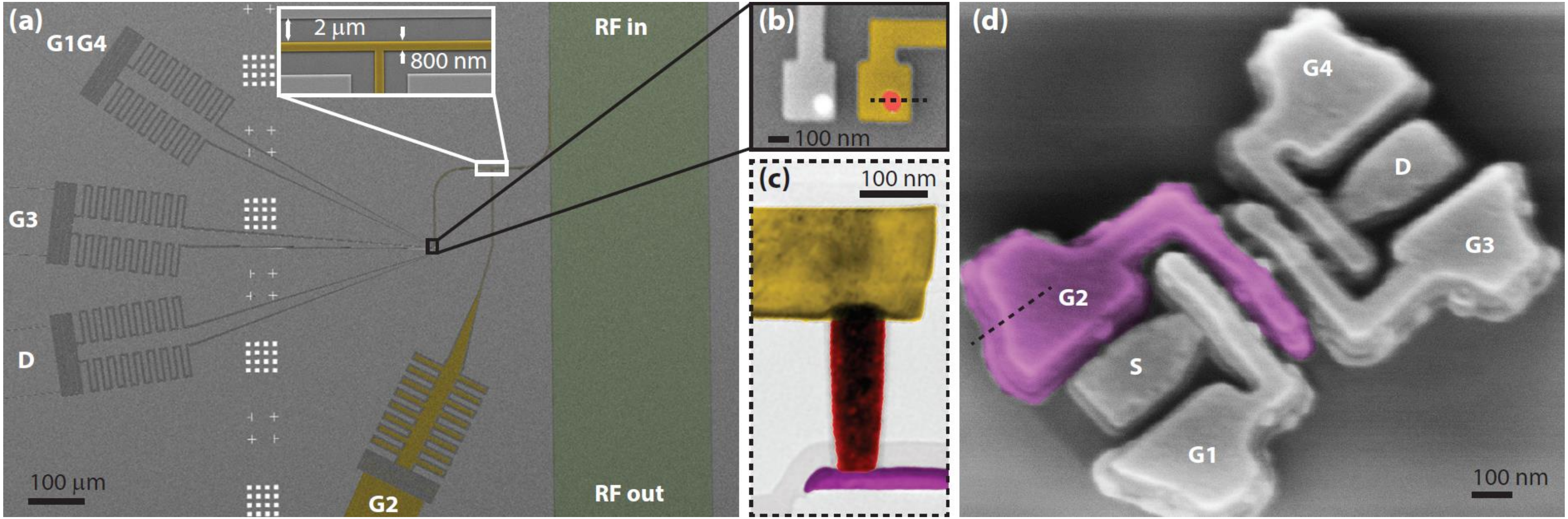

- NbN CPW resonator $Z_c = 2.5k\Omega$
- Cavity characteristics: $\omega_r/2\pi = 5.43$ GHz, $\kappa/2\pi = 13.5$ MHz $\kappa_{int}/2\pi = 10$ MHz, $\kappa_{ext}/2\pi = 3.5$ MHz
- Galvanic connection from the cavity to a plunger gate of the nanowire device

Hybrid circuit QED architecture with hole spins

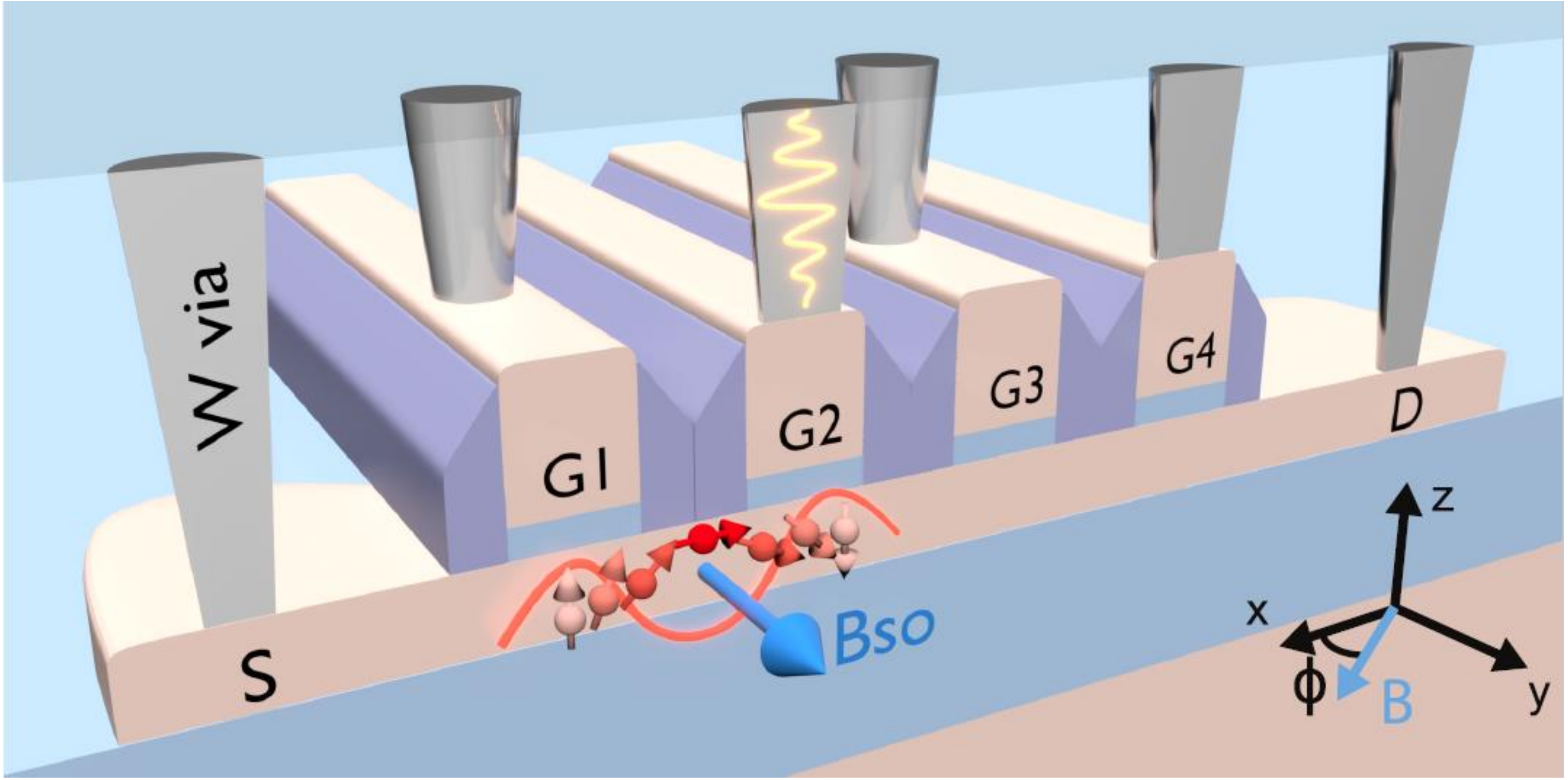

Charge-photon interaction

$$H_c = \begin{pmatrix} \epsilon/2 & t_c \\ t_c & -\epsilon/2 \end{pmatrix}, \begin{pmatrix} |L\rangle \\ |R\rangle \end{pmatrix}$$

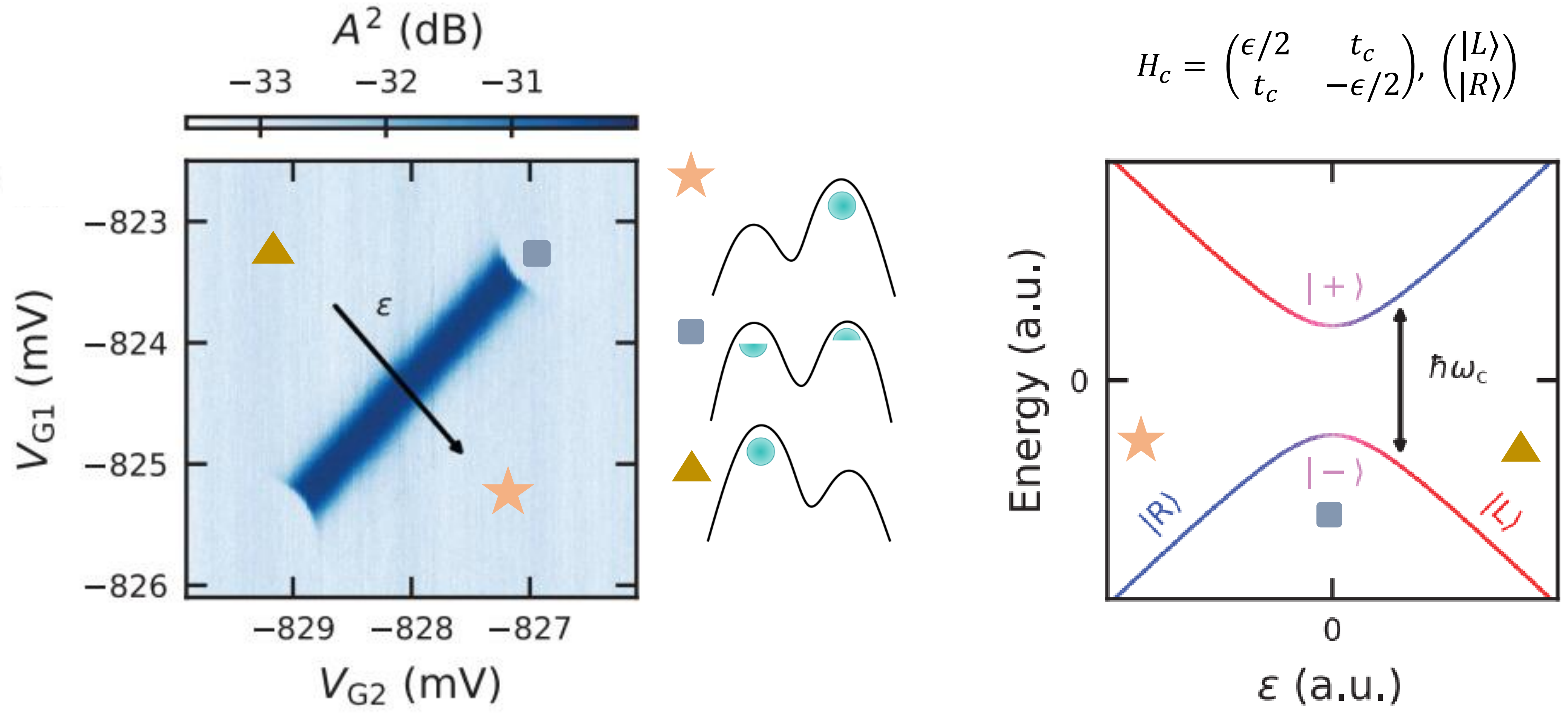

Charge-photon interaction

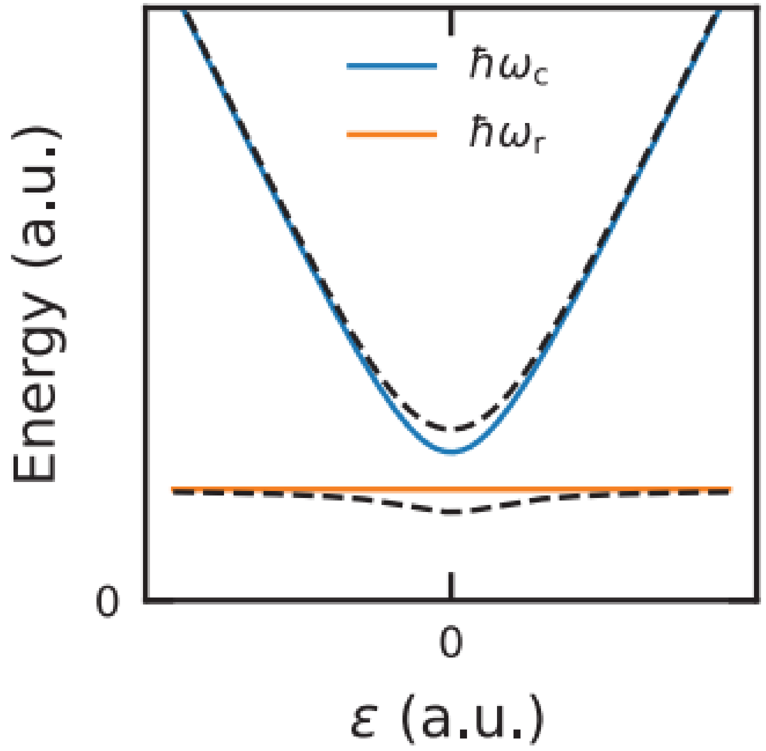

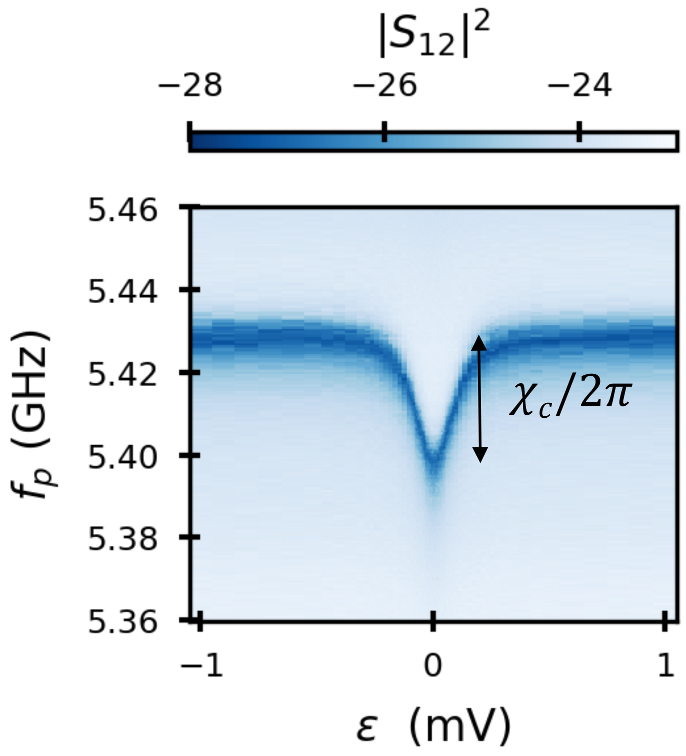

$$\hbar\omega_c = \sqrt{\epsilon^2 + 4t_c^2} > \hbar\omega_r$$

$$\chi_c = g_c^2 \cdot \left(\frac{1}{|\omega_q - \omega_r|} + \frac{1}{\omega_q + \omega_r}\right)$$

$\boldsymbol{g_c/2\pi}$ **= 513 MHz**

$\boldsymbol{t_c/h}$ **= 9.6 GHz**

$\boldsymbol{\frac{g_c}{f_r}}$ **~ 10 %**

Where is the spin?

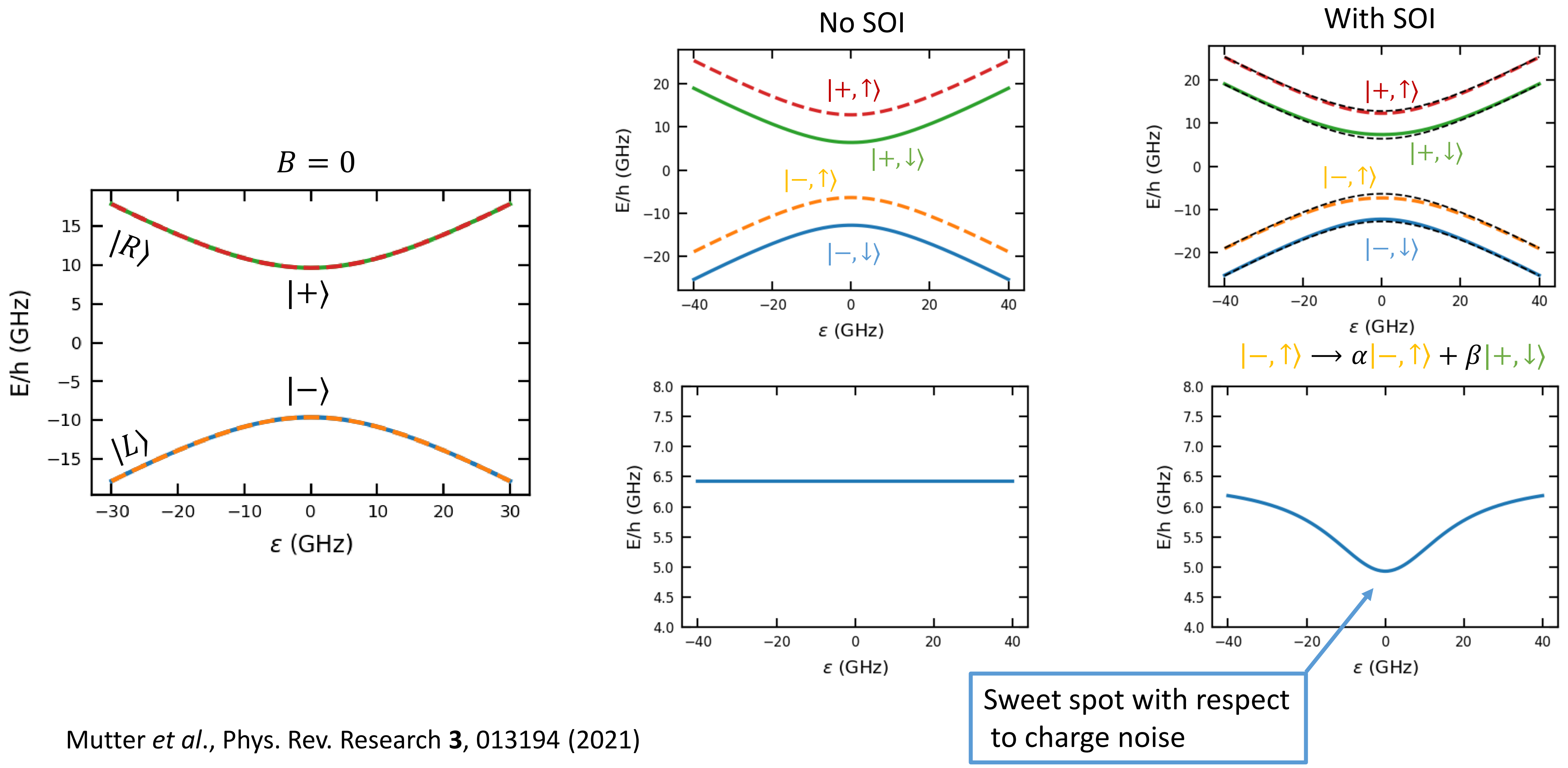

Mutter *et al.*, Phys. Rev. Research **3**, 013194 (2021)

Strong spin-photon coupling

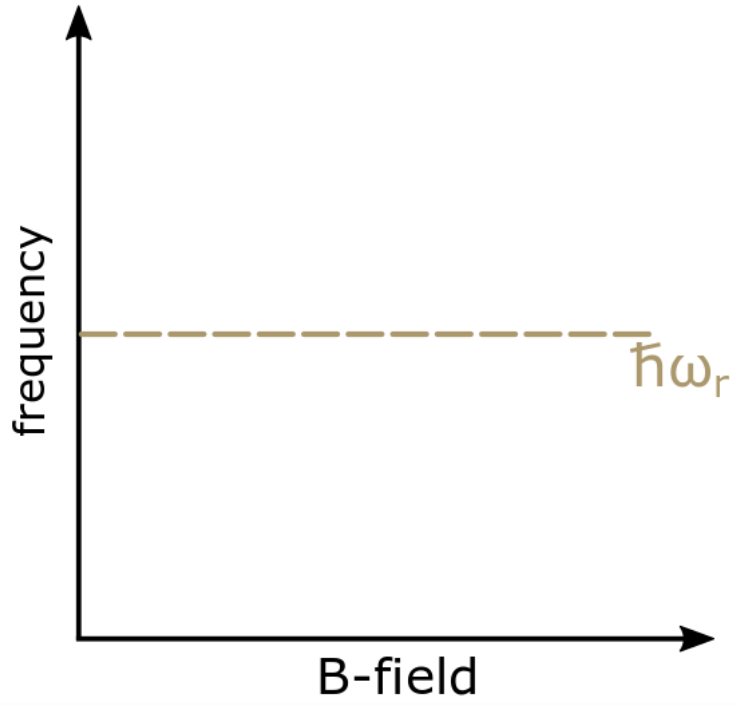

Strong spin-photon coupling

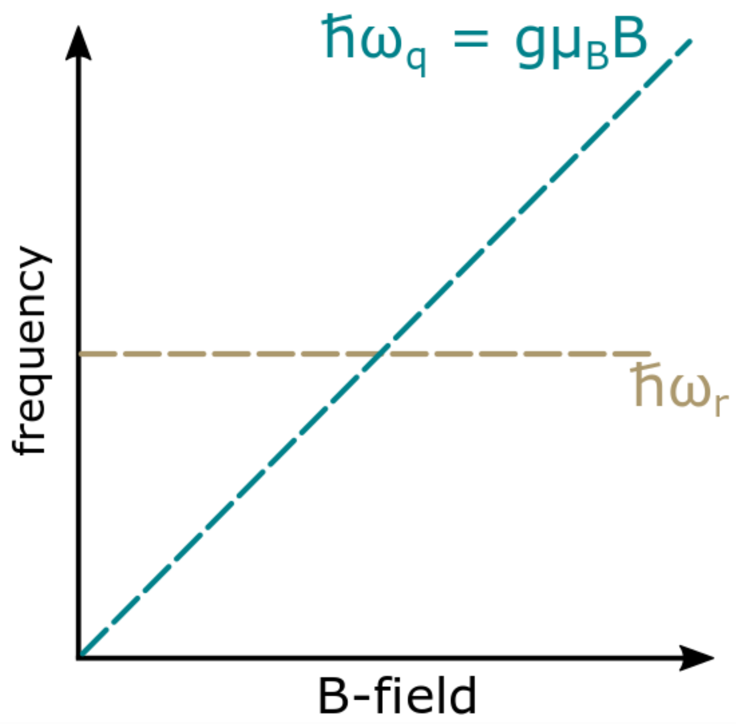

Strong spin-photon coupling

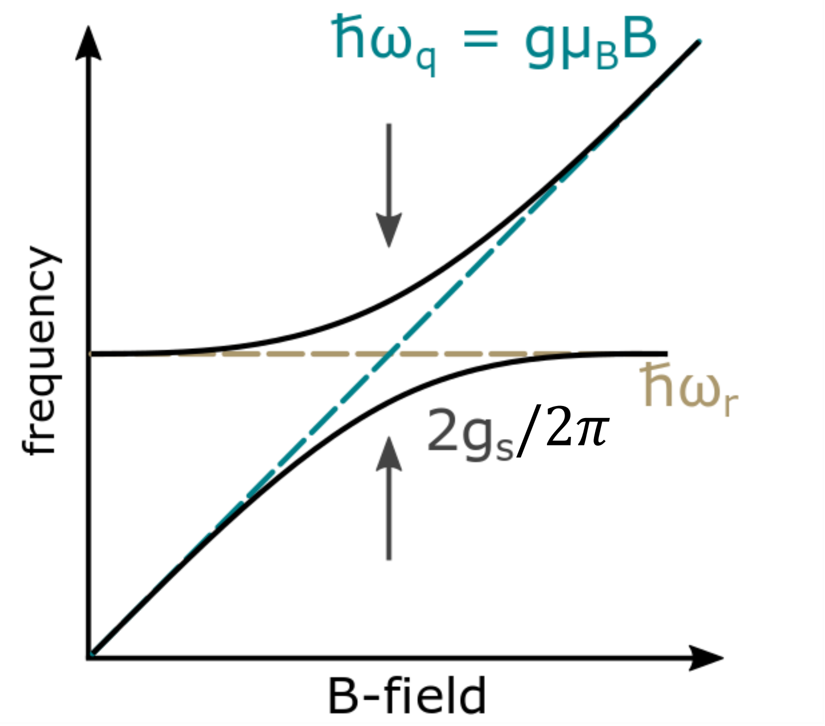

Vacuum Rabi splitting: signature of strong spin-photon coupling

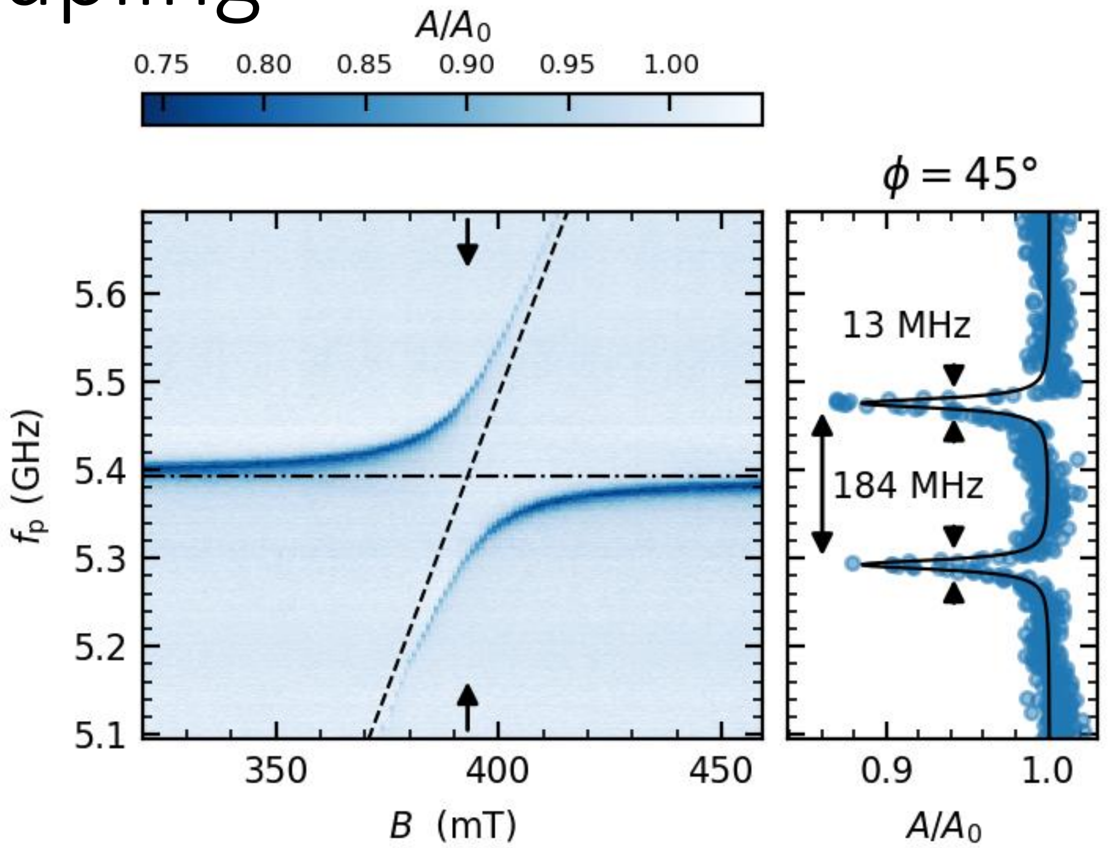

Strong spin-photon coupling with $2g_s/2\pi = 184$ MHz $\gg 13$ MHz

Angular dependence of g_s

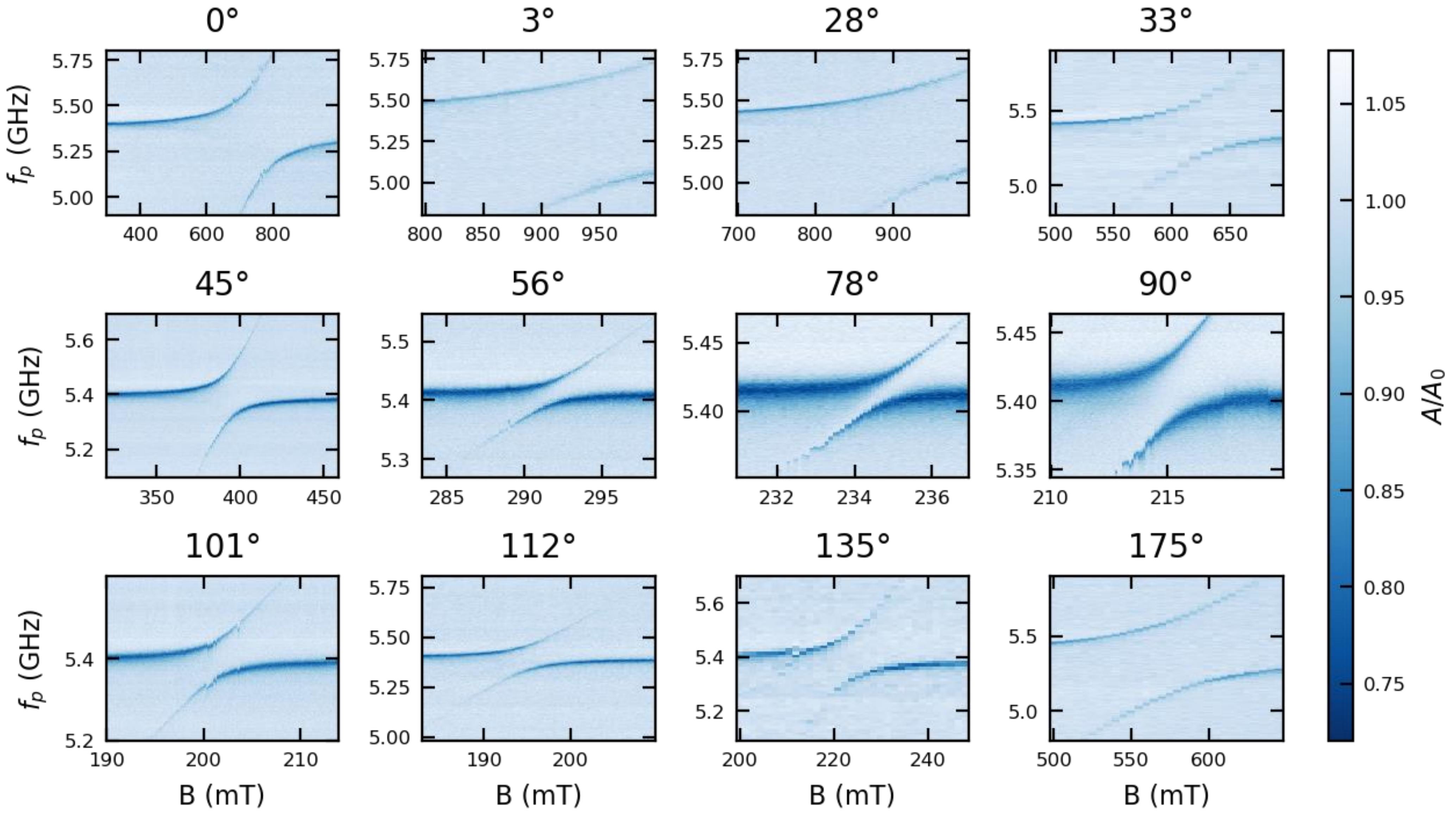

Strong spin-photon coupling: angular dependence

Kloeffel *Phys. Rev. B* **97**, 235422 (2018).

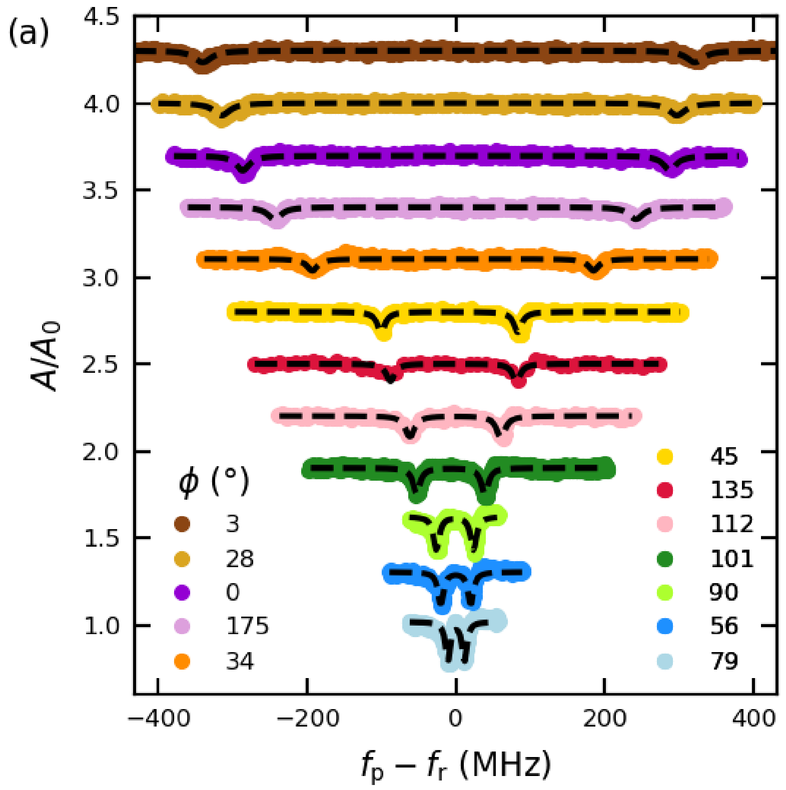

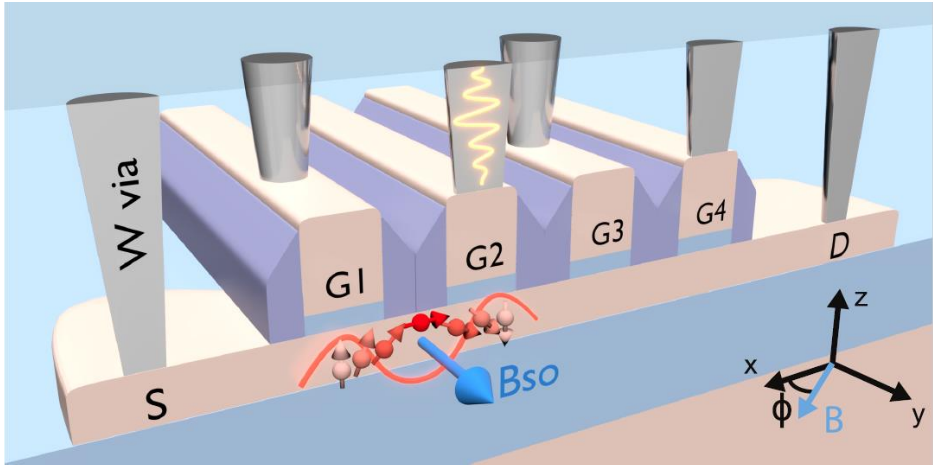

Direct 1-dimensional Rashba spin-orbit interaction

$\hat{g} \cdot \vec{B} \parallel \hat{g} \cdot \vec{B}_{SO}$ → minimal g_s

$\hat{g} \cdot \vec{B} \perp \hat{g} \cdot \vec{B}_{SO}$ → maximal g_s

spin-orbit field

$$g_s \propto g_c |(\hat{g} \cdot \vec{B}) \times (\hat{g} \cdot \vec{B}_{so})|$$

anisotropic Larmor vector

Modeling

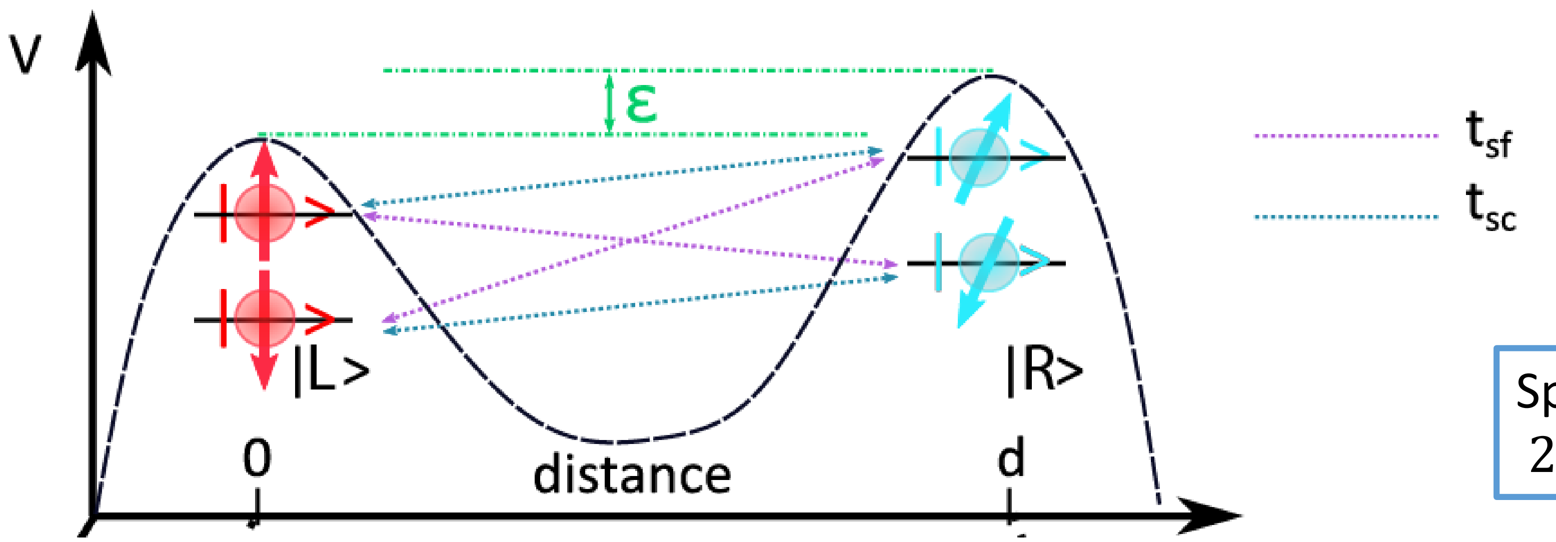

Spin-charge mixing angle:
$2\eta = 2d/\ell_{so}$

$$H_{DQD} = \begin{pmatrix} (\epsilon + g_L\mu_B B)/2 & 0 & t_{sc} & t_{sf} \\ 0 & (\epsilon - g_L\mu_B B)/2 & -t_{sf} & t_{sc} \\ t_{sc} & -t_{sf} & -(\epsilon - g_R\mu_B B)/2 & 0 \\ t_{sf} & t_{sc} & 0 & -(\epsilon + g_R\mu_B B)/2 \end{pmatrix}, \quad \begin{pmatrix} |\mathrm{L},\downarrow\rangle \\ |\mathrm{L},\uparrow\rangle \\ |R,\downarrow\rangle \\ |R,\uparrow\rangle \end{pmatrix}$$

Note: $\mathrm{g_L}(\phi)$, $\mathrm{g_R}(\phi)$, $t_{sf} \simeq t_c \sin\eta \,|\, (\hat{g}\cdot\vec{B}) \times (\hat{g}\cdot\vec{B}_{so})|$ and $t_c = \sqrt{t_{sf}^2 + t_{sc}^2}$

Modeling

Theory: J.C Abadillo-Uriel, V. Michal, M. Filippone, Y-M Niquet

$\omega_r/2\pi$	$g_c/2\pi$	α	t_c/h	$g_u^{(L)}$	$g_v^{(L)}$	ϕ_L	$g_u^{(R)}$	$g_v^{(R)}$	ϕ_R	η	Φ	Ψ
5.42835 GHz	513 MHz	0.607	9.57 GHz	1.002	2.186	29.24°	0.922	2.248	21.03°	83.31°	6.16°	19.75°
±0.06 MHz	±2 MHz	±0.004	±0.06 GHz	±0.047	±0.078	±1.18°	±0.037	±0.083	±1.23°	±3.06°	±2.54°	±3.32°

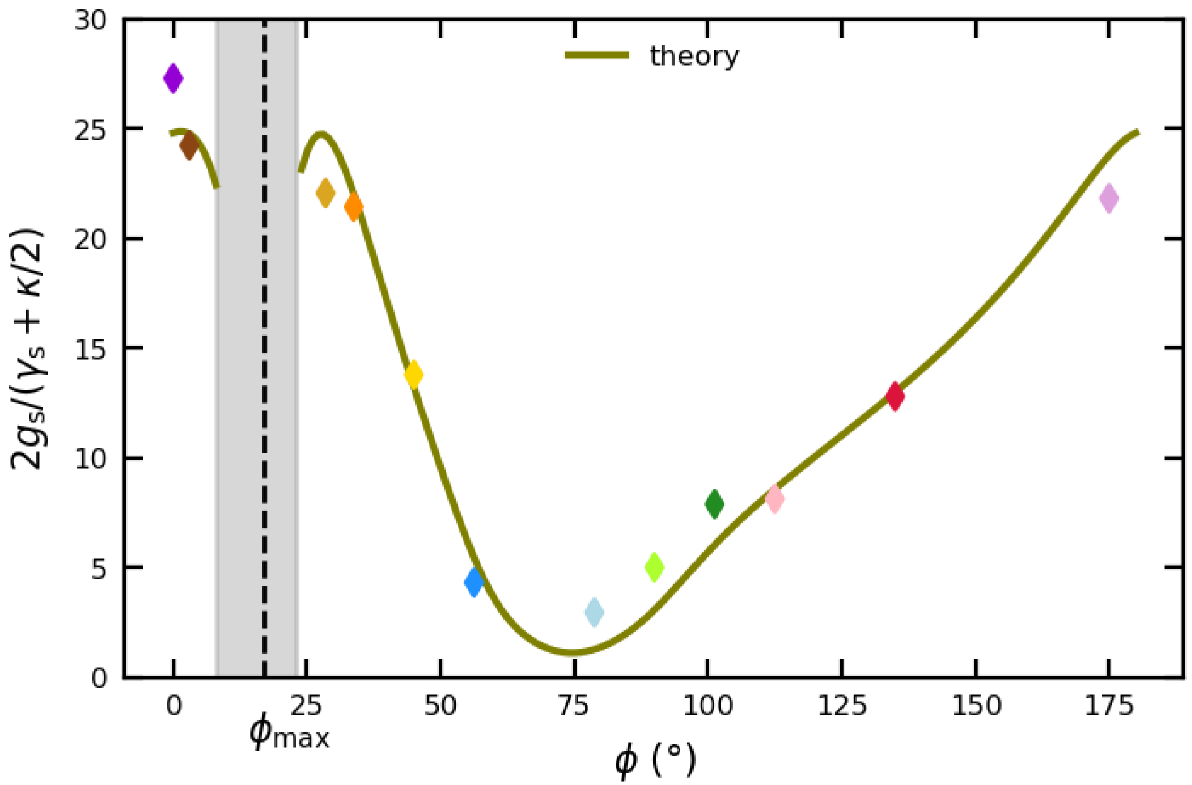

Dispersive regime

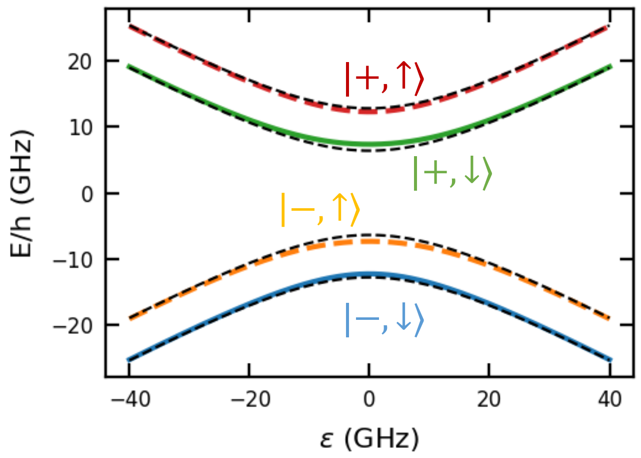

$$|-,\uparrow\rangle \longrightarrow \alpha|-,\uparrow\rangle + \beta|+,\downarrow\rangle$$

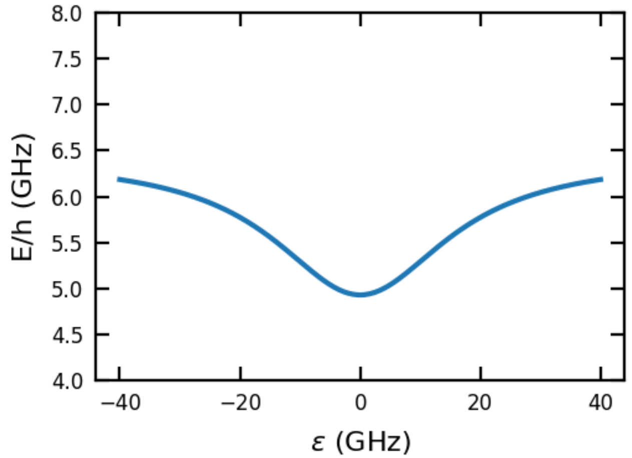

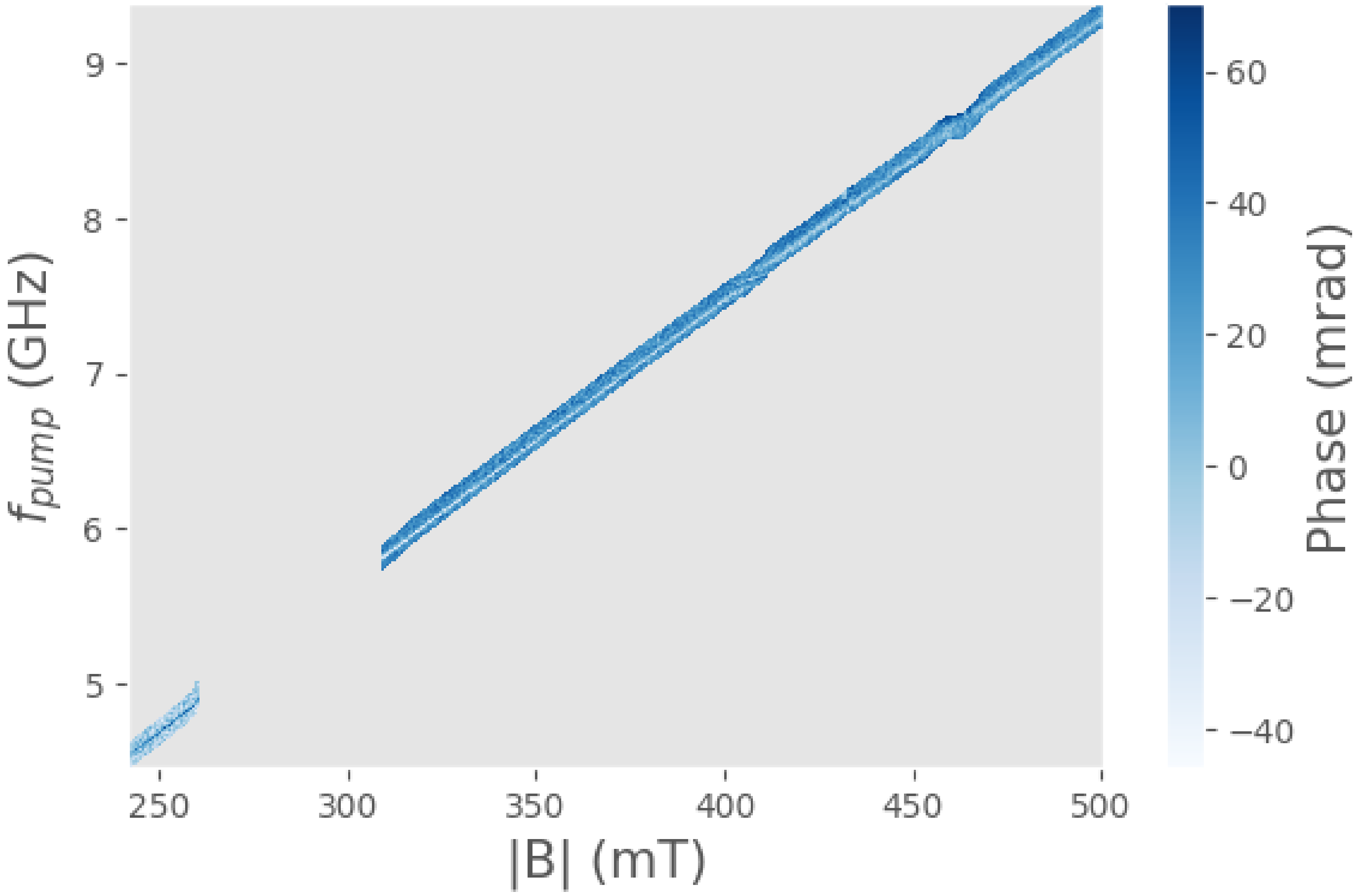

Dispersive regime

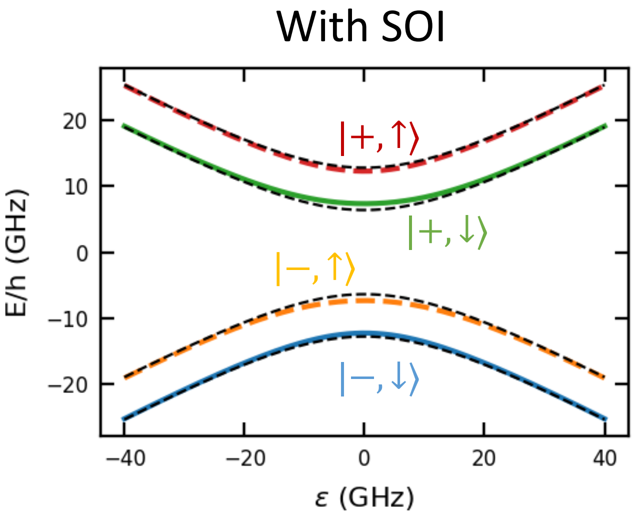

$$|-,\uparrow\rangle \longrightarrow \alpha|-,\uparrow\rangle + \beta|+,\downarrow\rangle$$

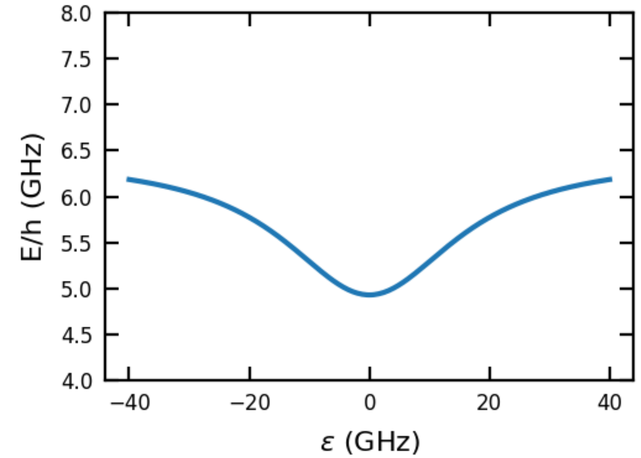

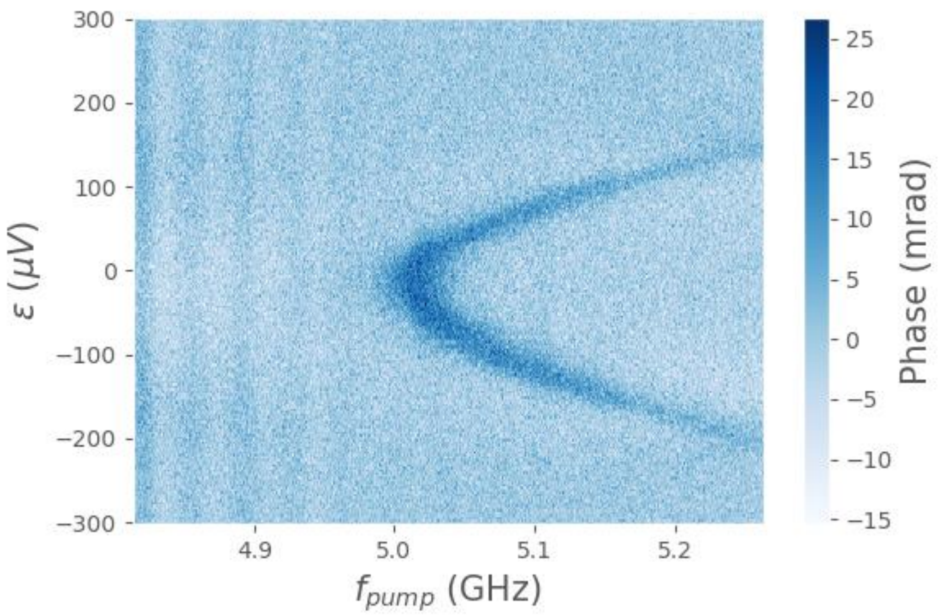

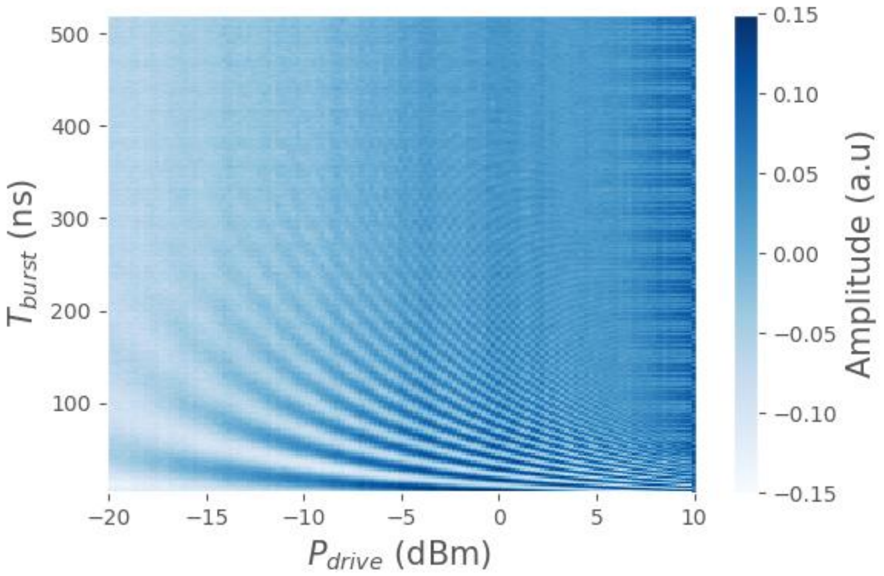

Spin-photon experiment with a single dot

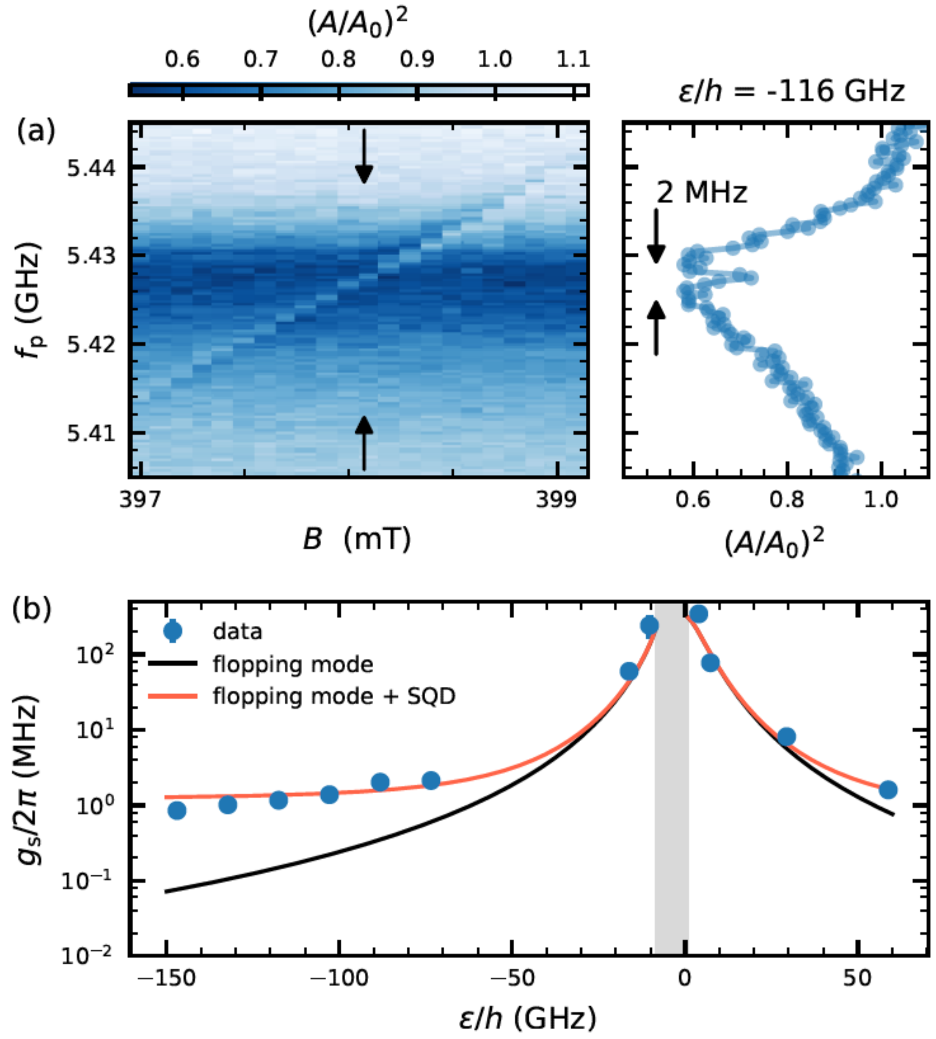

Bad cavity limit: needs a higher quality cavity

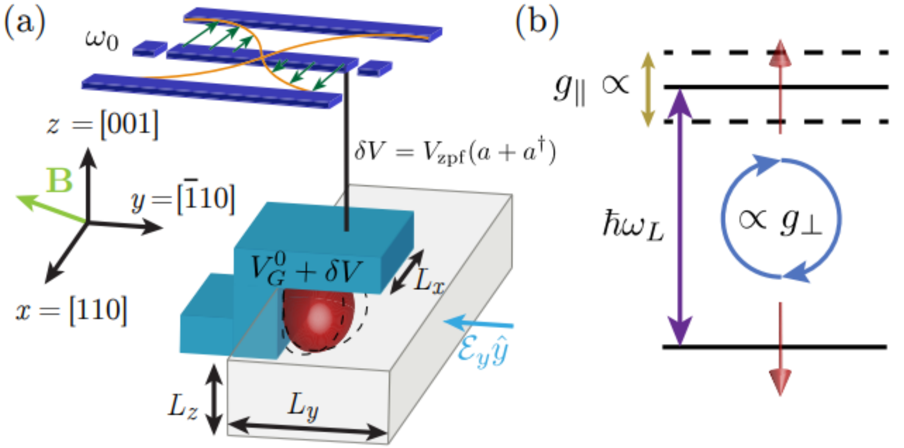

Michal, V *et al. Phys.Rev. B* 107, L041303 (2023)

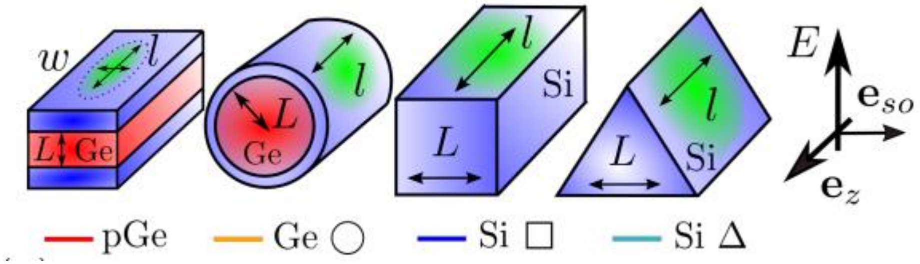

Bosco et al. PRL 129, 066801 (2022)

Take home message

- Nanowire MOS → ultra strong charge photon coupling

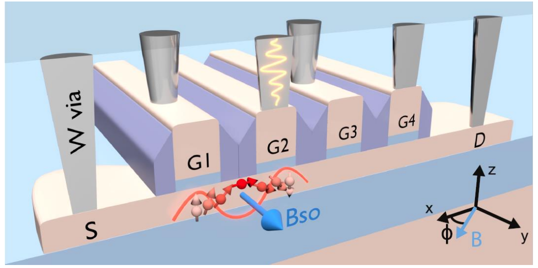

- Spin-photon coupling ruled by Spin-Orbit ~ 300MHz

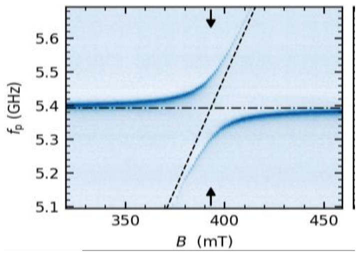

- Exploring with CQED the hole spin electric susceptibility

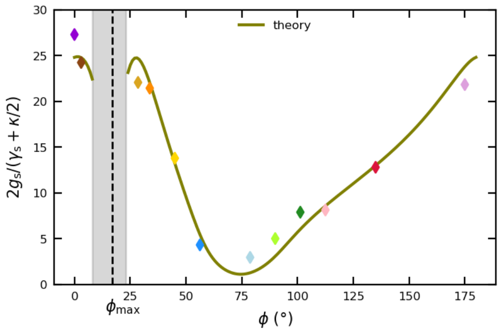

It is teamwork!

Special thanks to

- **Cécile Yu**
- **Nicolas Piot**
- **Simon Zihlmann**
- **Boris Brun-Barrière**
- **Léo Noirot**
- Xavier Jehl
- Silvano De Franceschi
- Etienne Dumur

- **José Abadillo-Uriel**
- **Vincent Michal**
- **Yann-Michel Niquet**

- Jean-Luc Thomassin
- Frédéric Gustavo

- Benoit Bertrand
- Heimanu Niebojewski
- Thomas Bedecarrats
- Maud Vinet

leti ceatech